

INTERPLAY OF MICROBIAL SHORT CHAIN FATTY ACIDS AND HOST  
G-PROTEIN COUPLED RECEPTORS IN BLOOD PRESSURE  
REGULATION

by  
Niranjana Natarajan

A dissertation submitted to Johns Hopkins University in conformity with  
the requirements for the degree of Doctor of Philosophy

Baltimore, Maryland

July 2016

© 2016 Niranjana Natarajan  
All Rights Reserved

## Abstract:

The role of commensal microbiota in modulating host physiology is a rapidly emerging and expanding concept. The composition of microbiota is diverse and dynamic depending on diet and environmental factors. Changes in the composition of the microbiota have been correlated with a variety of pathophysiological processes, including cardiovascular disease and hypertension. One of the well-characterized classes of gut microbial metabolites are short chain fatty acids (SCFAs), which are produced by the breakdown of dietary fiber in the colon. Recent studies have found that SCFAs produced by the gut microbiota modulate host physiology by acting as ligands for host G-protein coupled receptors (GPCRs), including Gpr41, Gpr43 and Olfr78. Gpr41, also referred to as Ffar3, is a member of the free fatty acid receptors family (FFAR), comprising of Gpr40, Gpr41, Gpr43, Gpr109a and Gpr120. These receptors are activated by free fatty acids. Gpr41, Gpr43 and Olfr78 are activated by SCFAs, while Gpr109a is activated by niacin and butyrate, Gpr40 and Gpr120 are activated by long chain fatty acids.

It has been previously reported that Olfr78 and Gpr41 differentially modulate blood pressure (BP) in response to acute delivery of SCFAs. Olfr78 is expressed in vascular smooth muscle cells and Olfr78 KO mice are known to be hypotensive in comparison to Olfr78 WT mice. The



broad goal of the work presented here was to better understand the role of Gpr41 in blood pressure regulation. It was hypothesized based on previous knowledge that Gpr41 KO mice would be hypertensive in comparison to Gpr41 WT mice.

In the work presented, Gpr41 was localized to the vascular endothelium, in contrast to Olfr78, which is found in the vascular smooth muscle, initially by RT-PCR and substantiated by antibody staining of primary endothelial cells. Continuous telemetry blood pressure measurement in 3 – month old male Gpr41 KO and WT mice determined that Gpr41 KO mice exhibit systolic hypertension in comparison to Gpr41 WT mice. In addition, Gpr41 KO mice present with elevated pulse wave velocity at 6 months of age, but not at 3 months (time point of baseline blood pressure measurement). Examination of blood vessel tensile properties did not reveal differences in stiffness of intact aorta from Gpr41 KO and WT mice. Furthermore, Gpr41 KO mice do not exhibit salt sensitive hypertension, but interestingly, do not have an adaptive decrease in systolic pressure on a low salt diet, exhibited by the Gpr41 WT mice.

In an attempt to understand the signaling behind SCFA – mediated vasodilation, it was observed that the vascular endothelium is essential for SCFA mediated vasodilation to occur, as vasodilation is absent in endothelium-denuded vessels ex vivo, consistent with a role for Gpr41 in

decreasing blood pressure / mediating vasodilation. The work presented sheds light on the novel role of Gpr41 in the endothelium in blood pressure regulation. SCFA receptors expressed in both the vascular endothelium (Gpr41) and vascular smooth muscle (Olf78) form a complex network to regulate BP in response to signals produced by the microbiota. In the future, better understanding of these pathways has the potential to further our understanding of BP regulation as a whole, as well as to more fully uncover the unique role of the gut microbiota in regulating both BP and vascular tone.

<b>TABLE OF CONTENTS</b>		
<b>1. Front matter</b>		
1.1.	Title page	i
1.2.	Abstract	ii
1.3.	Table of contents	v
1.4.	List of figures	vii
1.5.	List of tables	xi
1.6.	Acknowledgements	xii
1.7.	Dedication	xiv
1.8.	Author's declaration	xv
1.9.	Abbreviations	xvi
<b>2. Introduction</b>		
2.1.	Background	1
2.2.	G – protein coupled receptors	3
2.3.	Short chain fatty acid receptors	4
2.4.	Hypertension	8
2.5.	Microbiome and microbe – to – host signaling	11
2.6.	Specific aims	14
2.7.	Significance	16
<b>3. Localization and characterization of Gpr41</b>		
3.1.	Abstract	18
3.2.	Introduction	20

3.3.	Materials and methods	23
3.4.	Results	35
3.5.	Discussion	51
<b>4.</b>	<b>Role of Gpr41 in blood pressure regulation</b>	
4.1.	Abstract	57
4.2.	Introduction	60
4.3.	Materials and methods	66
4.4.	Results	74
4.5.	Discussion	98
<b>5.</b>	<b>Signaling mechanism of SCFAs in blood vessels</b>	
5.1.	Abstract	105
5.2.	Introduction	106
5.3.	Materials and methods	107
5.4.	Results	108
5.5.	Discussion	114
<b>6.</b>	<b>References</b>	116
<b>7.</b>	<b>Curriculum vitae</b>	134

**List of figures:**

<b>Figure</b>	<b>Title</b>	<b>Page number</b>
2.1	Hypothetical schematic of blood pressure regulation by a push – pull mechanism involving Gpr41 and Olfr78	6
2.2	Hypothetical pathway of Gpr41 signaling	14
3.1	Dual luciferase assay to assess olfactory receptor / Gs coupled GPCR activation by ligands.	32
3.2	$\beta$ – gal stain is not observed in Gpr41 KO tissues, indicating that insertion of LacZ gene into the coding region of Gpr41 may have disrupted Gpr41 IRES	36
3.3	Gpr41 is expressed in the endothelium (by RT-PCR)	37
3.4	Sequence alignment of epitope in rat and murine Gpr41	38
3.5	Gpr41 antibody faithfully detects over-expressed Gpr41 in HEK293T cells	39
3.6	Murine Gpr41 is detected as a monomeric 37kDa band and a dimeric 75kDa band in a western blot	40
3.7	Immunohistochemical stain of kidney sections from (A) Gpr41 WT and (B) Gpr41 KO mice.	41
3.8	Gpr41 is detected by western blot in aorta from Gpr41	42

	WT mouse.	
3.9	Immunohistochemical stain of kidney sections from (A) Gpr41 WT and (B) Gpr41 KO mice.	43
3.10	Beta hydroxybutyrate, a ketone body, is an agonist of Gpr41	44
3.11	Lactate is a weak agonist of Olfr78	46
3.12	EC50s of Olfr78 for SCFAs and lactate	47
3.13	Olfr78 and OR51E2 are activated by “microbial” SCFAs derived from <i>B. vulgatus</i> ,	49
4.1	Placement of telemetry catheter in the carotid artery for continuous blood pressure monitoring.	62
4.2	Representative blood pressure traces from telemetry system	63
4.3	Experimental scheme of chronic propionate treatment	72
4.4	Experimental scheme of high salt diet regime	73
4.5	SCFAs stimulate renin secretion via Olfr78, which results in a BP increase	78
4.6	Angiotensin – I standard curve	79
4.7	H&E stained sections of Gpr41 KO kidney moderate nephritis	81
4.8	Gpr41 KO mice exhibit isolated systolic hypertension	82
4.9	Pulse pressure is significantly elevated in Gpr41 KO	83

	mice, there are no differences in heart rate	
4.10	Gpr41 KO mice have significantly higher dP/dt	83
4.11	Pulse wave velocity is elevated in 6 – month old Gpr41 KO mice	86
4.12	Blood vessel tensile properties are similar in intact aorta, decellularized aorta from Gpr41 KO mice are more compliant.	87
4.13	Chronic propionate administration (200mM sodium propionate in the drinking water) doesn't stably alter blood pressure in Gpr41 KO mice	89
4.14	Mean arterial pressure and diastolic pressure in Gpr41 KO and WT mice during the treatment periods, both light cycle and dark cycle values are shown.	90
4.15	Heart rate is not significantly different between Gpr41 KO and Gpr41 WT mice during sodium propionate and sodium chloride treatment.	90
4.16	Body weight of Gpr41 KO mice increases on propionate and sodium chloride treatment.	92
4.17	Plasma sodium increases during chronic sodium propionate treatment in both Gpr41 WT and Gpr41 KO mice	93
4.18	Gpr41 KO mice do not exhibit salt – sensitive	96

	hypertension.	
4.19	Diastolic pressures are mostly not different between genotypes during salt loading	97
4.20	Gpr41 KO mice do not exhibit any trend in heart rate on high salt or low salt diets.	98
5.1	SCFAs induce vasodilation in murine tail resistance arteries. A: microvascular chamber setup, B: representative trace	109
5.2	Endothelium mediates SCFA – mediated vasodilation – representative traces	110
5.3	Endothelium mediates SCFA – mediated vasodilation (summarized data)	111
5.4	L-NAME doesn't significantly inhibit SCFA – induced vasodilation – representative trace	112
5.5	L-NAME doesn't significantly inhibit SCFA – induced vasodilation – summarized data	113



**List of tables:**

<b>Table</b>	<b>Title</b>	<b>Page number</b>
3.1	Primer sequences for RT-PCR	24
3.2	EC50s of Olfr78 for SCFAs and lactate	47
4.1	Plasma electrolytes in Gpr41 KO and Gpr41 WT mice	75
4.2	Plasma renin concentration in 3 month old mice	79
4.3	Plasma renin concentration, 6 month old mice	79
4.4	Plasma electrolytes during baseline, sodium propionate and sodium chloride treatments	94

### Acknowledgements:

I am who I am because of my family. My parents have gone through a tremendous amount of effort hardship just to make sure that I got the very best at every stage in life and enjoyed opportunities that they never had. My mother has been a pillar of support, encouragement and motivation throughout my life. She has always encouraged me to expand my horizons, not just limited to science and research but in a wide range of interests, from music and literature to science and technology. My father has been my most ardent supporter and enthusiast, stimulating me to do better than my best. My most important source of support, encouragement and inspiration was my maternal grandmother, a retired schoolteacher, who first taught me to read and write as a child and continued to support me in my academic endeavors throughout. She was there to support me in every way, every day of my childhood. Her ardent desire to learn new things and expand her horizons was my greatest inspiration. I proudly say that at the age of 80, she tried her best to learn science, so that she could understand what I worked on. I cannot say that any other person would be more proud of my achievements than my grandmother. I would be amiss if I do not mention my little sister, who has been a great support, friend and partner in crime. My life would never be as bright and colorful without her. It has been a joy and stimulating journey to watch her grow and take on research projects of her own.

In my academic life, I was very fortunate to have been part of the Khorana fellowship, which first exposed me to an academic research environment in the United States. My experience as an intern at University of Wisconsin, Madison made me want to pursue research as a career and go into graduate school. At Johns Hopkins, I am very fortunate to have found an inspirational, creative and amazing mentor like Dr. Jennifer Pluznick. Jen strives to bring the best out in her trainees. In addition to research, she taught me how to approach a scientific problem, helped me develop scientific writing skills and showed me to not be afraid of mistakes, but to learn from them and move forward. My thesis committee members, Dr. William Guggino, Dr. Lawrence Schramm and Dr. William Wong have been very supportive of my work and have encouraged me with feedback on my work. I was also lucky to be in a very friendly lab environment with people from diverse backgrounds. I learned a lot from Blythe, a postdoctoral fellow in our laboratory. I have also enjoyed the camaraderie with my fellow lab mates, in both scientific and casual settings.

Finally, it would have been impossible to go through graduate school without the support of my husband, Jishnu Das. He has been a friend, intellectual peer and motivation throughout my career. He just wrapped up his Ph.D at Cornell University.

## **Dedication**

Dedicated to my grandmother, Rajalakshmi, who was an integral part of my life and instrumental in getting me to where I stand today.



Mrs. S. Rajalakshmi Oct 10, 1934 – June 20, 2016

Author's declaration:

The investigations and results shown were conducted by the author. No part of the work presented in this dissertation has previously been presented in fulfilment of the regulations for any degree or diploma, either at this University or at any other institution.

Abbreviations:

GPCR	G – protein coupled receptor
SCFA	Short chain fatty acids
BP	Blood pressure
mmHg	Millimeters mercury (unit for measuring blood pressure)
PBS	Phosphate buffered saline
TBS	Tris buffered saline
DMEM	Dulbecco's eagle modified medium
HEK	Human embryonic kidney cells
HUVEC	Human umbilical vein endothelial cells

## **2. Introduction**

### **2.1 Background**

Chemosensory receptors on the cell surface recognize a variety of signals and relay information into a cell, initiating an appropriate cellular response and enabling communication between cells, tissues and organs. These cell surface receptors are grouped into three families based on homology and function – ion channel linked receptors, enzyme linked receptors and G – protein coupled receptors (GPCRs). Seven trans-membrane domain G-protein coupled receptors (GPCRs) comprise the largest superfamily of cell surface receptors in the human proteome[1-3]. GPCRs are potential therapeutic targets due to their ability to be modulated by pharmaceutical agents. GPCRs respond to a variety of stimuli ranging from light to neurotransmitters, odorants, nucleotides, small peptides and lipids to fatty acids, biogenic amines and hormones[1-3]. Many tissues express and employ GPCRs as chemosensors, in order to respond to metabolites and extracellular signals[4-9].

It has recently been reported that metabolites produced by commensal microbiota act as ligands for GPCRs of the host organism, allowing for an entirely novel paradigm of microbe-to-host GPCR signaling pathways[10-15]. These metabolites produced by the commensal microbiota act on key regulatory pathways in the host, playing important roles in regulating

host physiology and pathophysiological processes like obesity, immune disorders, atherosclerosis, irritable bowel syndrome and chronic kidney disease[10-20].

A major class of metabolites generated as a by-product of microbial metabolism is short chain fatty acids, (SCFAs, namely formate, acetate, propionate and butyrate, pentanoate and hexanoate), produced primarily from the fermentation of dietary fiber[12, 21-23]. The predominant species of SCFA produced are acetate, butyrate and propionate, in order of decreasing abundance in the colon[14, 22]. Gut microbiota-derived SCFAs have been shown to activate a subclass of GPCRs commonly referred to as Free Fatty Acid Receptors (FFARs), including Gpr41, Gpr43[24, 25]. In addition, an olfactory receptor (subfamily of GPCRs) Olfr78 (human homolog hOR51E2 is also activated by SCFAs[5, 26].

SCFAs mediate a significant component of microbe – to – host signaling by activating SCFA receptors and acting in a receptor – independent manner[12-14, 27-29]. SCFAs were reported to modulate host blood pressure via Gpr41 and Olfr78 and FFARs and Olfr78 were expressed in blood vessels[5, 26]. Understanding a microbe-to-host signaling pathway that modulates blood pressure is of fundamental importance in the development of hypertension therapeutics. The aim of the work presented



in this dissertation is to uncover the molecular mechanism underlying the hypotensive response to SCFAs.

### **2.1.2 G-protein coupled receptors**

GPCRs are members of the largest gene family in the human genome. They are characterized by the presence of 7 – transmembrane helices, with an extracellular N – terminus and an intracellular C – terminus. The distinct name G – protein coupled receptors arises from the association of GPCRs with downstream signaling proteins that have GTPase activity[2, 30-32]. A majority of GPCRs are associated with trimeric G – proteins,  $G_\alpha$ ,  $G_\beta$ ,  $G_\gamma$ , while some GPCRs are known to associate with smaller GTPases.  $G_\alpha$  possesses GTPase activity and aids in translation of ligand binding – mediated receptor activation to a cellular response. GPCRs serve the function of transducing an extracellular stimulus to an intracellular response. A wide variety of stimuli ranging from pH, light, ions, amino acids and nucleotides to lipids and proteins are known to activate GPCRs, which upon activation initiate downstream signaling responses in the cell aided by the heterotrimeric G proteins[1, 31]. When a GPCR is activated by ligand binding, it undergoes a conformational change and subsequently acts as a Guanine Nucleotide Exchange Factor for the associated  $G_\alpha$  protein. The GPCR activates the associated  $G_\alpha$  protein by exchanging the bound GDP for GTP. The activated  $G_\alpha$  protein dissociates from the  $\beta$  and  $\gamma$  subunits to elicit a downstream signaling

response. There are different  $G_\alpha$  proteins known, each of which initiate a different downstream response in the cell ( $G_{\alpha s}$ ,  $G_{\alpha i/o}$ ,  $G_{\alpha q/11}$ ,  $G_{\alpha 12/13}$ )[33]. The two major signal transduction pathways initiated by GPCRs are the cAMP pathway and phosphoinositol pathway[1, 2, 31, 33, 34]. In addition, activated  $G_\alpha$  subunits can signal via calcium, cGMP and MAPK pathway[35]. The signal transduction pathway initiated by a GPCR upon activation depends on the associated  $G_\alpha$  subunit.  $G_{\alpha s}$  and  $G_{\alpha i/o}$  signal via cAMP as the second messenger, synthesized by the enzyme adenylate cyclase. While  $G_{\alpha s}$  activates adenylate cyclase, increasing cellular cAMP levels,  $G_{\alpha i/o}$  inhibits adenylate cyclase, decreasing cellular cAMP levels.  $G_{\alpha q/11}$  signal via phospholipase C, with calcium and phosphoinositol as second messengers;  $G_{\alpha 12/13}$  signal via small cytosolic Rho GTPases[2, 32, 34, 36]. Aside from the cellular response initiated by  $G_\alpha$  proteins,  $G_\beta$  and  $\gamma$  modulate ion channel function in the cell.

### **2.1.3 Short chain fatty acid receptors**

A total of 4 SCFA receptors have been identified till date, Gpr41, Gpr43, Gpr109a and Olfr78.

#### **Gpr41 (free fatty acid receptor 3, Ffar3)**

Gpr41 and Gpr43 were identified as SCFA receptors when they were de-orphanized together by two independent groups in 2003[37, 38]. Gpr41

couples to inhibitory G – protein, Gi and is best activated by propionate (EC50: Gpr41 = 2 $\mu$ M), although a variety of other SCFAs including formate, acetate, butyrate, and isobutyrate elicit varying degrees of activation[37, 38]. Importantly, the human and rat orthologs of Gpr41 displayed similar SCFA response profiles, indicating that the signaling of this receptor is likely to be evolutionarily conserved[37-39]. An additional receptor present in humans, Gpr42, has a very high level of homology to Gpr41, but it is unclear whether Gpr42 is a functional gene created due to duplication or a pseudo gene[38-40].

Acetate, propionate and butyrate, which are stronger ligands for Gpr41, are produced as byproducts of microbial metabolism. Gpr41 is expressed in a variety of tissues and cell types including the colon, kidneys, sympathetic nervous system and blood vessels, where they respond to microbiota-generated SCFAs to mediate physiological responses of the host[10, 37, 38, 41-45]. In the conventional state, Gpr41 KO mice weigh less and gain weight at a slower rate compared to their Gpr41 WT littermates; furthermore, the differences in weight gain are dependent on gut microbiota (as illustrated by the lack of weight differences between genotypes in germ-free animals)[10]. On the cellular level, other studies have shown that Gpr41 inhibits cell proliferation and induces apoptosis via the activation of p53 and MAPK[46]. Furthermore, Gpr41 is expressed in vasculature and plays a role in regulating blood pressure in response

to dietary SCFAs (Figure 2.1.1). Gpr41 and Olfr78 work in opposing directions to regulate blood pressure upon activation by SCFAs. The work presented in this dissertation focuses on the role of Gpr41 in blood pressure regulation and the mechanism of Gpr41 signaling[5, 26].

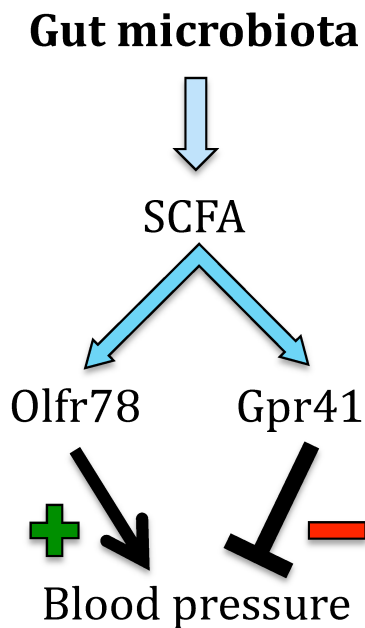


Figure 2.1 Hypothetical schematic of blood pressure regulation by a push – pull mechanism involving Gpr41 and Olfr78

### **Gpr43 (Free fatty acid receptor 2, Ffar2)**

Like Gpr41, Gpr43 was also found to be most responsive to propionate (EC<sub>50</sub>: 300  $\mu$ M), although other SCFAs exhibit varying levels of activation, with acetate, propionate and butyrate being the strongest three ligands[37, 38]. While Gpr41 couples to Gi, Gpr43 was found to couple to both Gi and Gq. Gpr43 is expressed mainly in the vasculature

and immune cells including lymphocytes, neutrophils, monocytes and peripheral blood mononuclear cells (PBMC)[45, 47]. Functionally, Gpr43 has been shown to regulate host inflammatory responses in response to microbial SCFAs. SCFAs have been shown to activate cytokines and chemokines both in cultured intestinal epithelial cells and in mice via the activation of Gpr43, as the response was absent in cells from Gpr43<sup>-/-</sup> mice. In addition, Gpr43<sup>-/-</sup> mice have extensive dysregulation of inflammatory responses, showing excessive inflammation in models of colitis, arthritis and asthma[45, 47-49].

### **Gpr109a**

Gpr109A was initially identified as a receptor for niacin[50], and subsequently was also found to respond to beta-D-hydroxybutyrate as well as butyrate[51]. Interestingly, this receptor does not respond to acetate or propionate, but has an EC<sub>50</sub> for butyrate around ~1mM. Gpr109A has been localized to epithelial cells in the colon, where its level of expression is suppressed in the absence of commensal microbiota[50, 52].

### **Olfactory receptor 78 (Olfr78)**

Olfactory Receptor 78 (Olfr78) is a chemosensory receptor, expressed in non-sensory tissues outside the olfactory epithelium[5, 26]. Olfr78 responds to acetate and propionate (EC<sub>50</sub> 2.35mM and 920  $\mu$ M,

respectively), but does not respond to butyrate (in contrast, Gpr109A responds only to butyrate). Importantly, the human ortholog of Olfr78, OR51E2 also responds to SCFAs, indicating that the function of this receptor is conserved through the course of evolution. Olfr78 localizes to the kidney, blood vessels, autonomic neurons and the olfactory epithelium. In the kidney, it is expressed in the afferent arteriole and in vascular smooth muscle cells in resistance blood vessels. Both of these cell types are important in blood pressure regulation.

#### **2.1.4 Hypertension**

Blood pressure (BP) is the pressure developed by circulating blood pressing against the walls of blood vessels. The term “blood pressure” commonly refers to arterial pressure and is measured in mmHg. BP is expressed in two values, the systolic pressure (higher pressure developed during contraction of the left ventricle to deliver blood to the aorta) and diastolic pressure (lower pressure observed when the left ventricle is relaxed and being filled with blood). Blood pressure of a healthy adult at rest falls within 100 - 140 mmHg systolic and 60 - 90 mmHg diastolic.

Hypertension is defined as a condition wherein the systolic / diastolic pressure of an individual is persistently greater than 140 / 90 mmHg or when the BP is the normotensive range only upon administration of anti-hypertensive medication[53-55]. Hypertension is a major, worldwide

health problem owing to its high prevalence and association with increased morbidity and mortality as a result of cardiovascular complications. Approximately 7.1 million deaths per year can be directly attributed to poor control of blood pressure. An estimated 29% of the adult US population is hypertensive and an equivalent percentage suffers from prehypertension; evidence shows that individuals with prehypertension are at particular risk of developing overt hypertension[53, 54].

Hypertension is classified as primary or essential hypertension and secondary hypertension. 90 – 95% of cases have primary hypertension, usually due to a combination of nonspecific lifestyle, genetic or unknown factors, while the remaining 5 -10% of cases have attributable causes leading to increased blood pressure like narrowing of arteries, chronic kidney disease or endocrine disorders [56, 57]. Essential hypertension is a complex trait resulting from the interaction of multiple genes and environmental factors. 35 genetic loci that affect blood pressure have been identified by GWAS and several genetic variants that have effects on blood pressure have been identified[58-60]. Blood pressure is the product of vascular resistance and cardiac output. In people with essential hypertension, an increase in total peripheral vascular resistance is observed, which results in increased arterial blood pressure. Precise reasons for the increase in vascular resistance are unknown, it is

presumed that renal dysfunction leading to disruption of salt – water balance, increase[61, 62] of sympathetic output or endothelial dysfunction may lead to an increase in vascular resistance in hypertension[63-65].

In addition to the contribution of renal dysfunction, vascular resistance and sympathetic nervous system, the immune system, also contributes to the development and manifestation of hypertension[66]. Animals with hypertension exhibit an increase in inflammatory cells in the blood and bone marrow resulting in immune infiltration of kidneys and other tissues, leading to end-stage organ damage[67]. This inflammatory response also leads to the production of cytokines that increase sodium retention in the kidney and vasoconstriction, resulting in increased peripheral resistance, which further augments the hypertensive condition[67, 68].

Management of hypertension is of utmost importance because increased arterial pressure over a prolonged period of time results in a host of cardiovascular and renal complications, and increases the risk of stroke. A combination of antihypertensive medication and lifestyle modifications are prescribed to reduce blood pressure to 140 – 160mmHg systolic and 90 – 100 mmHg diastolic pressure[69]. Pharmacological intervention for hypertension is carried out using one or a combination of thiazide



diuretics, calcium channel blockers, angiotensin – I converting enzyme (ACE) inhibitors or alpha / beta-adrenergic receptor antagonists[61, 62].

Advances in the diagnosis and treatment of hypertension have had a major impact on management of this chronic disease. However, despite these advances, it is estimated that 1.56 billion people will suffer from hypertension by 2025[53]. Further methods are therefore needed to manage hypertension and its associated risks. The development of such therapeutic interventions will be facilitated by an increased understanding of the pathogenic mechanisms underlying this condition.

#### **2.1.5 Microbiome and microbe – to – host signaling**

The population of commensal microbes that reside mainly in the gut and several other sites in the body are collectively referred to as the microbiota and the collective genome of these microbes is called the “microbiome”. There has been an explosion of literature on microbiota and their effect on host health and disease in the recent few years. Microbiota play an integral role in modulating host physiology, immune system and pathophysiology. Metabolites produced by gut microbiota act as ligands for host receptors and GPCRs [70, 71], allowing for an entirely novel paradigm of microbe-to-host GPCR signaling pathways. These metabolites produced by the gut microbiota act on key regulatory pathways in the host, playing important roles in regulating host

physiology and pathophysiological processes like immune disorders[72], atherosclerosis[73], irritable bowel syndrome[74, 75] and chronic kidney disease[76, 77]. Recent studies suggest that development and onset of cardiovascular and metabolic diseases are influenced by microbial composition and metabolites[15, 78-80].

The composition of microbiota of an individual, referred to as the “enterotype”, is dynamic and constantly changing due to changes in diet and environment[81]. Recent data suggests that a disruptive change in microbial composition to a pathological state, "dysbiosis"[16], is related to chronic inflammatory diseases like asthma and inflammatory bowel disease[15, 47, 82-84]. Balance of the abundance of different species in the gut is key to maintaining homeostasis in the intestinal environment and normal physiology of the host. An individual's microbiota is diverse and comprises of many species, but 4 phyla are most abundant - *firmicutes*, *actinobacteria*, *proteobacteria*, *bacterioidetes*. A ratio of the relative abundance of two microbial species Firmicutes and Bacterioidetes (F/B ratio) is potentially used as a biomarker for pathological conditions[85-87].

Dysbiosis was observed in a small cohort of hypertensive humans with a marked increase in the F/B ratio, treatment with antibiotic minocycline to alter the microbiota resulted in a decrease in BP[79, 88]. An

independent study reported differences in microbiota composition between salt –sensitive and salt – resistant rats[20]. Decreased systolic and diastolic BP have been reported with a regular consumption of probiotics and dietary fiber in population studies[89, 90]. Furthermore, the dysbiosis observed in hypertensive individuals resulted in a decrease in SCFA production by the microbiota[87, 91], indicating that microbiota affect host BP via SCFAs and that in a state of dysbiosis, microbiota could contribute to the manifestation of hypertension by modulating the immune system.

Understanding the basis of microbiota and SCFA – mediated BP regulation could enable development of alternate dietary strategies for management of hypertension that could be combined with existing pharmaceutical intervention approaches.

### 2.1.6 Specific aims

The goal of the work presented in this dissertation is to understand the role of Gpr41, a propionate receptor, in microbe-to-host signaling pathways that regulate blood pressure. Gpr41, also referred to as Free fatty acid receptor 3 (Ffar3), is activated by SCFAs such as propionate and butyrate. Gpr41 plays an important role in mediating a hypotensive response to SCFAs. It is hypothesized (Figure 1) that Gpr41 regulates blood pressure by playing a role in endothelium-mediated vasodilation via the release of vasoregulatory factors such as nitric oxide and prostacyclins. To address both the mechanism underlying Gpr41's role in vasodilation, as well as the physiological implications of this SCFA – mediated signaling pathway in blood vessels, the following aims were pursued.

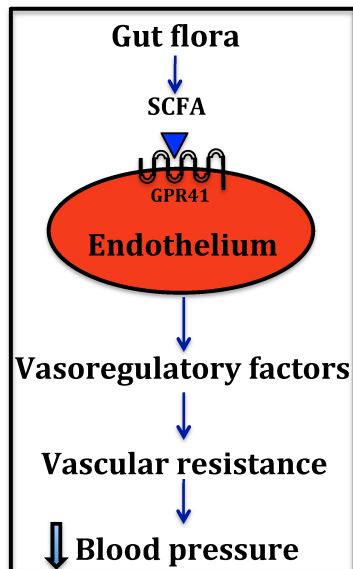


Figure 2.2: Hypothetical pathway of Gpr41 signaling

**Aim 1:** Localization and signaling of Gpr41

- (a) To determine the localization of Gpr41 and identify the cell – type in which Gpr41 is localized in a blood vessel
- (b) To elucidate the signaling mechanism of Gpr41
  - a. at the cellular level by studying the signaling of Gpr41 in endothelial cells at the tissue level
  - b. in blood vessels *ex vivo*; by examining the effect of SCFAs on vascular resistance of tail resistance arteries from Gpr41 KO and Gpr41 WT mice.

**Aim 2:** Role of Gpr41 in blood pressure regulation

- (a) To study the role of Gpr41 in blood pressure regulation – baseline blood pressure in Gpr41 WT and KO animals
- (b) To explore the effect of chronic SCFAs administration on blood pressure in Gpr41 KO and WT mice
- (c) To examine the effect of high salt and low salt diets on blood pressure in Gpr41 KO and WT mice.

### **2.1.7 Significance**

Modulation of blood pressure and vascular resistance by microbial metabolites is a novel pathway that is not understood clearly. Most digestion and nutrient assimilation occurs in the small intestine, whereas, breakdown of dietary fiber occurs in the colon. Significant quantities of SCFAs are produced following a meal, resulting in vasodilation, which may facilitate efficient absorption of nutrients into the circulation. An increase in plasma SCFA after a meal causes a transient postprandial hypotension documented especially in elderly populations[92].

There are two SCFA receptors (Olf78 and Gpr41) that signal in response to SCFAs in order to modulate blood pressure. The primary response to an increase in plasma SCFAs in wild-type mice is a decrease in blood pressure, which is driven by Gpr41[5, 26]. This hypotensive response, however, is opposed by the actions of Olf78, which acts to increase blood pressure upon activation by SCFAs[5, 26]. It is hypothesized that commensal microbiota play an integral role in maintaining blood pressure by producing SCFA metabolites that act predominantly via Gpr41 to modulate blood pressure. The purpose of having two receptors for the same ligand work in opposing directions is related to the fact that Gpr41 and Olf78 have very different EC<sub>50</sub>s for SCFAs (Propionate: Gpr41, EC<sub>50</sub> 274  $\mu$ M; Olf78, EC<sub>50</sub> 0.9 mM)[26, 37, 38]. Therefore,

under basal conditions (in which plasma SCFAs are 0.1-10mM) one would expect Gpr41 but not Olfr78 to be tonically active. When plasma SCFAs begin to rise (i.e., following a meal), Gpr41 would be further activated and therefore would further lower blood pressure. However, once SCFA concentrations are elevated such that Olfr78 is activated as well, activation of Olfr78 would act as a 'brake' on the hypotensive pathway, acting as a failsafe against dangerous levels of hypotension when SCFA concentrations are high.

Detection of environmental cues by GPCRs has gained significant attention recently. Studies have shown that complex signaling networks enable cells and tissues to respond to external signals, altering physiological processes. Microbe-to-host signaling is a recent and upcoming area of investigation, as the ability of commensal organisms to alter host physiology reveals an entirely new layer of physiological regulation. The results presented indicate a novel source (gut microbiota) of molecules, which can affect blood pressure regulation. The hypotensive effects observed with the elevation of SCFAs in plasma imply that, in the future, it is possible that manipulation of gut microbiota could be an alternative therapy for hypertension.

### **3. Localization and characterization of Gpr41**

#### **3.1 Abstract**

we previously showed that 3 SCFA receptors, Gpr41, Gpr43 and Olfr78 are expressed in major blood vessels (aorta, renal artery and iliac artery). In this section Gpr41 was localized to the vascular endothelium by a combination of RT-PCR from murine aorta and immunohistochemistry of primary aortic endothelial cells. An antibody against rat Gpr41 was characterized and showed to reliably detect murine Gpr41 by immunohistochemistry and western blotting. Furthermore, attempts are made to localize Gpr41 in the kidney by immunohistochemistry of Gpr41 WT tissue sections; Gpr41 KO serves as control to validate antibody-based detection.

Although Gpr41 and Olfr78 have been deorphanized and shown to be SCFA receptors, there are other small molecule agonists and partial agonists for these receptors that have been identified. For instance, 2-hydroxybutyrate, a ketone body has been shown to be a Gpr41 agonist by several groups, while other groups argue that it's an antagonist of Gpr41. On a different note, lactate was shown to be a ligand for Olfr78 and it plays a role in Olfr78 our work is to understand the role of these receptors in blood pressure regulation, it is crucial to assess receptor activation by novel ligands in-house, to identify target molecules that could affect blood pressure via these receptors. Activation of Gpr41 by 2-



hydroxybutyrate and activation of Olfr78 by sodium lactate was assayed. Since these receptors respond to SCFAs in circulation and SCFAs are mainly a by-product of microbial metabolism, it is important to assess receptor activation by “microbial” SCFAs that are a complex mixture of individual SCFA species, in contrast to purified SCFA salts used in most laboratory assays. Activation of Olfr78 and OR51E2 by “microbial” SCFAs derived from isolated microbe *Bacillus vulgatus* was demonstrated.

### **3.2 Introduction**

In this section, we will investigate and establish the localization and the ligands for Gpr41, and will additionally investigate the ligand profile for Olfr78. With regards to the tissue localization of Gpr41, there is a minor conflict in the literature. According to different reports, Gpr41 is expressed in adipose tissue, lungs, heart, kidneys, enteroendocrine cells in the colon, sympathetic nervous system and blood vessels[26, 37, 38, 93-95]. Expression of Gpr41 in blood vessels is of most importance in order to attempt to understand its role in BP regulation. All three SCFAs receptors, Gpr41, Gpr43 and Olfr78 are expressed in major blood vessels – the aorta, renal artery and the iliac artery[5, 26]. X-gal staining in the Olfr78 KO tissues (LacZ inserted into Olfr78 coding region, driven by the native Olfr78 promoter) co-localizes with smooth muscle actin, indicating the expression of Olfr78 in vascular smooth muscle cells[26]. Since Olfr78 and Gpr41 act to oppose each other and Gpr41 is likely involved in mediating a hypotensive response to SCFAs, the cell type in which Gpr41 is expressed in a blood vessel is key to understand its physiological role and downstream signaling components.

Blood vessels are comprised of outer vascular smooth muscle cell layers and an inner single cell layer of endothelial cells. Cellular pathways that mediate vasodilation and vasoconstriction are different in these two cell types. The endothelial cell layer initiates signaling in response to shear

stress or stimuli in the blood to elicit a change in the compliance of vascular smooth muscle cells via the secretion of vasoactive substances. In addition, the endogenous G – proteins available for signaling may be different in the vascular smooth muscle cells and endothelial cells. Identifying cell type of Gpr41 expression is key to understanding its signaling machinery and pathway.

Metabolites produced by commensal microbiota modulate host pathways by acting as ligands for host receptors and GPCRs, allowing for an entirely novel paradigm of microbe-to-host GPCR signaling pathways[10-15]. One well – studied class of microbial metabolites is SCFAs, produced by breakdown of complex dietary polysaccharides by *Bacterioides*, *Clostridiales* and *Bifidobacteria*[22, 39, 96]. SCFA concentrations peak in the colon after a meal, following which they are transported into the bloodstream by SCFA transporters or free diffusion[13, 26, 97]. SCFAs have been shown to act as ligands for several GPCRs, referred to as free fatty acid receptors, Gpr41, Gpr43, Gpr109a and Olfr78. In addition to GPCR – mediated effects in the host, SCFAs can mediate receptor – independent effects by modulating histone acetylation and cell proliferation. SCFAs have been shown to affect host adiposity and metabolism, immune system and blood pressure[26, 96-104]. Being a class of major microbial metabolites, it is important to understand the cellular effects mediated by SCFAs and their signaling pathways. In the

future, it is especially exciting to consider that modulating metabolite production by the gut microbiota may be a useful tool to obtain beneficial effects on host physiology.

Although broadly known as SCFA receptors, Gpr41 is activated by acetate, propionate and butyrate while Olfr78 is activated by acetate and propionate[26, 37, 38, 94, 105]. In addition to these ligands, there have been reports in the literature about a few small molecule ligands for these receptors[25, 43, 93, 106]. Olfr78, like all other olfactory receptors, couples to Golf in the nasal epithelium and in heterologous systems, can couple and signal via native G<sub>s</sub> (stimulatory G – protein) in the cell[107]. This fact is utilized to assess the ability of small molecules to act as an agonist for Olfr78. A dual luciferase system with a constitutive luciferase renilla, that acts as control and a CRE – driven luciferase firefly which is expressed upon an increase of cellular cAMP elicited by GPCR activation is used to test potential ligands for Olfr78 (Figure 4.1). Since activation is read out as an increase in firefly expression driven by increased amounts of cytosolic cAMP generated by G<sub>s</sub> activation, this assay cannot be directly used to assay G<sub>i</sub> coupled receptor activation, which decreases cytosolic cAMP. Therefore, an additional step is used to adapt this G<sub>s</sub> based GPCR assay to extend it for screening ligands for G<sub>i</sub> coupled GPCRs like Gpr41. Forskolin is added to the cells to increase cytosolic cAMP and ligand addition, which activates G<sub>i</sub> would decrease cAMP

levels leading to an observable decrease of firefly from forskolin treated cells, compared to ligand and forskolin treated condition.

### **3.3 Materials and methods**

#### **RT-PCR from murine aorta**

Reverse transcript – PCR (RT-PCR) was used to localize Gpr41. Thoracic aortas were dissected from 3 month old C57BL/6 male mice and total RNA was extracted using Qiagen RNeasy Mini kit with DNase digest performed before elution. To remove the endothelium, thoracic aortas were sliced open longitudinally and the endothelium was mechanically denuded before RNA extraction was performed. RNA was reverse transcribed using Biorad iScript reverse transcriptase kit (random primers), according to the protocol provided in the kit. Primer sequences for Gpr41, eNOS and  $\beta$ -actin are given in Table 2.1. In a subset of samples, reverse transcriptase was omitted from the RT reaction (mock RT) as a negative control. PCR was carried out using Invitrogen Platinum Taq Mastermix for 35 cycles; all PCR products were sequenced to confirm.

Table 3.1: Primer sequences for RT-PCR

Gpr41 (685 bp)	Fwd:	ACGGCGGTGAGCATCGAACG
	Rev:	TTCCACCCCCTCCTGCGGTC
$\beta$ -actin (353 bp)	Fwd:	GCTCGTCGTCGACAACGGCTC
	Rev:	CAAACATGATCTGGGTCATCTTCTC
eNOS (230 bp)	Fwd:	CTGCTGCCCCGAGATATCTTC
	Rev:	CTGGTACTGCAGTCCCTCCT

## Cell culture

### HEK293T cells

Human embryonic kidney cells stably expressing the SV40 large T-antigen (HEK293T) were grown in Dulbecco's modified Eagle's medium supplemented with 10% fetal bovine serum and 2mM L-glutamine (described below). Cells were grown in a humidified incubator of 95% air/5% CO<sub>2</sub> at 37C. Cells were frozen in culture medium with 10% DMSO added.

### HEK 293T cell medium (500ml)

DMEM, 4.5 g/L glucose	450 ml
Fetal bovine serum (FBS)	50ml
Penicillin / Streptomycin	5ml
L – Glutamine	5ml

### **HUVEC cells**

Human umbilical vein endothelial cells (pooled) were grown in MCDB – 131 basal medium with 20% FBS, 2mM L – Glutamine, Heparin and endothelial cell growth substrate (composition below). Cells were grown in a humidified incubator of 95% air/5% CO<sub>2</sub> at 37C. Cultures were propagated by trypsinizing and passing cells. A freezing medium of culture medium with 10% DMSO was used.

### **HUVEC cell medium (500 ml)**

MCDB-131 basal medium	400ml
Fetal bovine serum (FBS)	100ml
Penicillin / Streptomycin	5ml
L – Glutamine	5ml
Endothelial cell growth substrate	50 µg / ml
Heparin sodium	50 µg/ml

### **Medium for primary aortic endothelial cells**

Primary aortic endothelial cells were isolated as follows

- Aortas were harvested from Gpr41 WT and KO mice and cut into 2-3 mm rings
- Aortic rings were cut open to expose intima, suspended in DMEM with 2mg/ml collagenase A, penicillin, streptomycin and amphotericin and gently agitated for 30 minutes at 37C.

- The medium with aortic rings was centrifuged at 1000xg for 3 minutes and the pellet was resuspended in DMEM with 20% FBS, penicillin, streptomycin and amphotericin and placed in a collagen-coated tissue culture dish.
- Aortic rings were removed in 2 hours and the medium was replaced with primary endothelial cell growth medium described below.
- Endothelial cells grew to confluency in 2 weeks after isolation

#### **Primary aortic endothelial cell medium**

DMEM / F12	400ml
Fetal bovine serum (FBS)	100ml
Penicillin / Streptomycin	5ml
Amphotericin	50 µg/ml
L – Glutamine	5ml
100X Non-essential amino acid mix	5ml
Endothelial cell growth substrate	50 µg/ml
Heparin sodium	50 µg/ml

#### **HEK293T cell transfection with lipofectamine 2000**

Lipofectamine 2000 (Invitrogen) was used to transiently transfect Gpr41 and Olfr78 into HEK293T cells according to manufacturer instructions. Reverse transfections were performed, HEK293T cells were passed onto



12 – well dishes (on coverslips for immunofluorescence, in dishes for western blotting) and transfected simultaneously.

### **Cell immunofluorescence staining protocol**

HEK293T cells transfected with Gpr41 or any other olfactory receptor and non-transfected cells (control) were grown on coverslips for 24 hours post-transfection. Immunostaining was performed 24 hours after transfection. The protocol followed comprised of the following steps

1. Coverslips were washed in cold PBS++
2. Cells were fixed with 4% formaldehyde in PBS++ for 30 minutes at room temperature
3. Coverslips were washed in PBS++ and cells were permeabilized for 15 minutes. (Permeabilization buffer: 0.1% BSA, 0.3% Triton – X 100 in PBS++)
4. Blocking was carried out with 1% BSA in PBS++ for 30 minutes
5. Cells were incubated overnight with primary antibody (anti – Gpr41 polyclonal, raised in rabbit, monoclonal flag antibody, raised in mice) at 1:100 dilution in blocking buffer.
6. After three washes with permeabilization buffer, coverslips were incubated with fluorescent tagged secondary antibody (1:1000 in blocking buffer) and Hoescht (nuclear stain, 1:2500) for 45 minutes at room temperature

7. Coverslips were washed and mounted with vectashield and viewed under a fluorescence microscope.

### **Tissue immunostaining protocol**

This protocol was used to stain tissue sections from Gpr41 KO and Gpr41 WT mice. Mice were euthanized by CO<sub>2</sub> asphyxiation and tissues were harvested. The harvested tissues were post fixed in 10% neutral buffered formalin for 2 days and sucrose treated for 3 days following which they were set in blocks with OCT for sectioning. The blocks were sectioned to get 10 – 12  $\mu$ M tissue cryosections for immunostaining. The following steps were performed:

1. Slides were washed in 1X TBS
2. Antigen retrieval in citrate buffer was performed with 10mM citrate buffer, pH 6.0. Citrate buffer was preheated and slides were placed in hot citrate buffer for 20 minutes and then allowed to cool down to room temperature.
3. Slides were washed in TBS and placed in s 1% SDS solution in TBS for 5 minutes, then washed again in TBS.
4. Blocking was carried out with 1% BSA and 0.2% milk in TBS, for 30 minutes at room temperature.
5. Sections were incubated overnight in a humidified chamber with primary antibody, diluted appropriately in blocking buffer.

6. Slides were washed first in TBS with 0.1% BSA, then in TBS with 0.1% BSA and 0.8% NaCl and then in TBS – 0.1% BSA.
7. Sections were then incubated with secondary antibody (fluorescent labeled) at 1:1000 dilution with Hoescht stain at 1:2500 dilution for 45 minutes at room temperature.
8. After secondary labeling, slides were washed similarly (step 6), with an additional wash in TBS in the end.
9. Slides were dried and mounted in vectashield and observed through a fluorescence microscope.

Buffers for tissue immunohistochemistry

Citrate buffer for antigen retrieval

5ml of 0.1 M Citric Acid) and 45 ml 0.1 M Na citrate in 500 ml total.

1% SDS in TBS

12.5 ml 20% SDS in 250ml total TBS

Blocking buffer

TBS with 1% BSA and 0.2% blocking milk

TBS/HS/BSA

500ml TBS, 0.5 g BSA, 8g NaCl

TBS/BSA

500ml TBS, 0.5g BSA

### **SDS-PAGE**

Protein samples were resolved using sodium dodecyl sulfate polyacrylamide gel electrophoresis (SDS-PAGE). Cell lysates were mixed with 5X Laemmli buffer and heated at 95C for 5 minutes and cooled before loading. SDS-PAGE gels with a 3% stacking gel and 12% resolving gel were cast and loaded with samples and molecular weight markers. 1X western running buffer was used to resolve the lysates on the gel.

### **Western blotting**

Following resolution of cell lysates by SDS-PAGE, the samples are electrophoretically transferred onto nitrocellulose membrane. Proteins were transferred at 100V for 90 minutes in 1X transfer buffer. Upon completion of transfer, the membranes were stained with Ponceau S to visualize transferred protein bands. The membrane was then blocked with 5% non-fat milk in PBS with 0.1% Tween 20 for 30 minutes and then incubated with primary antibody overnight in blocking milk. After incubation with primary antibody, the membrane was washed in PBS-T (1X PBS with 0.1% Tween 20) and incubated with secondary antibody (HRP linked) in milk for 1 hour at room temperature. The blot was developed with chemiluminescent ECL substrate after washing the

membrane thoroughly, following incubation with secondary antibody.

Dilutions of primary and secondary antibody are listed below

Primary antibodies

Gpr41: 1:1000 in milk, overnight

Mflag: 1:1000 in milk, overnight

Secondary antibodies

Goat anti mouse, HRP tagged: 1:10,000 in milk, 1-hour incubation

Goat anti rat, HRP tagged: 1:10,000 in milk, 1-hour incubation

### **Dual luciferase assay to monitor Gs coupled GPCR activation**

- HEK293T cells are plated in 96 – well black plates.
- The cells were transfected with olfactory receptor / GPCR construct (71%), luciferases firefly and renilla (14% each) using lipofectamine, according to manufacturer instructions.
- 20 hours post transfection, media is removed, cells are washed with PBS and incubated with STIM (CD293) medium for 30 minutes to decrease background cellular signaling.
- Ligands to be tested are prepared in various concentrations and 75µl ligand is added to each test wells. Non-treated wells are used as control. Cells are incubated with ligands for 4 hours.
- After ligand incubation, cells are washed and lysed in passive lysis buffer (manufacturer supplied) for 15 minutes at room temperature.

- Using a plate reader, 35μl Lar II (firefly, measure of GPCR activation) and Stop and Glo (renilla, constitutively active, measure of cell number) are added sequentially to the wells and the luminescence is recorded.
- Activation of GPCR is measured as ratio of firefly to renilla (Figure 3.1).

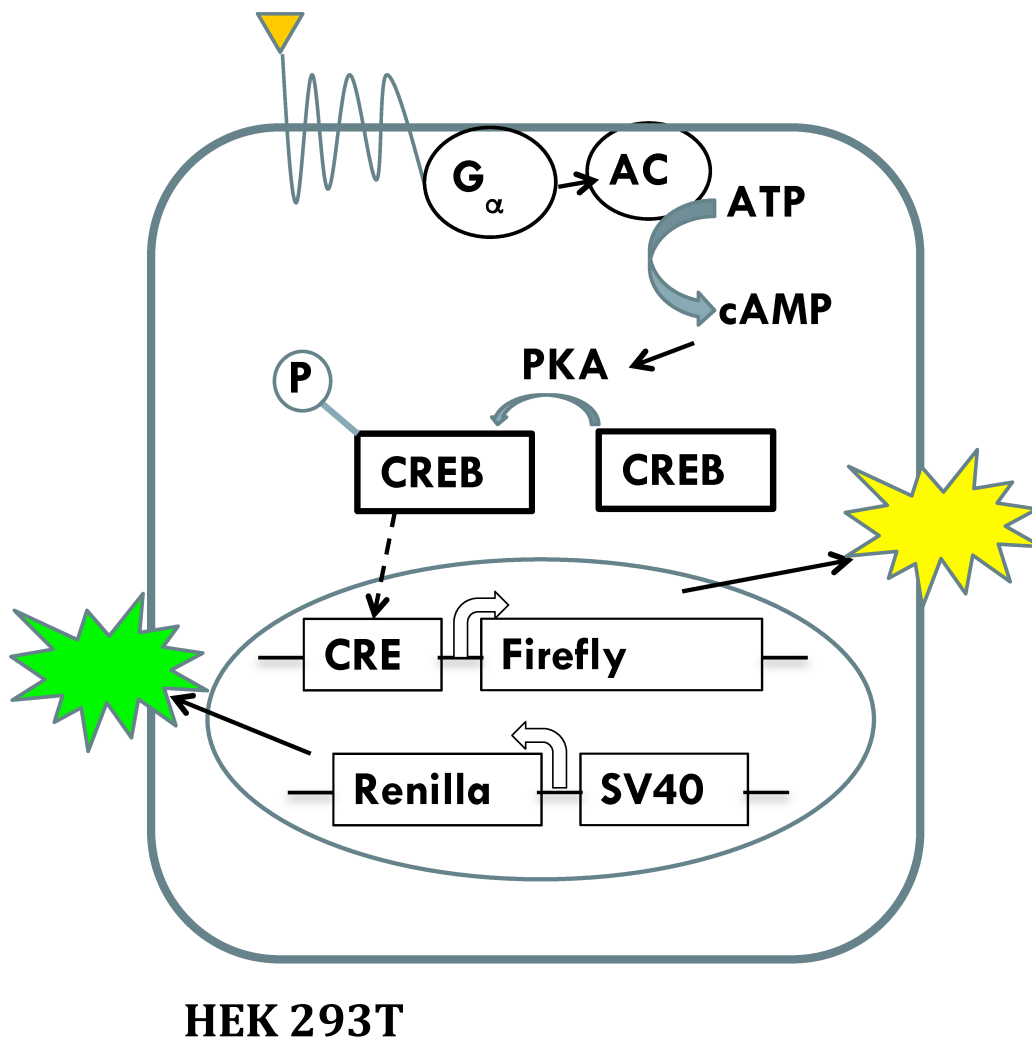


Figure 3.1 Dual luciferase assay to assess olfactory receptor / Gs coupled GPCR activation by ligands.

### ***B. vulgatus* culture**

*Bacillus vulgatus*, an isolated human colonic bacterial species, known to produce SCFAs was grown in brain heart infusion medium under 95% CO<sub>2</sub> for 48 hours.

### **Buffers**

#### ➤ **50X TAE (1 liter)**

242g Tris base (MW=121.14)

57.1ml Glacial Acetic Acid

100 mL of 0.5 M EDTA (pH 8.0)

pH 8.5

#### ➤ **10X Tris buffered saline (TBS, 1 liter)**

24.08g Tris base

80g NaCl

13ml 6M HCl

pH to 7.6 with HCl

#### ➤ **10X Phosphate buffered saline (PBS, 1 liter)**

25.6 g Na<sub>2</sub>HPO<sub>4</sub>·7H<sub>2</sub>O

80 g NaCl

2 g KCl

2 g  $\text{KH}_2\text{PO}_4$

➤ **10X SDS – PAGE running buffer**

35mM SDS

250mM Tris base

1.92M Glycine

➤ **10X transfer buffer**

250mM Tris base

1.92M Glycine

1X buffer made up with 20% Methanol.

➤ **Cell lysis buffer**

50mM Tris

150mM NaCl

5mM EDTA

1% NP-40

0.1% Triton X-100

Protease inhibitor cocktail

➤ **Laemmli buffer**

0.1% 2-Mercaptoethanol



0.0005% Bromophenol blue

10% Glycerol

2% SDS

63mM Tris-HCl, (pH 6.8)

### **3.4 Results**

#### **Gpr41 KO does not have detectable expression of $\beta$ – galactosidase**

Initial attempts to localize Gpr41 in tissue were made using commercially available antibodies, X-gal staining and  $\beta$  – galactosidase antibody staining in Gpr41 KO mice. Commercially available antibodies for Gpr41, shown to detect Gpr41, were found to be unreliable in our hands[108, 109]. Although sc-131166, raised against the amino acid 106 – 180 of human Gpr41 was reported to recognize Gpr41 in tissues[108], in our hands it gave similar staining in Gpr41<sup>-/-</sup> and Gpr41<sup>+/+</sup> mice. On the other hand, sc-98332[109], raised against a cytoplasmic epitope of human Gpr41, failed to recognize overexpressed Gpr41 in HEK293T cells. Gpr41 KO mice have LacZ inserted into the coding region of Gpr41[10]. X-gal staining was not detected in tissues from Gpr41 KO. Staining with  $\beta$  – galactosidase antibody also did not detect expression of lacZ specific to Gpr41 KO tissues (Figure 3.2). Interestingly, Gpr41 doesn't have a defined promoter, the expression of Gpr41 is driven by the promoter of Gpr40, which is the adjacent gene in the chromosome, via an internal ribosome entry site (IRES)[40, 42]. This explains the absence of

X-gal staining and  $\beta$  – galactosidase antibody staining in Gpr41 KO tissues. Hence Gpr41 was localized by RT-PCR.

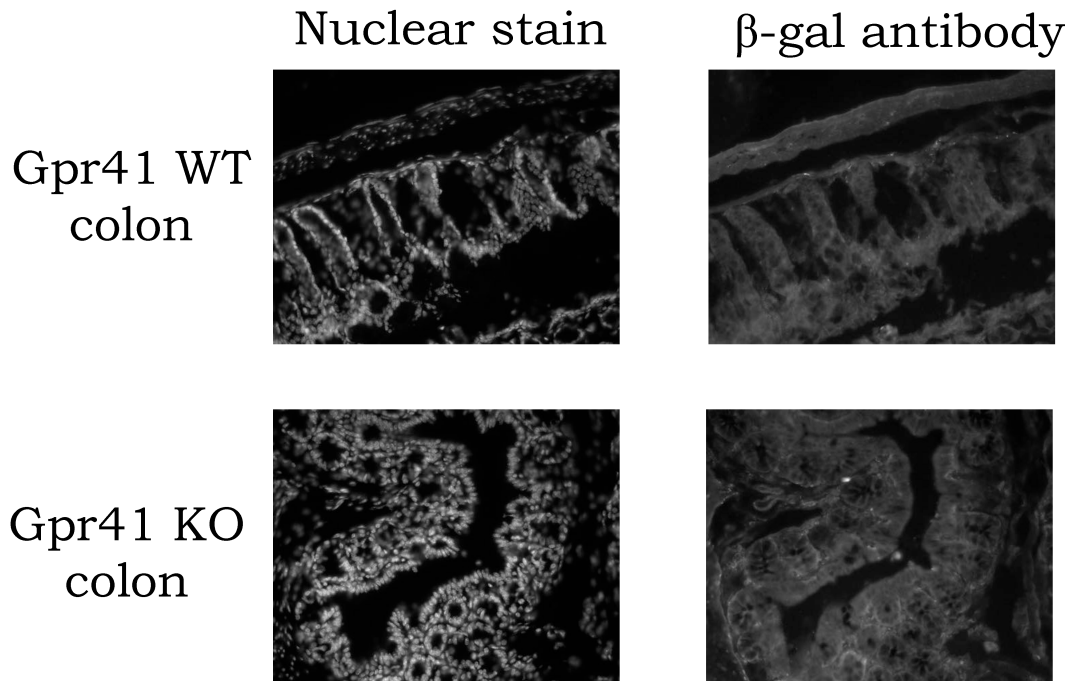


Figure 3.2:  $\beta$  – gal stain is not observed in Gpr41 KO tissues, indicating that insertion of LacZ gene into the coding region of Gpr41 may have disrupted Gpr41 IRES.

### **Gpr41 is expressed in the vascular endothelium**

Blood vessels primarily comprise of two cell types – outer vascular smooth muscle cells and one inner endothelial cell layer. Therefore, to determine whether Gpr41 also localizes to smooth muscle cells or to the endothelium, Gpr41 expression was assayed by RT-PCR in intact blood vessels versus blood vessels from which the endothelium had been

denuded. Gpr41, like eNOS (endothelial Nitric Oxide Synthase, an endothelial marker), is detected in intact blood vessels but not in blood vessels from which the endothelium has been mechanically denuded (Figure 3.3). Therefore, Gpr41 localizes to endothelial cells (EC).  $\beta$ -actin (housekeeping gene) is robustly detected in all samples. Bands were sequenced to confirm and mock RT controls (no reverse transcriptase) were negative.

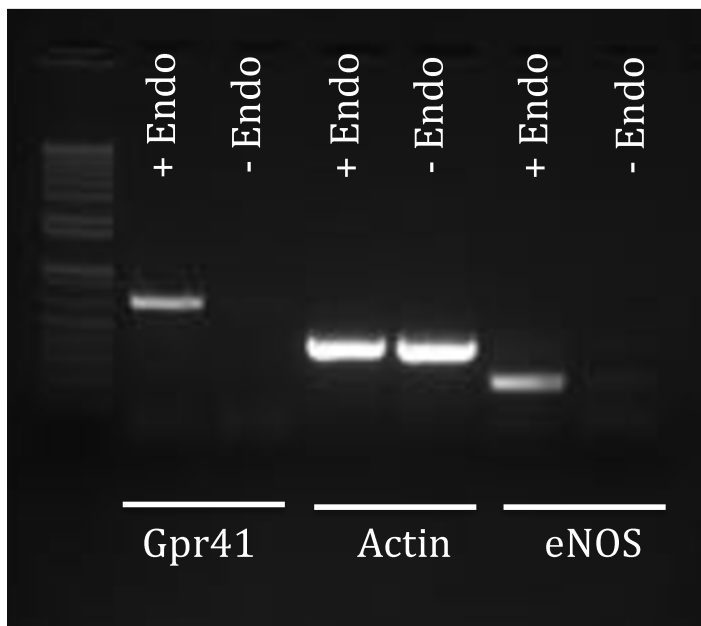


Figure 3.3: Gpr41 is expressed in the endothelium (by RT-PCR). Gpr41 is detected in intact aorta (vascular smooth muscle cells + endothelium, lane 1), but not in denuded vessels (vascular smooth muscle cells only, lane 2). Similarly eNOS (endothelial nitric oxide synthase), an endothelial marker, is detected in intact vessels (lane 5, +Endo) but not in vessels lacking endothelium (lane 6, -Endo). B-actin, as a control, is detected in both +endo and -endo vessels (lane 3,4).

### Characterization and validation of Gpr41 antibody

An antibody generated against the amino acids 296 – 319 in the C – terminal end of rat Gpr41 was recently obtained from Izumi Kaji and colleagues at UCLA[110]. 27 out of the 28 amino acids used to generate the antibody are conserved in murine Gpr41 (Figure 3.2) Preliminary control experiments showed that the antibody specifically detected overexpressed murine Gpr41 in HEK293T cells. HEK 293T cells transfected with flag – tagged Gpr41 was used for this experiment. Cells transfected with Olfr78 and OR51E2 (flag – tagged) were used as additional control to test the specificity of the antibody. Minimal cross – reaction with Olfr78 and OR51E2 was observed upon staining with Gpr41 antibody, while cells transfected with mGpr41 exhibited robust staining, supporting the reliability and specificity of the antibody (Figure 3.4).

rat	PWTQEVSLKLVKNGEEPSKECPS
mouse	PWTQQVSLKLVKNGEEPSKECPS
	*****:*****

Figure 3.4 Sequence alignment of epitope from human and mouse.

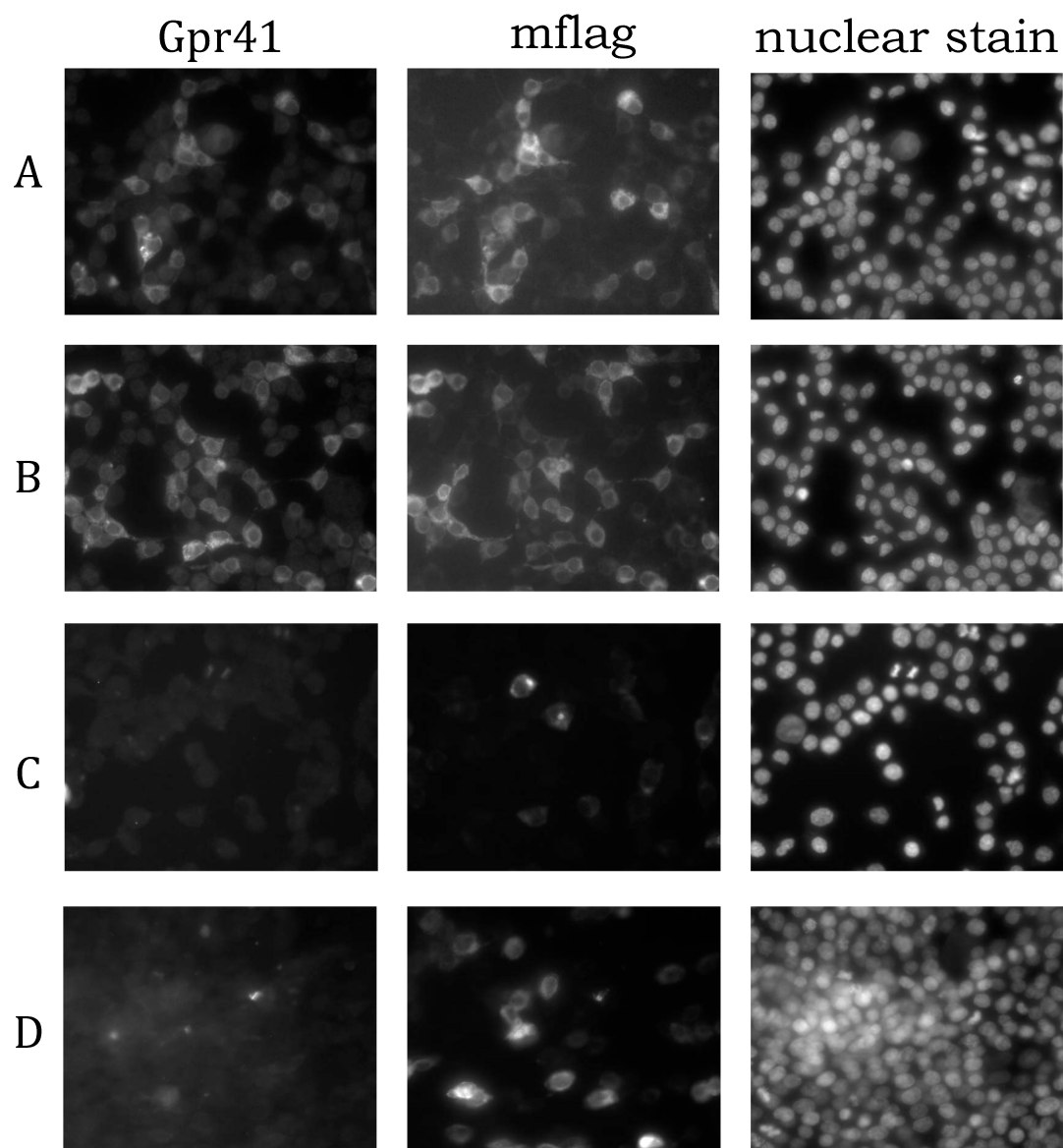


Figure 3.5: Gpr41 antibody consistently detects over-expressed Gpr41 in HEK293T cells. A, B: HEK 293T cells expressing murine Gpr41, stained with Gpr41 antibody, flag antibody and nuclear stain (left to right). C: Olfr78, D: OR51E2 expressing cells stained with Gpr41 antibody, flag antibody and nuclear stain (left to right).

In addition to being able to detect murine Gpr41 by immunohistochemistry, the antibody detected Gpr41 specifically in a western blot. Gpr41 from transfected HEK 293T cells is detected as a monomer (37kDa) and a possible dimer (75kDa) in an SDS-PAGE western blot (Figure 3.6).

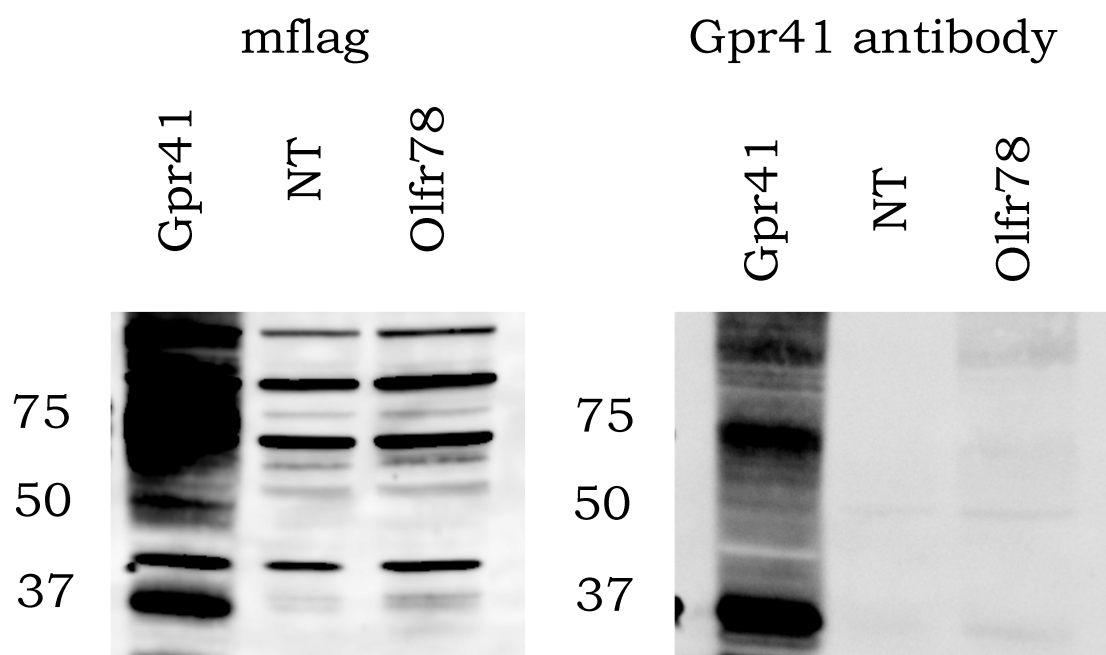


Figure 3.6: Murine Gpr41 is detected as a monomeric 37kDa band and a dimeric 75kDa band in a western blot. The blots shown used HEK 293T cell lysates transfected with Gpr41, Olfr78 and a non-transfected control (NT). Both Gpr41 and Olfr78 and flag – tagged and a flag blot of the lysates was used as positive control. The blot on the right used Gpr41 antibody for detection and a robust specific band is seen at 37kDa and 75kDa only in the lane with Gpr41 – transfected cell lysate.

### Detection of Gpr41 in endothelial cells

Following characterization and validation of the Gpr41 antibody for immunohistochemistry and western blot, attempts were made to confirm expression of Gpr41 at the protein level in aortic endothelial cells. Primary aortic endothelial cells were isolated from Gpr41 WT mice and stained with the Gpr41 antibody. Gpr41 (red) is detected in most of the cells in the field of view (nuclear stain in blue), confirming the expression of Gpr41 in the vascular endothelium (Figure 3.7). Staining observed with the antibody was competed off by the peptide when cells were stained with antibody preincubated with excess peptide.

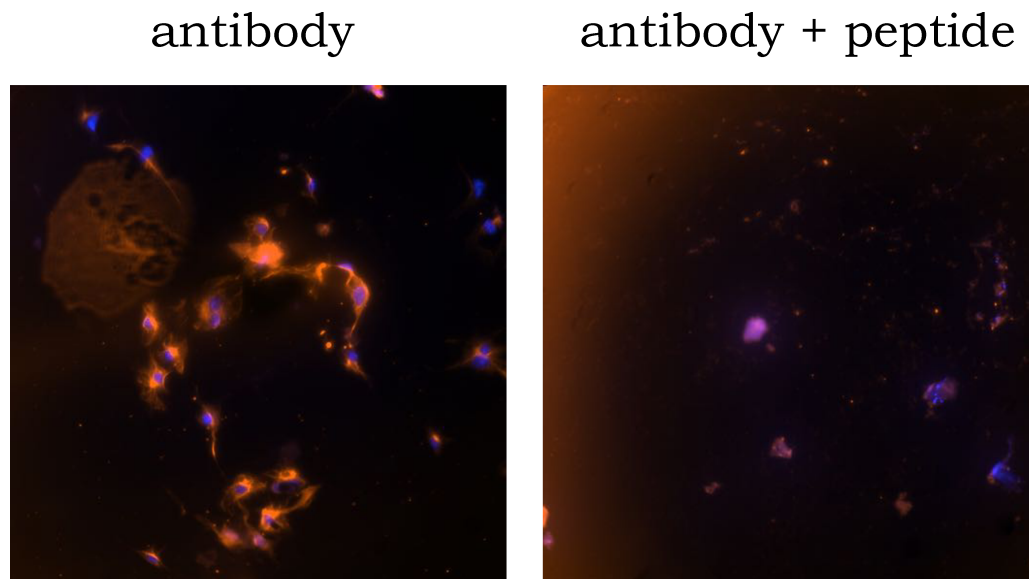


Figure 3.7: Gpr41 is detected in primary murine aortic endothelial cells. Gpr41 (red) staining is observed in most of the cells in the field of view (nuclear stain in blue).

The expression of Gpr41 was also confirmed in intact aorta from Gpr41 WT mice by western blot. A 37kDa monomeric band and a 75kDa (possible dimer) are detected by western blotting of aorta isolated from Gpr41 WT mice (Figure 3.8).

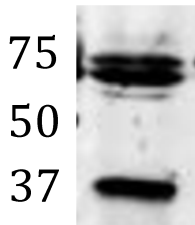


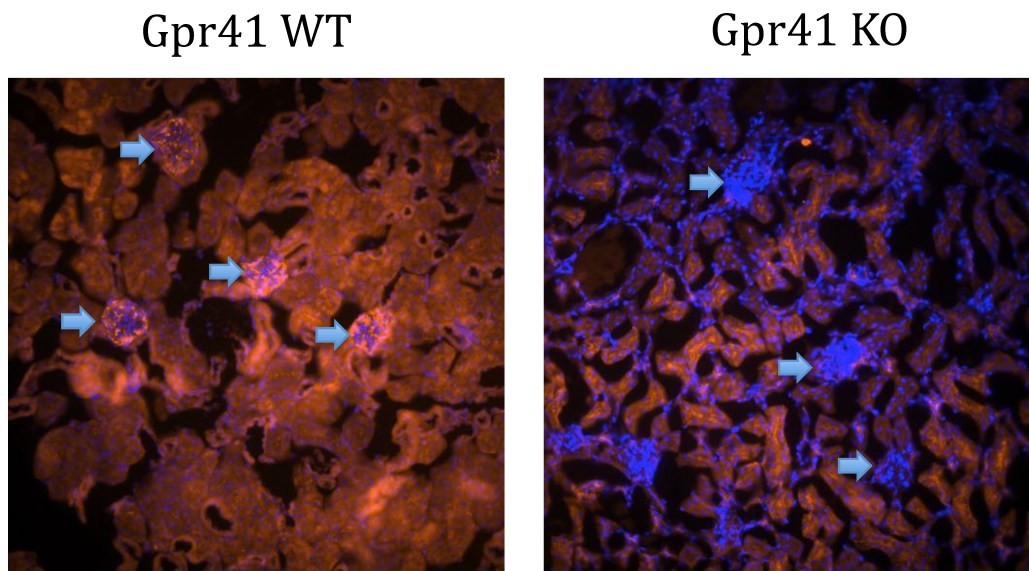
Figure 3.8: Gpr41 is detected by western blot in aorta from Gpr41 WT mouse.

### **Immunohistological staining of kidney sections from Gpr41 KO and WT mice**

Immunohistochemical staining of heart and kidney sections from Gpr41 KO and WT mice was performed to further validate the specificity of the antibody and to identify staining patterns unique to the Gpr41 WT mouse. Interestingly, in the kidney it was observed that glomeruli from Gpr41 WT sections were stained while there was no staining observed in the glomeruli from Gpr41 KO sections, although there seemed to be a non-specific apical tubular stain in the Gpr41 KO sections that was not observed in the Gpr41 WT sections (Figure 3.8).



A



B

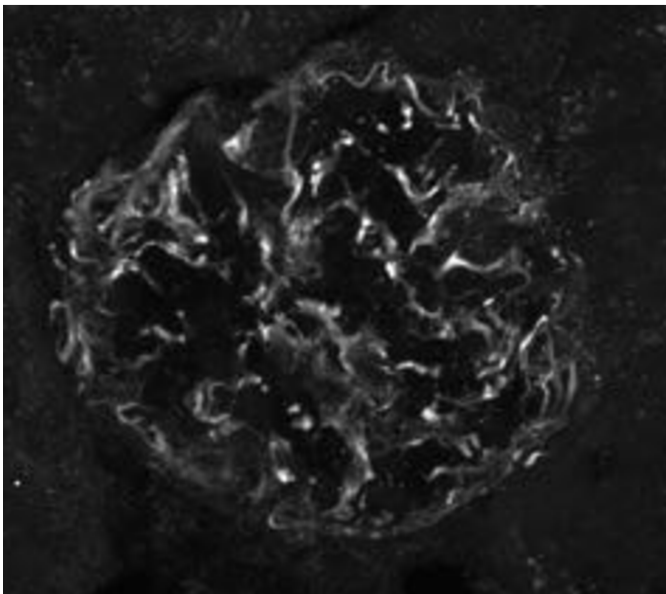


Figure 3.9: A: Immunohistochemical stain of kidney sections from Gpr41 WT and Gpr41 KO mice. Representative images are shown from stained sections with a pseudocolor overlay image of Gpr41 (red) and nuclear stain (blue) showing glomerular staining in the Gpr41 WT and absence of

stain in the glomeruli of Gpr41 KO sections. Arrows point to the glomeruli in the sections shown. B: Confocal image of Gpr41 WT glomerulus showing antibody staining.

### Is $\beta$ -hydroxybutyrate a ligand for Gpr41?

There has been some conflict in the literature regarding Gpr41 about  $\beta$ -hydroxybutyrate, a ketone body being an agonist or an antagonist[43, 111]. Several groups present evidence for  $\beta$ -hydroxybutyrate being an agonist and some other groups have evidence for the converse. Gpr41, being a Gi coupled receptor was screened with  $\beta$ -hydroxybutyrate in the modified assay with 10  $\mu$ M Forskolin. We found that Gpr41 was activated by  $\beta$ -hydroxybutyrate (Figure 3.10), supporting the claims that  $\beta$ -hydroxybutyrate is a Gpr41 agonist.

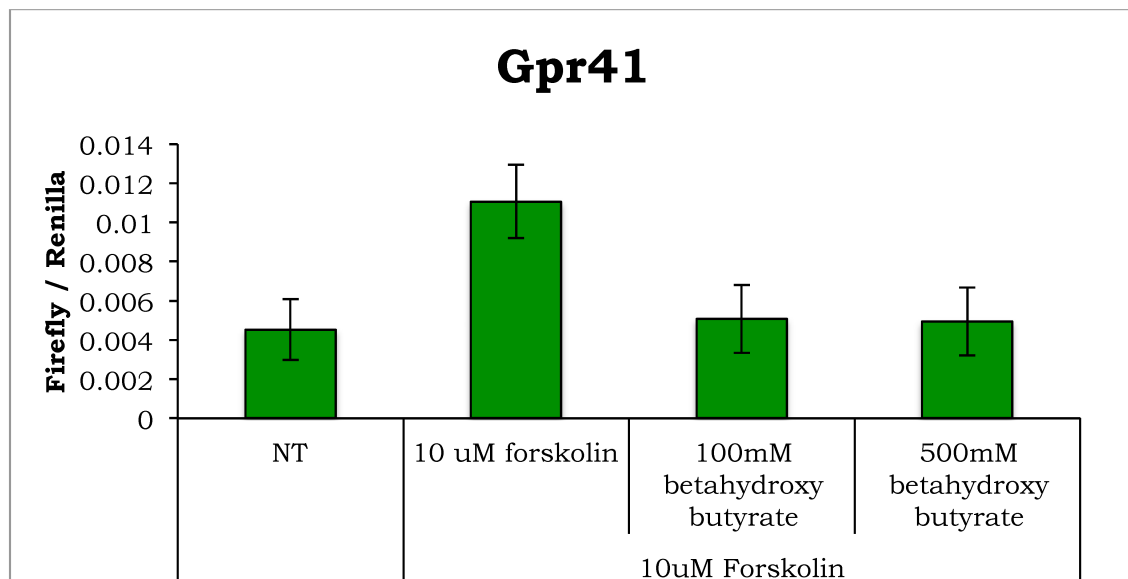


Figure 3.10 Beta hydroxybutyrate, a ketone body, is an agonist of Gpr41

### **Olf78 and OR51E2 – lactate**

A recent study reported that lactate was an agonist of Olf78 and Olf78 is expressed in the oxygen – sensitive glomus cells in the carotid body[106, 112]. The carotid body controls respiration rate and monitors blood oxygen levels[112]. In Olf78 KO mice, lactate – induced hyperventilation is not observed, raising the possibility that Olf78 KO could be activated by lactate[106]. Unlike the SCFAs, which are produced primarily as byproducts of microbial metabolism, lactate is generated in muscle under hypoxia and stress[23, 113]. If lactate were a strong agonist of Olf78, that would add another layer of complexity to the blood pressure regulation pathway involving Olf78 and Gpr41. D – Lactate and L – Lactate were tested in various concentrations with Olf78 and OR51E2 to see if the receptors were activated by either enantiomer of lactic acid. L – Lactate appeared to activate Olf78 at relatively higher doses compared to acetate and propionate and appeared to be, at best, a partial agonist (Figure 3.11).

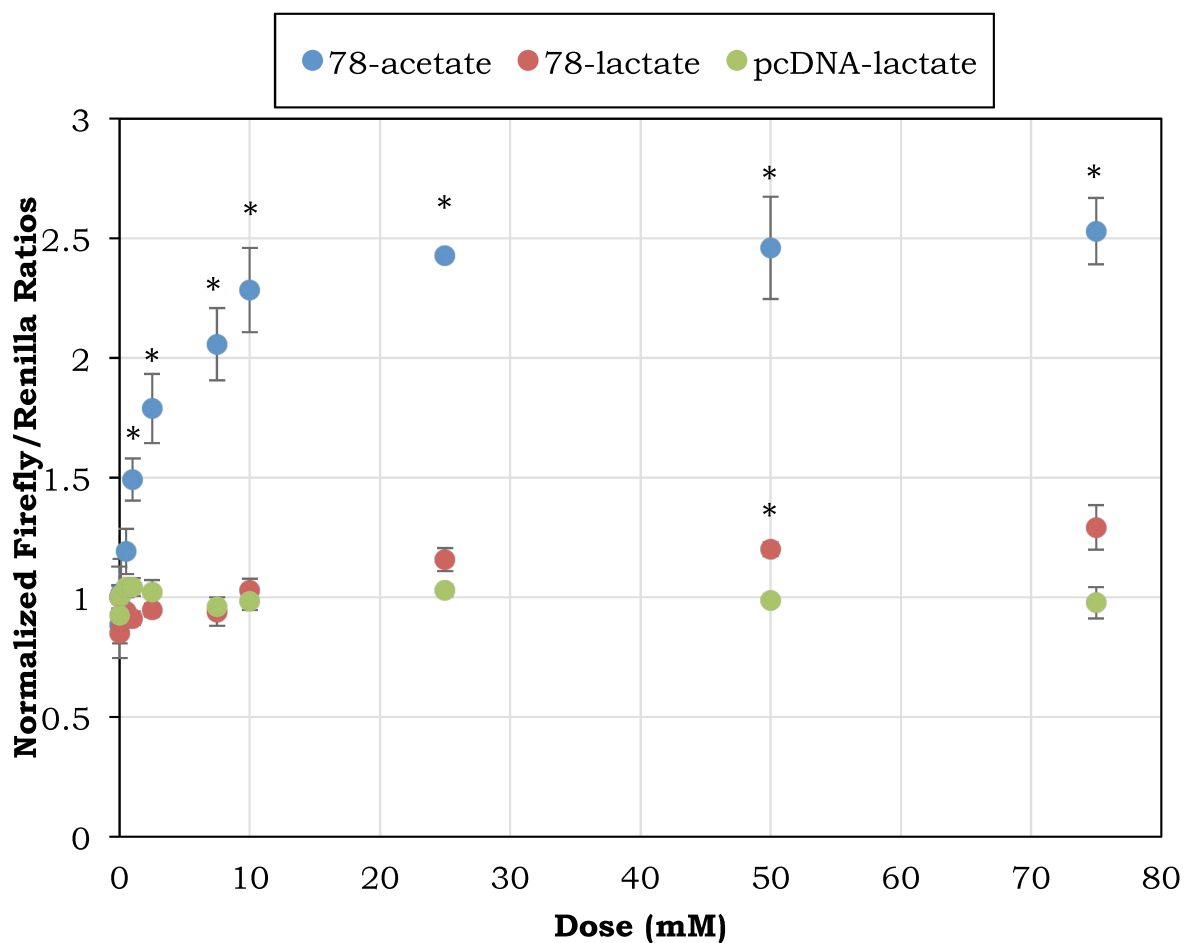


Figure 3.11 lactate is a weak agonist of Olfr78. Activation of Olfr78 by acetate (positive control) and lactate were tested along with a pcDNA (empty vector) control for lactate. \*  $p < 0.05$ , compared to pcDNA values.

EC50 values calculated from the assay shown matched accepted numbers for acetate and propionate, but L – Lactate had much higher EC50 (~21mM), opposed to the published value (4mM).

Table 3.2 EC50s of Olfr78 for SCFAs and lactate	
Ligands	EC50 (mM)
Sodium acetate	4.269
Sodium propionate	4.941
Sodium L - lactate	21.3949

OR51E2 was screened with similar doses of lactate to test the responses of the human ortholog. While Olfr78 had a weak response at high concentrations of lactate, OR51E2 did not exhibit any activation upon treatment with lactate in the luciferase assay (Figure 3.12).

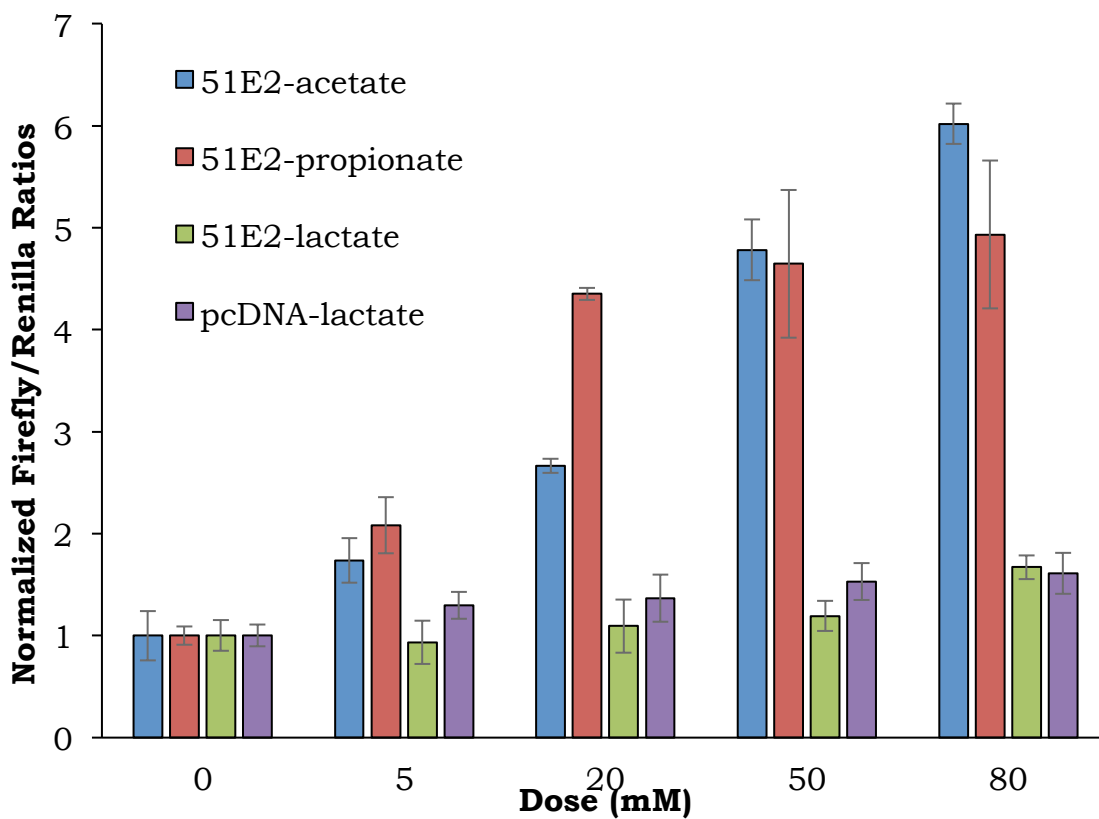
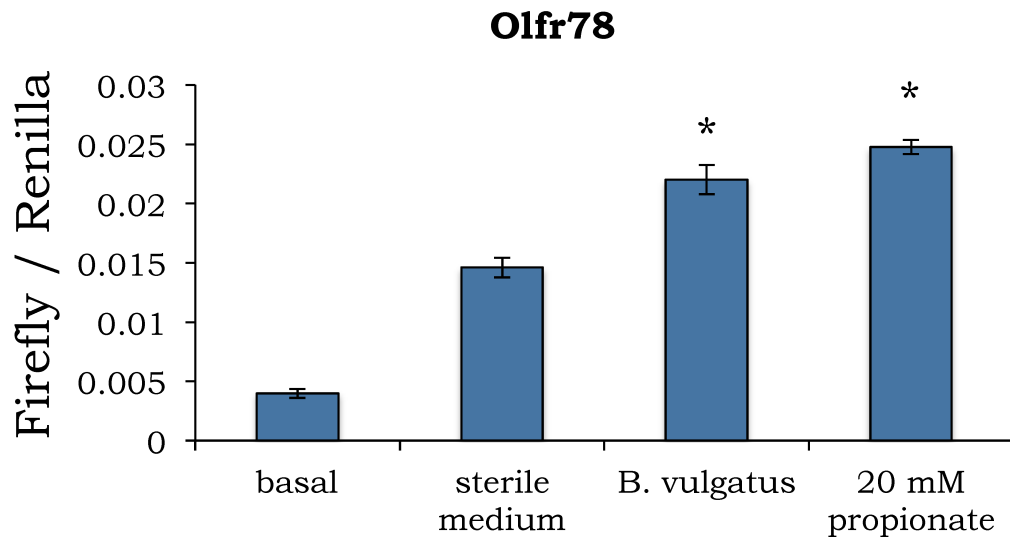


Figure 3.12 OR51E2 is not activated by lactate. Activation of OR51E2 is observed in a dose – dependent manner with acetate and propionate, while lactate doesn't show activation at any of the doses tested. \*  $p < 0.05$ , in comparison to non-treated (0mM) values.

### **Activation of Olfr78 and OR51E2 by “microbial” SCFAs**

Although Olfr78 and OR51E2 have been de-orphanized and shown to be SCFAs receptors, the SCFAs used for the de-orphanization assays were mostly purified sodium salts. SCFAs as made by the commensal microbiota is a complex mixture of different moieties mainly in the carboxylic acid form in contrast to the purified SCFAs which are in the ionized salt form. In order to derive SCFAs produced as a byproduct of microbial metabolism, filtered culture supernatant from an isolated species of human colonic bacteria, *Bacillus vulgatus* was obtained. The culture supernatant was used to screen Olfr78 and OR51E2 in a luciferase assay to monitor activation of the receptors by “microbial” SCFAs. *Bacillus vulgatus* is known to produce large quantities of SCFAs by breaking down dietary polysaccharides. Isolated *Bacillus vulgatus* is grown in brain heart infusion medium, background activation by the medium and by the culture supernatant were compared to assess activation of the receptors by microbial SCFAs. Both Olfr78 and OR51E2 (Figure 3.13) are activated by culture supernatant from *Bacillus vulgatus*, indicating that they are activated by microbiota –derived SCFAs. Given

previous reports that purified SCFAs activate Gpr41 and Olfr78, and our observation that microbial SCFAs activate Olfr78 and OR51E2, while lactate weakly activates Olfr78 and doesn't activate OR51E2 at all, it is possible that the function of being SCFA receptor is conserved through evolution in Olfr78 and OR51E2. Detection of lactate by Olfr78 could be an allosteric effect observed in the mouse homolog of the receptor.



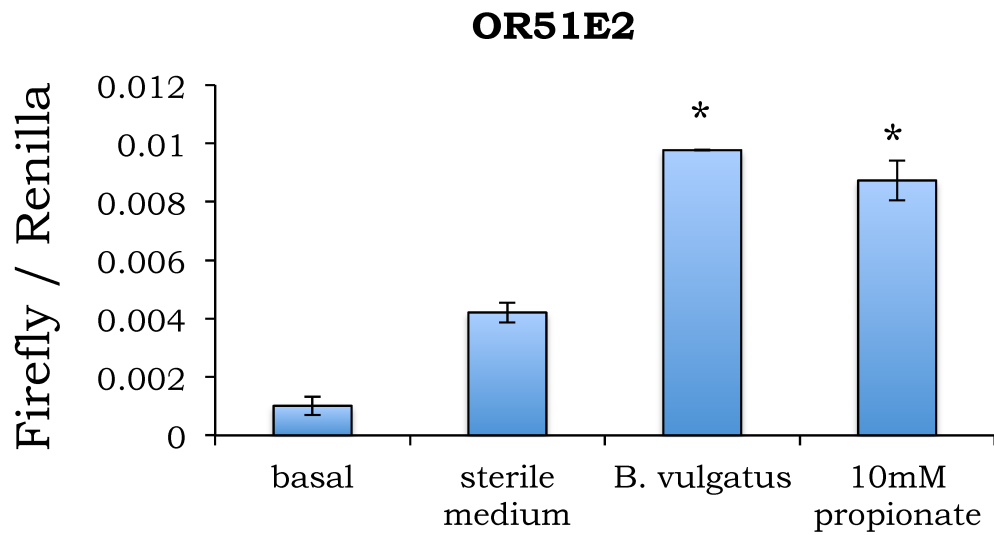


Figure 3.13 Olfr78 and OR51E2 are activated by “microbial” SCFAs derived from *B. vulgatus*, an isolated human colonic bacterial strain. Basal – background, sterile medium – microbial culture medium without any microbial inoculation, *B. vulgatus* – filtered culture medium used to grow a 48 – hour culture of *B. vulgatus*, prop 20mM – 20mM sodium propionate, a positive control. \*  $p < 0.05$ , in comparison to basal and sterile medium controls



### **3.5 Discussion**

SCFA metabolites act via GPCRs – Gpr41 and Olfr78 to modulate blood pressure. Gpr41 and Olfr78 are both expressed in major blood vessels and Olfr78 is expressed in the vascular smooth muscle cells and renal afferent artery. Based on acute dose responses, it was inferred that Olfr78 mediates a hypertensive response upon activation, while Gpr41 mediates a hypotensive response. The aim of the experiments presented in this section was to understand the cellular localization of Gpr41 in blood vessels, kidney and other tissues and to characterize ligands for Gpr41 and Olfr78. The major findings reported in this section are that Gpr41 is expressed in the vascular endothelium (by RT-PCR and antibody staining of primary mouse aortic endothelial cells) and renal glomeruli (tissue immunohistochemistry).

Gpr41 and Olfr78 are SCFA receptors that get activated by a variety of SCFA moieties. In addition to SCFAs, there are several reports of small molecules that act as agonists for Olfr78 (lactate, for instance) and Gpr41 ( $\beta$  – hydroxybutyrate). Since the role of these receptors in blood pressure regulation is our primary interest, it is crucial to identify the ligand range of these receptors and the sources of these ligands in order to know the source and mode of small molecules that regulate BP.

### **Gpr41 in the endothelium**

Localization of murine Gpr41 to the vascular endothelium is consistent with previous reports of human Gpr41 and Gpr42 expression in the endothelium of adipose tissue vasculature. Initially, it was thought that Gpr41 was expressed in adipose tissue since it was detected by RT-PCR in adipose tissue and played a role in regulating adiposity. Subsequently, Brown et.al. showed that hGpr41 and Gpr42 localized to the vasculature in adipose tissue, the vascular endothelium in particular.

The endothelial cell layer of blood vessels senses blood pressure and rate of flow by monitoring shear stress through their cilia. Being the inner layer of cells in a blood vessel, substances in circulation can affect endothelial cell function either directly by diffusing into the cell or by activating cell surface receptors in the cell. GPCRs in endothelial cells have been shown to detect shear stress and respond to reactive oxygen species in the cell. Expression of a SCFA receptor in endothelial cells is very interesting and is a novel finding regarding GPCR expression in the endothelium and their physiological role.

Endothelial cells secrete signaling molecules that act on the vascular smooth muscle cell layer to modulate their stiffness, thereby modulating vascular resistance and blood pressure. There are several well-studied mechanisms by which endothelial cells mediate vasodilation and

vasoconstriction. eNOS based nitric oxide signaling, prostacyclins and endothelial-derived hyperpolarizing factor mediate vasodilation, while endothelin and mediate vasoconstriction. Since Gpr41 mediates a hypotensive response upon activation, the localization of Gpr41 in the endothelium narrows down the potential signaling mechanisms to a handful of pathways by which the endothelium mediates vasodilation and subsequent decrease in BP. Furthermore, if the pathway of Gpr41 signaling is identified and validated, Gpr41 agonists can be used to target key downstream components to decrease BP in hypertension.

### **Localization of Gpr41 in renal glomeruli**

It was previously shown that Gpr41 is expressed in the vasculature and kidney, but localization to a precise cell type / structure in the kidney has not been established until now. Glomeruli are complex structures comprised of podocytes, epithelial cells and blood vessels. Localization of Gpr41 in the glomeruli could mean that Gpr41 potentially plays a role in renal function and regulation of glomerular filtration rate. It is important to identify the cell type of Gpr41 expression in the glomerulus to infer more about its function in the kidney. Analysis of gene expression in human studies have showed Gpr41 to be in top 10% under expressed in glomerulosclerosis[114], indicating that Gpr41 could play a very important role in regulating renal function.

Olf78, also a SCFA receptor that mediates a hypertensive response to SCFAs is expressed in the renal afferent artery. Expression of Gpr41 in the glomerulus puts Olf78 and Gpr41 in adjacent cell types in the kidney. Given that they have opposing effects on blood pressure, it is crucial to understand their function in the kidney and determine if their renal effects oppose or augment each other. Olf78 stimulates renin secretion from the renal afferent artery upon activation; it would be interesting to compare the renal effect of Gpr41 to plasma renin concentration to determine if Olf78 and Gpr41 exhibit crosstalk in the kidney.

### **$\beta$ – hydroxybutyrate and Gpr41**

$\beta$  – hydroxybutyrate is a ketone body produced under starvation conditions. In contrast to SCFAs, that are primarily produced by commensal microbiota,  $\beta$  – hydroxybutyrate is endogenously produced. Activation of Gpr41 by  $\beta$  – hydroxybutyrate is of great interest because that would identify an innate mechanism by which hypotension is induced in periods of prolonged physical activity or during starvation, to conserve energy. Given that there were conflicting reports in literature as to the nature of  $\beta$  – hydroxybutyrate's effect on Gpr41, it was important to assess its effect in the assay setup in house. In our hands,  $\beta$  – hydroxybutyrate works as a Gpr41 agonist. This indicates that Gpr41 may be activated by pathways other than microbe mediated to decrease

blood pressure. Furthermore, Gpr41 is also expressed in the sympathetic nervous system. Ketone bodies provide energy source for the brain during prolonged starvation. There could be novel mechanisms by which Gpr41 plays a role in energy metabolism via  $\beta$  – hydroxybutyrate.

### **Lactate and Olfr78**

It was recently shown that lactate activated Olfr78 expressed in the carotid body[106, 112]. Like  $\beta$  – hydroxybutyrate, lactate is also produced during starvation, mostly in muscle during exercise. According to the study, Olfr78 had an EC50 of 4mM for lactate. Since Olfr78 elicits a hypertensive response upon activation, it was important to test the activation of Olfr78 by lactate in our luciferase assay setup to verify its ability to activate the receptor. Upon extensive testing of lactate – mediated activation of Olfr78, it appeared that lactate is a weak, partial agonist of Olfr78 with ~ 20mM EC50 and the human ortholog of Olfr78, OR51E2 is not activated by lactate. This means that detection of lactate could be an allosteric effect that the murine ortholog exhibits, whereas that ability is not seen in the human ortholog. In contrast, SCFAs elicit a response from both Olfr78 and OR51E2, indicating that the ability to detect SCFAs has been conserved through evolution, reinforcing the role of Olfr78 as a “SCFA” receptor.

### **“Microbial” SCFAs and Olfr78**

De-orphanization assays to identify ligands for orphan receptors usually utilize purified chemical ligands that are a single isolated species. On the other hand, when SCFAs are made by the microbiota, it's a complex mixture of formate, acetate, propionate, butyrate, lactate and a few other minor SCFA species in the native state, not ionized in the salt forms. Mixtures of ligands and purity of ligands greatly influence the activation seen in vitro. Analysis of Olfr78 and OR51E2 activation with culture supernatants from isolated colonic bacterial strains known to produce SCFAs showed that microbially produced SCFAs could in fact activate the receptors. This can be very useful in further experiments looking at the effect of diet on increasing plasma SCFAs in order to activate Gpr41 and its downstream signaling effects.

## **4 Role of Gpr41 in blood pressure regulation**

### **4.1 Abstract**

Plasma electrolytes play a very important role in blood pressure regulation and renal function. Here, ten major plasma electrolytes and parameters were assessed in male and female Gpr41 KO and WT mice. There were no significant differences in plasma electrolytes between the genotypes / sexes. Plasma renin concentration (PRC) was assessed in Gpr41 KO and WT mice of 3 months and 6 months of age. There were no differences in the PRC of 3-month-old mice, while older 6-month-old KO mice tended toward a slight increase in PRC. Furthermore, renal morphology of Gpr41 KO and WT was studied and it appears that Gpr41 KO mice trend towards having smaller glomeruli.

Previously, acute bolus of SCFA (sodium propionate) was shown to mediate a quick and sharp decrease in BP with an equally quick recovery. Based on acute dose responses, it was hypothesized that Olfr78 mediates a hypertensive response to SCFAs and Gpr41 mediates a hypotensive response. Since Gpr41 mediates a decrease in BP, we hypothesized that Gpr41 knockout (KO) mice would be hypertensive at baseline. Concordant with our hypothesis, we found that Gpr41 KO (n=8) exhibit isolated systolic hypertension and elevated pulse pressures compared to wild-type (WT, n=6) mice; diastolic BP and heart rate was

not different between genotypes. In agreement with a phenotype of systolic hypertension, KO mice also exhibited elevated pulse wave velocity in vivo, but surprisingly, no increase in ex-vivo aorta stiffness (measured by tensile testing experiments).

Hypothesis: (i) Gpr41 KO mice would exhibit hypertension.

(ii) Chronic SCFA administration would elevate systolic BP in Gpr41 KO

(iii) Gpr41 KO may not exhibit salt sensitive hypertension

Acute sodium propionate doses decrease BP via Gpr41, while Olfr78 increases BP via a renin-dependent pathway. Sodium propionate was chronically administered to Gpr41 KO and WT mice to monitor its effect on BP and to explore the potential of elevation of plasma SCFAs by dietary intervention and its effect on BP. Chronic administration of 200mM sodium propionate (a Gpr41 ligand) and 200mM NaCl (control) did not significantly affect BP in Gpr41 WT or KO, although systolic pressure trended toward an increase for both treatments and genotypes. We hypothesize that the hypertensive effect of propionate in the KO is mediated by another SCFA receptor, Olfactory receptor 78, which increases in BP upon activation.

To determine the salt-sensitivity of hypertension observed, 3-month-old Gpr41 KO and WT mice were switched to a control diet with 0.49% NaCl



and implanted with telemetry devices. Following a baseline BP measurement, the mice were switched to a high salt diet (4% NaCl) for a week and then switched to a low salt diet (0.04% NaCl) for 5 days. Analysis of data obtained from this experiment shows that hypertension in Gpr41 KO mice is not salt sensitive, there is no increase of BP observed on the high salt diet. However a decrease in BP when moved from high salt diet to low salt diet is blunted in Gpr41 KO mice.

## **4.2 Introduction**

Hypertension is widely prevalent in today's adult population with ~30% adults having higher than normal BP values. Cardiac output and systemic vascular resistance regulate mean arterial pressure. The control of BP is complex and involves an intricate balance between the neurohormonal components that regulate vascular resistance, inotropy and salt balance. In addition to physiological factors, diet and lifestyle play major roles in the development of hypertension in individuals. Chronic hypertension, if untreated, leads to the development and progression of cardiovascular disease and associated complications. Despite the current pharmacological intervention methods for hypertension, some individuals develop resistant hypertension that mounts a greater challenge. BP regulation mediated by microbial SCFA metabolites offers an exciting novel pathway that could potentially be targeted by therapeutics.

Previous work in the Pluznick lab showed that Gpr41 is involved in blood pressure regulation by microbial SCFAs, and that acute activation of Gpr41 lowers blood pressure[5, 26]. Therefore, it was hypothesized that Gpr41 KO mice would be hypertensive in comparison to Gpr41 WT mice. To test this hypothesis, baseline blood pressure was measured in 3-month-old male Gpr41 WT and KO littermates using a telemetry – based continuous blood pressure monitoring system from DSI.

Since Gpr41 is expressed in the kidney and vasculature and Gpr41 KO mice exhibit a BP phenotype, it is important to analyze plasma electrolytes to assess renal function. The iSTAT method offers an easy way of estimating various plasma solutes and ions. Any obvious differences in plasma electrolytes between genotypes could indicate toward a defect in ion handling by the kidney or electrolyte homeostasis.

Olf78 works via an increase in plasma renin concentration (PRC) to increase blood pressure. Since chronic propionate administration did not produce a stable increase in BP in Gpr41 KO mice, PRC was measured in Gpr41 KO and WT mice to assess if there were any differences due to systolic hypertension. Finally, morphology of kidney sections from Gpr41 KO and WT mice were observed to identify any gross changes in histology in the KO mice, since Gpr41 was identified in the glomerulus.

Blood pressure can be measured by a couple of methods in animals, a tail cuff measurement for mice that is easier, but relatively inaccurate and continuous telemetry that involves implantation of pressure transmitters in the mice. Telemetry for blood pressure measurement is carried out with a pressure sensor and transmitter with a 5.0 cm catheter that is threaded in through the carotid artery to have the tip of the device situated in the free – flowing blood in the aortic arch (Figure 5.1). PA-C10 devices were used for telemetry and they measure

- (i) systolic pressure
- (ii) diastolic pressure
- (iii) mean arterial pressure
- (iv) pulse pressure
- (v) heart rate
- (vi) activity

An example tracing of blood pressure from an animal over a 3 – day period is shown in Figure 5.2 with the light cycle and dark cycle indicated in open rectangles and closed rectangles, respectively.

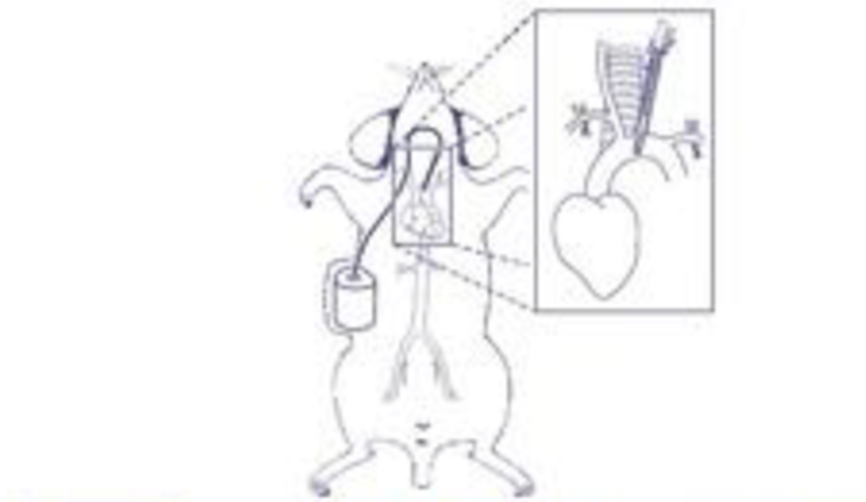


Figure 4.1 Placement of telemetry catheter in the carotid artery for continuous blood pressure monitoring.

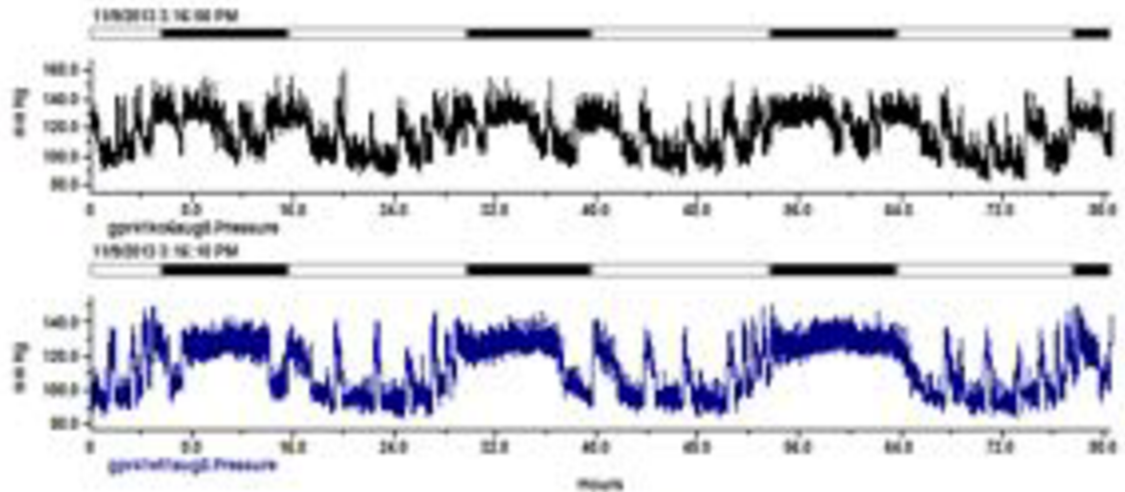


Figure 4.2 Representative blood pressure traces from telemetry system, dark boxes indicate night recordings (dark cycle), open boxes are the daytime recordings (light cycle).

To assess a hypertensive phenotype, blood vessel stiffness is analyzed. Blood vessels are comprised of an extracellular matrix rich in elastin, which bears aortic stress and enables expansion of the vessel. During a systole in the cardiac cycle, the aorta is subject to acute stress to cause expansion of the vessel to accommodate the stroke volume. The basic principles of material stress and fracture apply to the elastin fibers in a blood vessel and over time, in the aorta acute expansion results in the damage of elastin fibers[115]. Fracture of the elastin fibers results stretching of the aortic wall, resulting in vessel dilation. Consequently, stress is transferred to the less elastic collagen in the aortic wall causing a further increase in pressure. Increased stiffness of the aortic wall causes a corresponding increase in aortic pulse wave velocity[115, 116].

This increase in PWV causes the reflected pressure wave to return earlier to the heart and increase pressure in late systole.

It was previously demonstrated that acute intravenous delivery of SCFAs caused a rapid hypotensive response in wild-type mice, but a hypertensive response in Gpr41 KO mice[5, 26]. The nature of this blood pressure response observed to acute SCFA infusion was rapid and short-lived. SCFAs also trigger renin secretion from the juxtaglomerular apparatus, via Olfr78, which in-turn increases blood pressure[26]. The time course of this renin response is much slower and gradual compared to the blood pressure response. Olfr78 KO mice have lower renin secretion from the juxtaglomerular apparatus and exhibit a decrease of blood pressure in response to acute SCFA administration[26]. Gpr41, on the other hand decreases blood pressure and it was established that Gpr41 KO mice have higher systolic pressure. Gpr41 KO and WT mice were subjected to chronic SCFA delivery via drinking water to understand the mechanism of chronic SCFA signaling and to see if the acute effects observed would replicate in the chronic treatment scenario. The objective of the experiments presented in this section is to test the hypothesis that chronic SCFA treatment will similarly alter BP in wild type mice and Gpr41 KO mice.

A combination of dietary and genetic factors contribute to the development and manifestation of hypertension in an individual. In humans, dietary salt intake is an important causative factor that leads to hypertension, although the salt susceptibility of blood pressure varies in different individuals. Salt-sensitive hypertension develops in individuals, whose kidneys have an impaired ability to handle excess salt, leading to sodium retention, which increases BP by increasing cardiac output. Salt sensitivity of an individual can lead to the development of primary essential hypertension or can exacerbate an existing hypertensive condition, resulting in a three-fold increase of the occurrence of cardiovascular complications[117-119].

Since Gpr41 KO mice present with isolated systolic hypertension at baseline and Gpr41 localized to the glomeruli in kidney sections, it was important to assess the salt – sensitivity of the blood pressure phenotype. Exacerbation of the hypertension phenotype observed would indicate that sodium loading results in sodium retention and impairs the ability of kidneys to handle salt. Furthermore, if Gpr41 KO mice exhibited salt-sensitive hypertension, it forms a further link between microbial metabolism and salt consumption.

### **5.3 Materials and methods**

#### **Animal handling**

Mice were housed in accordance with institutional, state and national guidelines. All experimental protocols were approved by the Johns Hopkins University Institutional Animal Care and Use Committee (accredited by the AALAC). Gpr41 KO (a kind gift from Drs. Yanagisawa (UT Southwestern) and Gordon (Washington University)[10] were backcrossed onto C57BL/6 mice, and Gpr41 heterozygotes were then bred in-house to obtain Gpr41 KO and Gpr41 WT littermates. All animals were fed and watered ad-libitum.

#### **Blood chemistry and plasma electrolytes**

Blood chemistry of Gpr41 mice was analyzed using iSTAT Chem8+ cartridge with handheld iSTAT system 1 using samples taken from the superficial temporal vein.

#### **Plasma renin concentration**

Plasma renin concentration was measured using a modified angiotensin-I measurement kit (Peninsula labs S-1180). Prior to starting the assay, plasma was diluted 15 fold and incubated with excess porcine angiotensinogen (Sigma SCP0021) for 20 minutes at 37°C in a buffer containing 50mM sodium acetate (pH 6.5), 10mM AEBSF, 10mM EDTA



(pH 8.0), 1uM porcine angiotensinogen and 10mM 8-hydroxyquinoline. After incubation with angiotensinogen, the samples were analyzed according to the protocol provided with the kit. Plasma renin activity was assayed by competitive binding of angiotensin – 1 generated to its antibody.

### **Histology**

Kidneys were harvested from 3-month-old Gpr41 KO and WT mice and post-fixed in 10% buffered formalin. After fixation, the kidneys were set in paraffin blocks, section and stained with H&E to visualize histology.

### **Blood pressure measurement**

DSI TA11 PA-C10 devices were used to measure BP by radiotelemetry in Gpr41 KO and WT mice. 3-month-old male Gpr41 KO and WT mice were implanted with PA-C10 devices under 2% isoflurane anesthesia and allowed 7 days for recovery. BP was recorded continuously in the implanted mice after recovery. A 5-day recording period was used to assess baseline BP. Subsequently, mice were chronically treated with 200mM sodium propionate (Sigma P1880) in the drinking water for 7 days, followed by a return to regular water for 5 days, and then an additional 5 days with 200mM sodium chloride (equimolar sodium control, Fisher S641-212) in the drinking water. A separate cohort of age-

matched mice (no telemetry) on the same sequence of treatments was used to monitor body weights.

In order to assess the salt – sensitivity of blood pressure in Gpr41 KO and WT mice, they were subjected to 7 days of high salt diet (4% NaCl) followed by 5 days of low salt diet (0.04% NaCl). Blood pressure was continuously recorded during the experimental period. A separate cohort of age matched mice was used to monitor body weights and plasma electrolytes on the normal, high salt and low salt diets.

### **Pulse wave velocity**

Pulse wave velocity (PWV) was measured non-invasively in 3 month old and 6-month-old male Gpr41 KO and WT mice with a high frequency, high-resolution Doppler spectrum analyzer (Indus Instruments, Houston, TX). Under anesthesia with 1.5% isoflurane, mice were placed supine on a temperature-controlled platform. Core temperature was maintained at 37°C. Thoracic aortic outflow and abdominal aortic flow profiles were captured with two probes. The distance separating the probe locations was also measured. PWV was calculated by the thoracic – abdominal distance divided by the pulse transit time between flow pulses recorded at the thoracic and abdominal aortic sites. DSPW software (Indus Instruments) was used for data analysis[120].

### **Tensile testing of Gpr41 aorta**

Aortas from 6-month-old Gpr41 male mice were harvested and cut into 2-mm rings and mounted on the pins of an electromechanical puller (DMT560; Danish Myo Technology A/S, Aarhus, Denmark). After calibration and alignment, the pins were slowly moved apart using an electromotor at a rate of 50  $\mu\text{m}/\text{sec}$  to apply radial stress on the specimen until breakage. Force and displacement were continuously recorded. A 1-mm segment proximal to the ring was imaged at a 10x magnification. The inner and outer diameters of the vessel were measured at 4 locations using Image J software (National Institutes of Health [NIH], Bethesda, MD). Average inner and outer diameters were used to calculate sample thickness. Engineering stress ( $S$ ) was calculated by normalizing force ( $F$ ) to the initial area of the specimen;  $S = F/2tl$ ; where  $t$  = thickness and  $l$  = length of the sample. Engineering strain ( $\lambda$ ) was calculated as the ratio of displacement to initial diameter. The stress-strain relationship was represented by the equation  $S = \alpha e^{\beta\lambda}$  where  $\alpha$  and  $\beta$  are constants, determined by nonlinear regression for each sample[121]. A subset of aortas were decellularized for this measurement: for this, aortas from Gpr41 KO and WT mice were incubated in de-cellularization solution 1 (8 mM CHAPS, 1 M NaCl, and 25 mM EDTA in PBS) for 44 hours. Next, samples were incubated in de-cellularization solution 2 [1.8 mM sodium dodecyl sulfate (SDS), 1 M NaCl, 25 mM EDTA in PBS] for 44 hours. The de-cellularization solutions were changed every 22 hours with three 15-

min PBS washes. After incubation in de-cellularization solutions, aorta segments were washed and incubated in PBS for 2 days to remove residual detergents. All steps were conducted at room temperature under constant shaking. Finally, samples were incubated at 37°C for 1 day in endothelial cell media (ScienCell Research Labs) and washed thrice in PBS for 15-min each, to obtain decellularized specimen. These aortas were then analyzed (tensile testing) as described above.

### **Ex-vivo vascular relaxation experiments**

3-month-old male mice (Gpr41 WT and KO) were euthanized by CO<sub>2</sub> asphyxiation. Proximal segments of the tail artery were dissected rapidly and placed in cold Krebs-Ringer bicarbonate solution containing 118.3mM NaCl, 4.7mM KCl, 1.2mM MgSO<sub>4</sub>, 1.2mM KH<sub>2</sub>PO<sub>4</sub>, 2.5mM CaCl<sub>2</sub>, 25.0mM NaHCO<sub>3</sub>, and 11.1mM glucose (control solution). The tail arteries (either intact or with endothelium denuded) were cannulated at both ends with glass micropipettes, secured using 12-0 nylon monofilament suture, and placed in a microvascular chamber (Living Systems, Burlington, VT)[122, 123]. The arteries were maintained at a constant transmural pressure ( $P_{TM}$ ) of 60 mmHg in the absence of flow. The chamber was superfused with control solution, maintained at 37°C, pH 7.4, and gassed with 16% O<sub>2</sub>-5% CO<sub>2</sub>-balance N<sub>2</sub>. The chamber was placed on the stage of an inverted microscope (20X; Nikon TMS-F) connected to a video camera (CCTV camera; Panasonic). The vessel image

was projected on a video monitor, and the internal diameter was continuously determined by a video dimension analyzer (Living Systems Instrumentation) and was monitored using a BIOPAC (Santa Barbara, CA) data acquisition system[122, 123]. The tail vessels were allowed to equilibrate at  $P_{TM}$  of 60mmHg for 30 minutes. After equilibration, the vessels were constricted with phenylephrine (PE) and then treated with increasing doses of sodium propionate and sodium acetate in the superfusate and the internal diameter of the vessels were recorded over time. After propionate treatment, the reactivity of the vessels (and presence/absence of endothelium) was confirmed by acetylcholine.

SCFAs were delivered orally and blood pressure was continuously recorded over the treatment period. As shown in Figure 4.3, after an initial baseline measurement (5 days), mice were treated with 200mM sodium propionate in the drinking water for 7 days, followed by 5 days recovery, 5 days treatment with 200mM NaCl (control) in the drinking water, and then a final 5-day recovery.

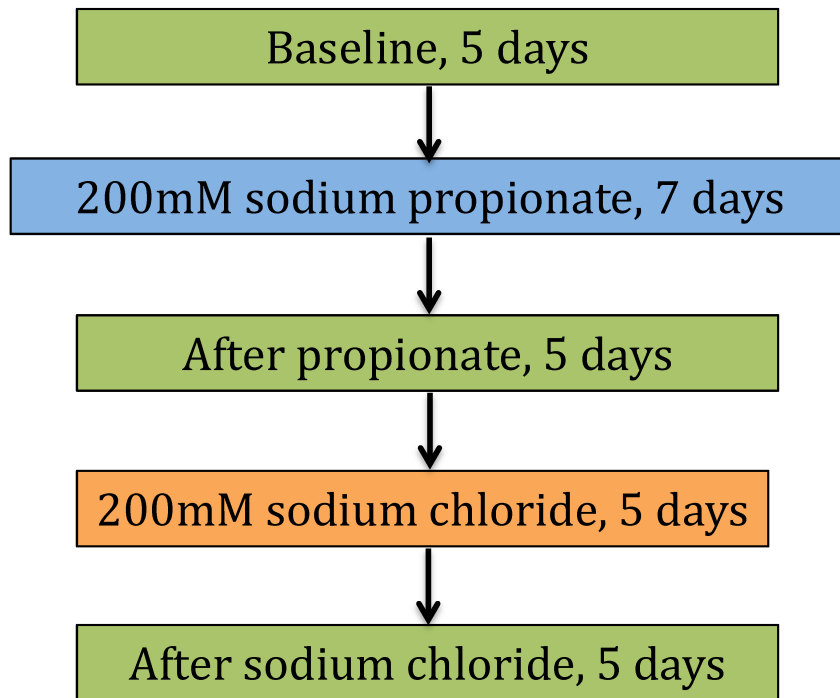


Figure 4.3: Experimental scheme of chronic propionate treatment

3-month-old male Gpr41 KO and Gpr41 WT were maintained on a normal sodium diet (0.49% sodium chloride). A 5 – day baseline was recorded on control (normal sodium diet, 0.49% sodium chloride), subsequently, mice were subjected to a regimen of high salt (4% sodium chloride) for 7 days and low salt diet (0.04% sodium chloride) for 5 days (Figure 4.4). Blood pressure was continuously recorded throughout the experimental period from baseline measurement to low sodium diet treatment and day – wise trends in BP values were analyzed.

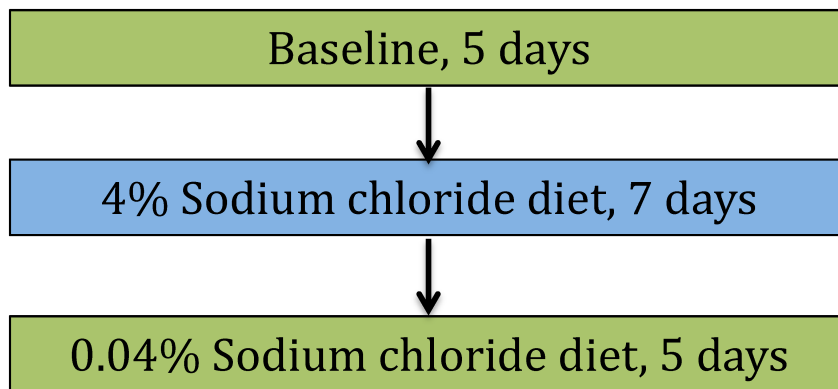


Figure 4.4: Experimental scheme of high salt diet regime

## **4.4 Results**

### **Plasma electrolytes in Gpr41 KO and WT mice**

Plasma electrolytes were assayed in 3 month old Gpr41 KO and Gpr41 WT, male and female mice using iSTAT cartridges that measure plasma sodium, potassium, calcium, chloride, glucose, creatinine, BUN, anion gap, hematocrit, TCO<sub>2</sub> and hemoglobin. Similar values of plasma electrolytes were observed in the KO and WT mice, both male and female (Table 4.1). The mice were not fasted prior to this experiment; so the trends in plasma glucose numbers cannot be used for predicting metabolic phenotypes. Plasma samples collected exhibit mild hemolysis; hence potassium values are higher than normal values.



Table 4.1: Plasma electrolytes in Gpr41 KO and Gpr41 WT mice					
		M, WT	M, KO	F, WT	F, KO
mmol / L	Na	146.71±0.61	148.10±0.53	151.5±1.85	148±0.70
	K	6.01±0.22	6.22±0.29	6.175±0.09	5.525±0.45
	Cl	116.86±1.3	118.60±1.09	113.25±0.75	113.75±1.38
	iCa	1.14±0.02	1.17±0.04	1.2925±0.01	1.2425±0.03
	TCO2	15.29±1.57	15.00±0.84	18.5±1.19	19.5±0.5
mg/dL	Glucose	205.43±11.36	184.70±11.75	182.75±12.17	179±13
	BUN	18.57±1.46	20.00±0.94	20±1.58	19±61
	creatinine	<0.2	<0.2	<0.2	<0.2
% PCV	hematocrit	46.00±0.44	41.35±4.59	47±1.47	47.75±0.75
g/dL	hemoglobin	15.63±0.15	15.60±0.23	15.975±0.5	16.25±0.27
mmol/L	AnGap	21.43±0.97	21.70±1.08	24.25±1.8	22±1.78

### **Plasma renin concentration**

SCFAs act via Olfr78 to stimulate renin secretion from the juxtaglomerular apparatus. Olfr78 localizes to the renal afferent arteriole, which stores and secretes renin and vascular smooth muscle cells. SCFAs trigger renin secretion from glomerular preparations via Olfr78 (Figure 4.5); Olfr78 KO mice have lower plasma renin compared to Olfr78 WT mice. Since SCFA mediated BP increase is via renin, plasma renin concentration in Gpr41 KO and WT mice was measured to determine if compensatory changes in plasma renin occur in Gpr41 KO mice, which could affect baseline blood pressure observed. PRC was measured using a modified Angiotensin-I ELISA kit and was determined in terms of ng Angiotensin-I produced per ml of plasma per hour. Concentration of Angiotensin-I in the samples is determined using a standard curve (Figure 4.6).

Shown in Table 4.2 and Table 4.3 are individual plasma renin concentration values from 3 – month – old and 6 – month – old Gpr41 KO and Gpr41 WT mice. In 3 – month old mice, the average plasma renin concentration values of Gpr41 male, WT mice is  $105.94 \pm 8.57$  and that of Gpr41 male, KO mice is  $115.3 \pm 16.25$  ng Angiotensin – I produced / ml / hour. Gpr41 WT female mice have a plasma renin concentration of  $129.88 \pm 5.92$  and that of Gpr41 KO female mice is  $139.55 \pm 9.87$  ng Angiotensin – I produced / ml / hour. There are no significant differences

in the plasma renin concentration between 3 – month old Gpr41 KO and Gpr41 WT mice (both male and female). Interestingly, 6 – month – old Gpr41 KO male mice have an average plasma renin concentration of  $149.56 \pm 32.57$  and that of Gpr41 WT mice is  $72.66 \pm 13.36$  ng Angiotensin – I produced / ml / hour. In these older mice, Gpr41 KO mice tend towards having lower plasma renin activity, though not significant. This indicates that the isolated systolic hypertension phenotype observed is a vascular phenotype and in older mice there are compensatory changes in renin levels to adjust to the hypertensive state.

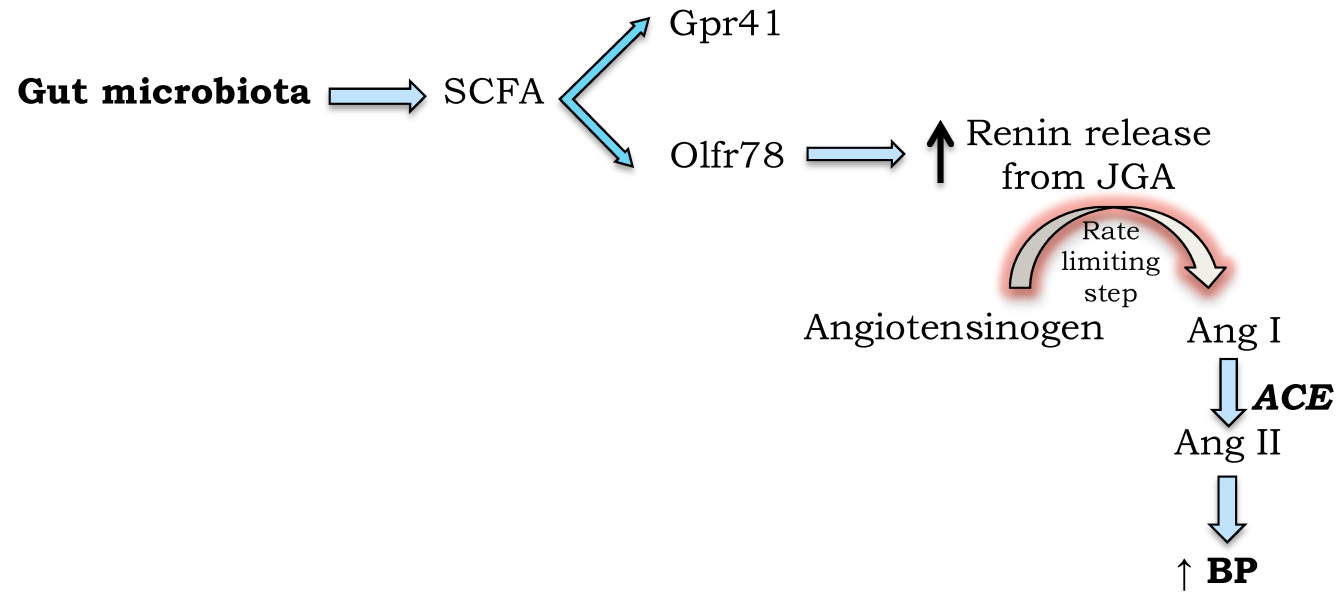


Figure 4.5: SCFAs stimulate renin secretion via Olf78, which results in an increase of BP

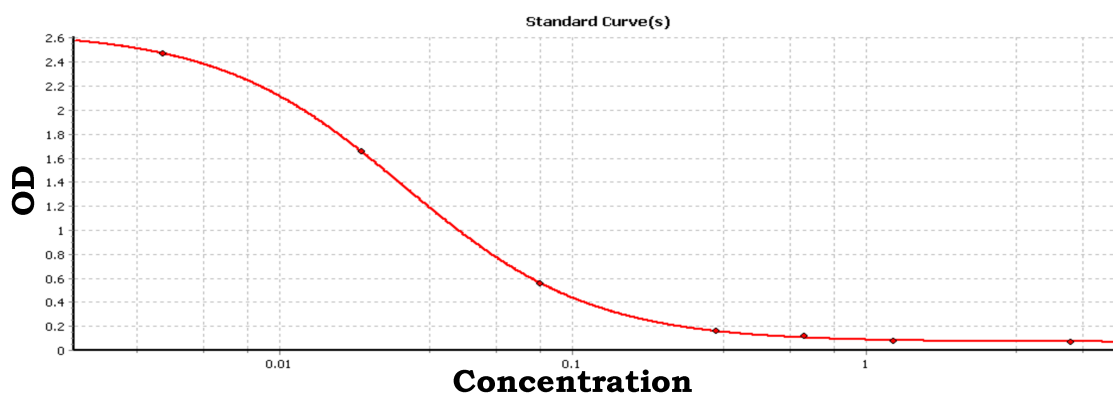


Figure 4.6 Angiotensin – I standard curve

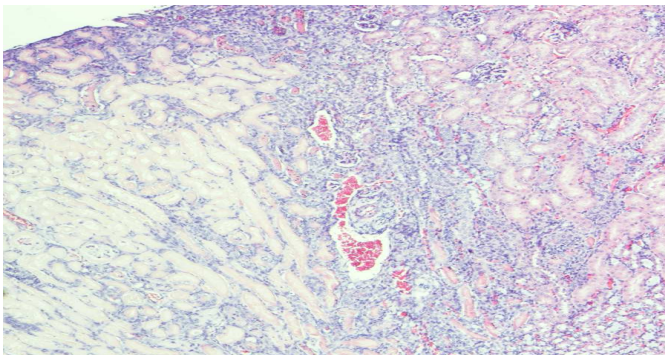
Table 4.2 Plasma renin concentration in 3 month old mice (ng Angiotensinogen I produced /ml / hour)	
Male, WT	105.94±8.57, n=7
Male, KO	115.3±16.25, n=7
Female, WT	129.88±5.92, n=6
Female, KO	139.55±9.87, n=6

Table 4.3: Plasma renin concentration, 6 month old mice (ng Angiotensin I produced / ml/ hour)	
M, KO	149.56±32.57
M, WT	72.66±13.36

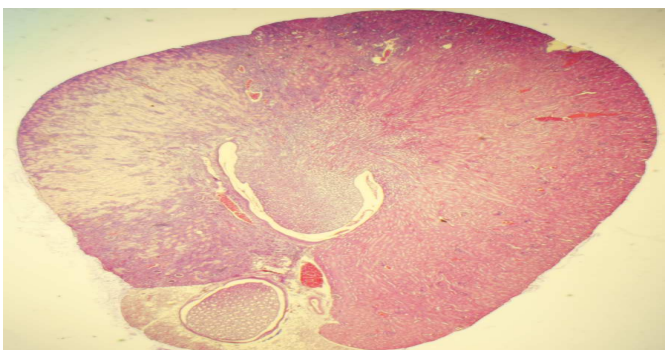
### Renal morphology of Gpr41 KO mice

Morphology of kidneys from Gpr41 KO and WT mice were analyzed using H&E stained paraffin sections of the kidney. At 10X magnification, some kidney sections from Gpr41 KO mice show a focally extensive area of

necrosis within the cortex and extending into the medulla (Figure 4.7 B). At 200X the tubular outlines are apparent, but within the tubules there is complete necrosis of tubular epithelial cells (Figure 4.7A). There is a sharp demarcation between the necrotic and viable areas of the kidney with several congested vessels and a cellular infiltrate with a densely cellular interstitium at this junction consisting of proliferative fibroblasts and infiltrating lymphocytes, plasma cells, macrophages, and neutrophils. However, some Gpr41 KO kidneys demonstrated no obvious lesions. Glomeruli in Gpr41 KO kidneys appear slightly shrunken compared to Gpr41 WT glomeruli.



A: 200X magnification



B: 10X magnification

Figure 4.7: H&E stained sections of some Gpr41 KO kidney sections demonstrated moderate nephritis.

### **Gpr41 KO mice exhibit isolated systolic hypertension**

At 3 months of age, male Gpr41 KO mice exhibited isolated systolic hypertension at baseline (Figure 4.8) both during the day and night. The reported values (Fig. 4.8) represent averages from a 5 – day recording of BP in 3-month-old male animals of both genotypes. Consistent with higher systolic pressures in the Gpr41 KO animals, the pulse pressures of Gpr41KO were significantly elevated during both dark and light cycles (Figure 4.9). The mean arterial pressure, diastolic pressure, and heart rate were similar between the two genotypes (Figure 4.8, 4.9). However,  $dP/dt$  (a measure of LV contractility) was elevated in the Gpr41<sup>-/-</sup> mice, which alludes to a lower compliance of blood vessels and increased preload in the Gpr41 KO animals (Fig 4.10).

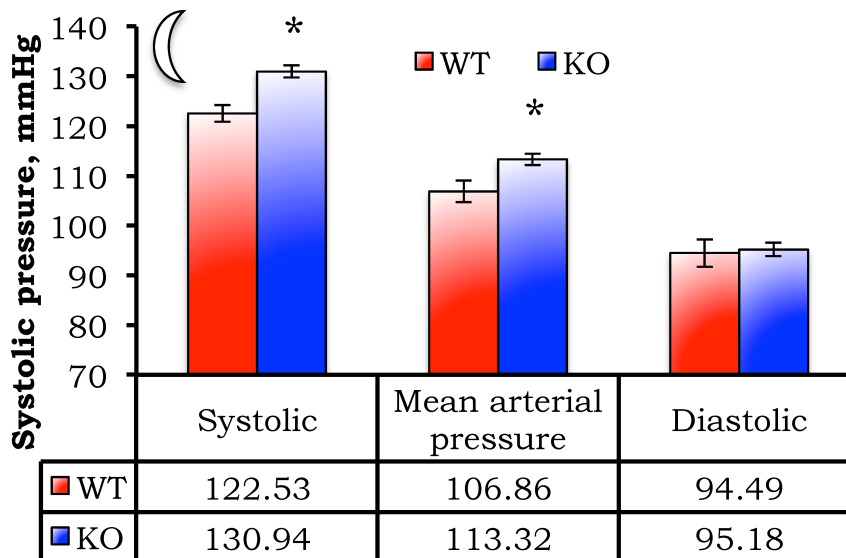
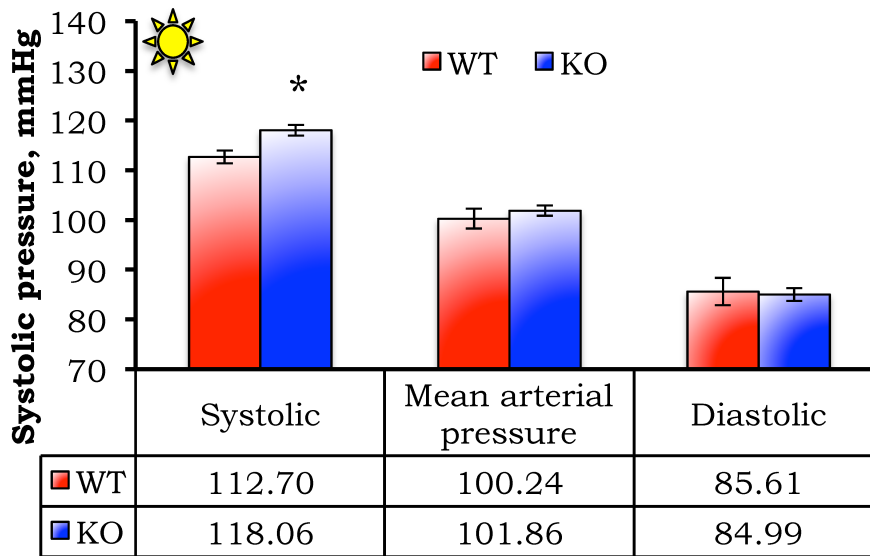


Figure 4.8: Gpr41 KO mice exhibit isolated systolic hypertension. Average blood pressure values (systolic pressure, mean arterial pressure, diastolic pressure) from a 5-day baseline recording period are summarized in the figure, light cycle (day) – top panel, dark cycle (night) – bottom panel. \*  $p < 0.05$ , comparison between genotypes



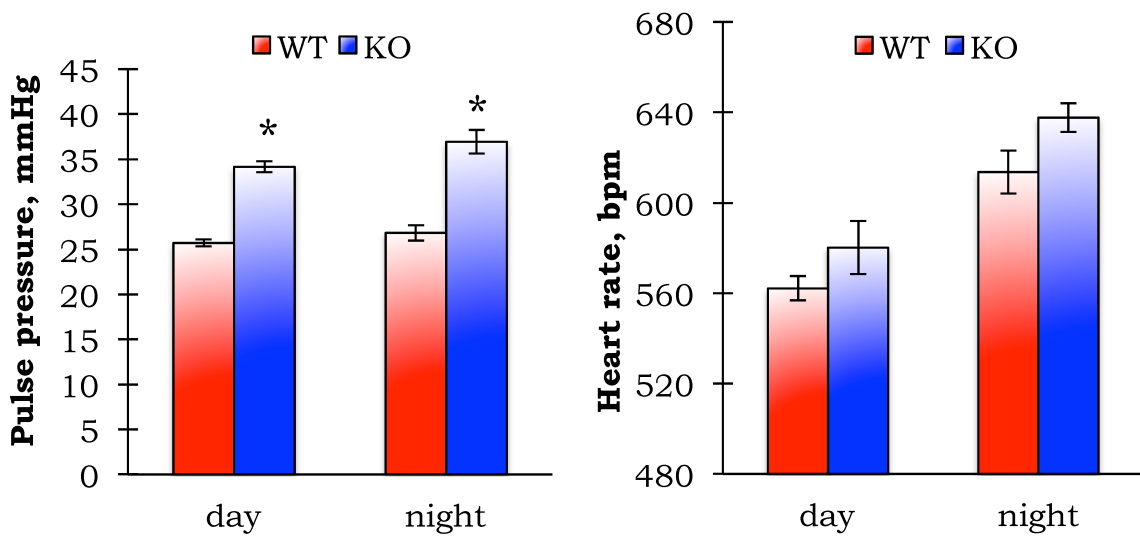


Figure 4.9: Pulse pressure is significantly elevated in Gpr41 KO mice, both at day and night, while there are no significant differences in the heart rate between the two genotypes. \*  $p < 0.05$ , comparison between genotypes

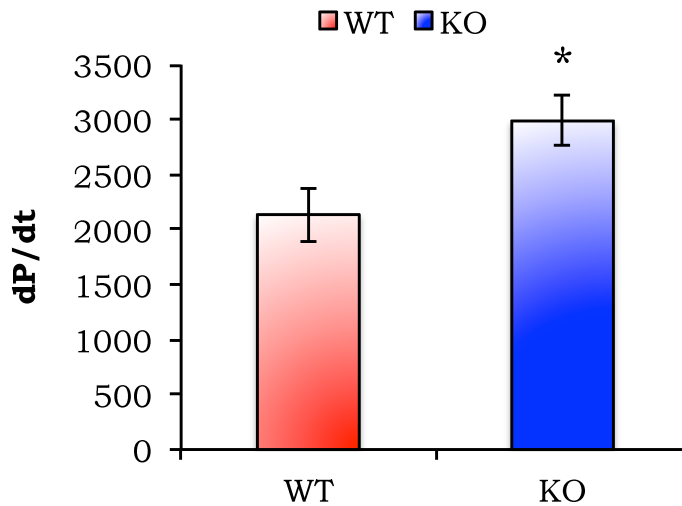


Figure 4.10: Gpr41 KO mice have significantly higher dP/dt during the dark cycle. \*  $p < 0.05$ , comparison between genotypes

Isolated systolic hypertension is associated with a two- to five-fold increase in mortality due to cardiovascular complications. Isolated systolic hypertension is most commonly attributed to large inelastic arteries and aortic insufficiency. It is also presumed that systolic hypertension arises with aging as a result of inelastic rigid arteries. In older populations, systolic hypertension is related to hypertensive cardiac failure, stroke and coronary heart disease[112, 116, 124, 125].

Now, with the evidence that Gpr41 KO mice exhibit isolated systolic hypertension, the first parameter to assess to determine causality was large vessel stiffness. Two approaches were used to assess blood vessel stiffness in the Gpr41 KO and Gpr41 WT mice, pulse wave velocity to assess vessel stiffness *in vivo* and tensile testing of aortas to assess blood vessel stiffness *ex vivo*[121, 126].

In order to assess blood vessel stiffness *in vivo*, we measured pulse wave velocity in Gpr41 KO and Gpr41 WT animals. Pulse wave velocity (PWV) is a measure of arterial stiffness, the rate at which pressure waves move down the blood vessels. PWV is a highly reliable prognostic parameter for cardiovascular morbidity and mortality in patients with end-stage renal disease, diabetes and hypertension[115, 116, 124, 125].

In a cardiac cycle, blood moves out of the left ventricle, into the aorta and subsequently through the vessels of the circulatory system. Left ventricular contraction during systole to eject blood into the ascending aorta acutely dilates the aortic wall and generates a pressure wave that moves along the aorta and its branches. The velocity of the pressure wave gives a measure of arterial compliance. Changes in the arterial wall as a result of aging or other causes, result in stiffer vessels and under these circumstances, the velocity of the pressure wave is increased. Pressure waves generated constantly due to cardiac function traverse through the arteries and are also reflected back at the end of systole. When the pressure waves move faster under inelastic conditions of the aorta, the reflected waves move back quicker too, causing an increased afterload on the ventricle, resulting in a greater systolic pressure requirement to overcome this afterload[115, 116, 124, 125]. PWV is collected by using two pressure catheters placed a known distance (pulse wave distance) from each another. The time taken by the pressure wave to go from the upstream pressure catheter to the downstream pressure catheter is the Pulse Transit Time (PTT). PWV is then calculated by dividing the distance by the transit time.

In a cohort of age - matched Gpr41 KO and Gpr41 WT mice at 3 months of age, there was no observed difference in the PWV. However, at 6 months of age, PWV was significantly elevated in Gpr41 KO as compared

to age-matched wild-type littermates (Figure 4.11). This interesting observation suggests that it could be possible that elevated systolic pressure over a prolonged period of time results in increased PWV.

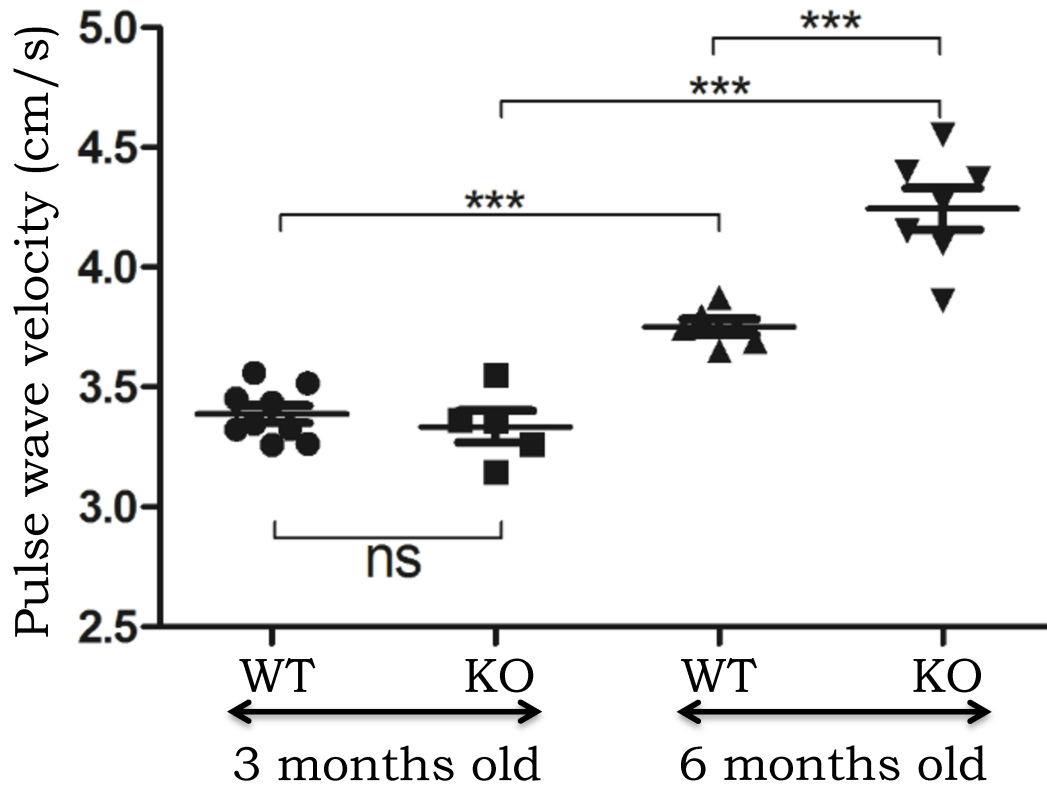


Figure 4.11: Pulse wave velocity is elevated in 6 – month old Gpr41 KO mice, pulse wave velocity is similar in Gpr41 KO and Gpr41 WT mice at 3 months of age (time point of baseline BP measurements) \*\*\*  $p < 0.01$ , comparison between genotypes.

Since older Gpr41 KO mice exhibited increased PWV in addition to systolic hypertension, tensile properties of aortas was assayed from Gpr41 KO and Gpr41 WT mice to examine if remodeling of the aortic media as a result of elastin fracture due to systolic hypertension could

cause the increased PWV observed in older Gpr41 KO mice. Tensile properties of aortas from Gpr41 KO and Gpr41 WT mice was examined by applying varying amounts of strain on the blood vessel followed by measurement of stress developed. Tensile properties of intact aortas was assayed and a subset of aortas were decellularized to measure tensile properties of the aortic media in the absence of cells. Surprisingly, intact aortas from Gpr41 KO and Gpr41 WT animals do not show any differences in their tensile properties, while decellularized Gpr41 KO aortas have increased compliance (Figure 4.12). This result rules out the possibility of changes in extracellular matrix in the aortic media or elastin fracture as a potential cause of increased PWV. On the other hand, the inherent cause of systolic hypertension and increased PWV in older animals could stem from impaired signaling in the endothelium that hampers blood vessel relaxation.

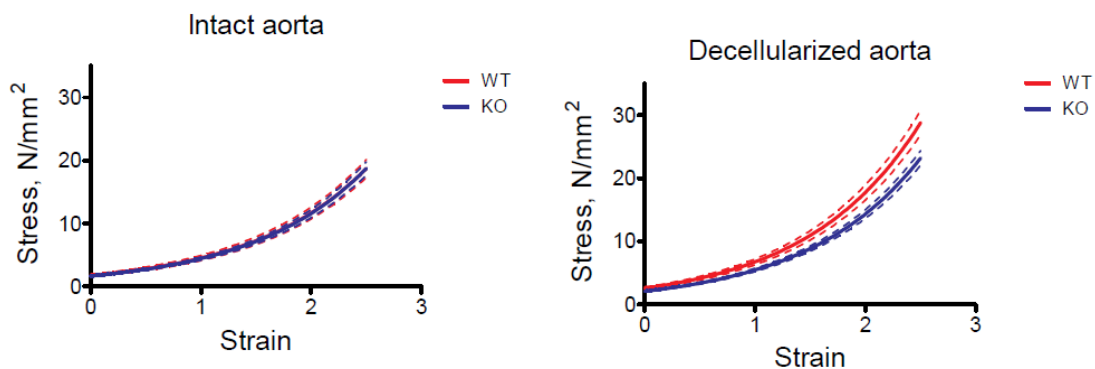


Figure 5.7: Blood vessel tensile properties are similar in intact aorta from Gpr41 KO and Gpr41 WT mice, decellularized aorta from Gpr41 KO mice are more significantly compliant,  $p < 0.0001$

### **Chronic sodium propionate administration doesn't elicit a blood pressure response in Gpr41 KO mice**

200mM SCFA treatment in drinking water has previously been shown to be sufficient to activate SCFA receptors in mice. However, contrary to our hypothesis, we found that neither sodium propionate nor sodium chloride treatment significantly altered systolic, mean, or diastolic BP (Figure 4.13, 4.14), systolic hypertension in Gpr41 KO mice was observed throughout the experimental duration (Figure 4.13). Pulse pressure was consistently higher in Gpr41 KO mice throughout the experiment (Figure 4.14), although a minor decrease in heart rate was observed upon propionate treatment in Gpr41 KO (Figure 4.15).

Since we observed a blood pressure response in WT and Gpr41 KO mice upon acute SCFA administration, but didn't observe any stable effects of chronic SCFA delivery on BP, it could be possible that SCFA – induced blood pressure changes are transient and become negligible in the average values for the treatment periods.

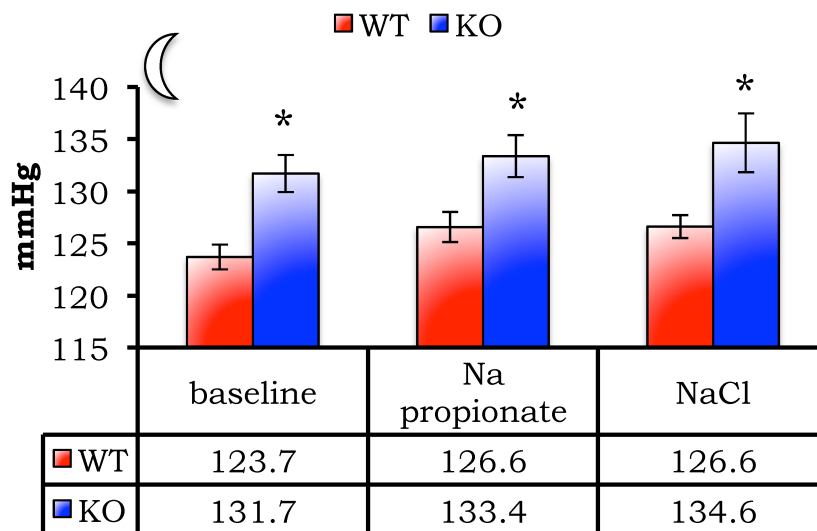
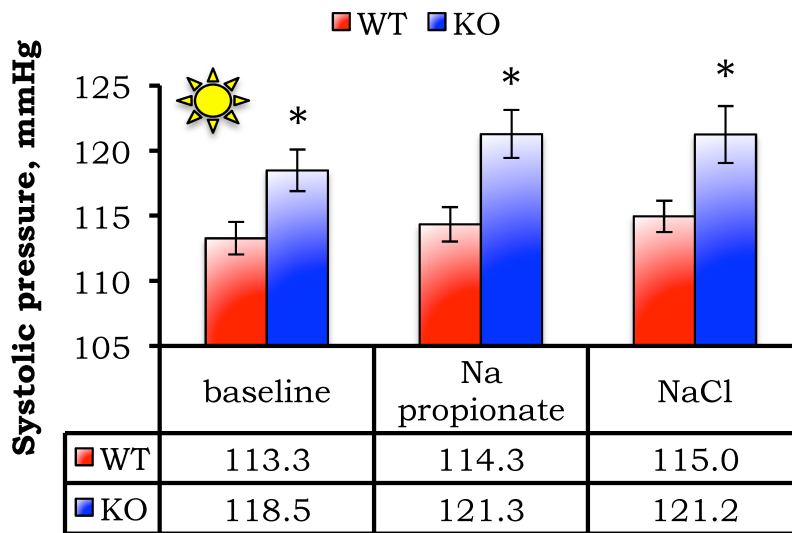


Figure 4.13: Chronic propionate administration (200mM sodium propionate in the drinking water) doesn't stably alter blood pressure in Gpr41 KO mice. \*  $p < 0.05$ , comparison between genotypes.

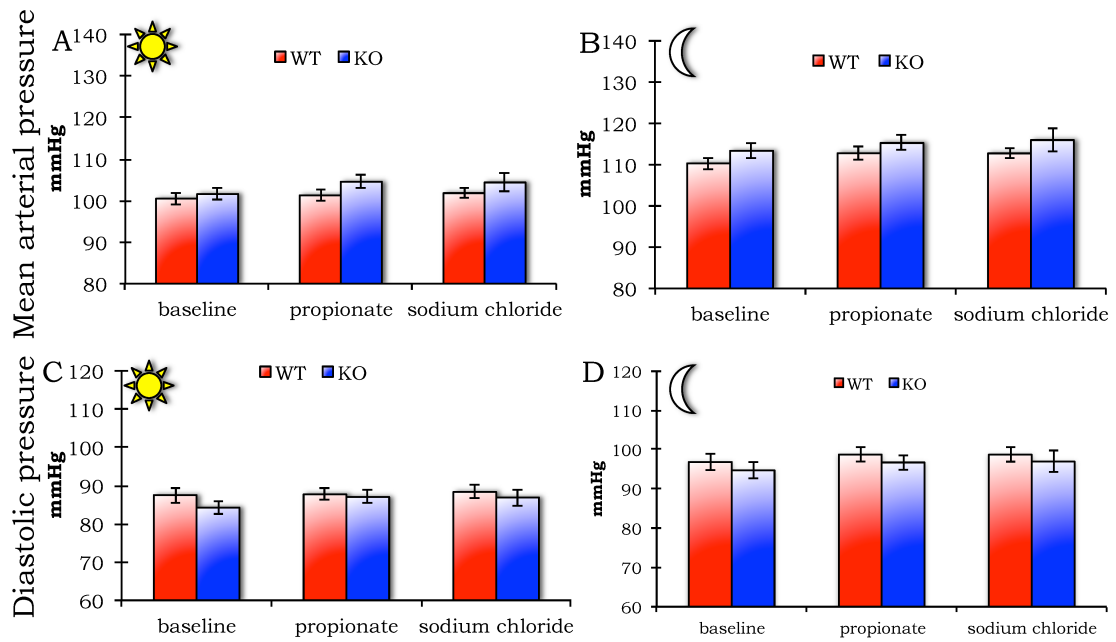
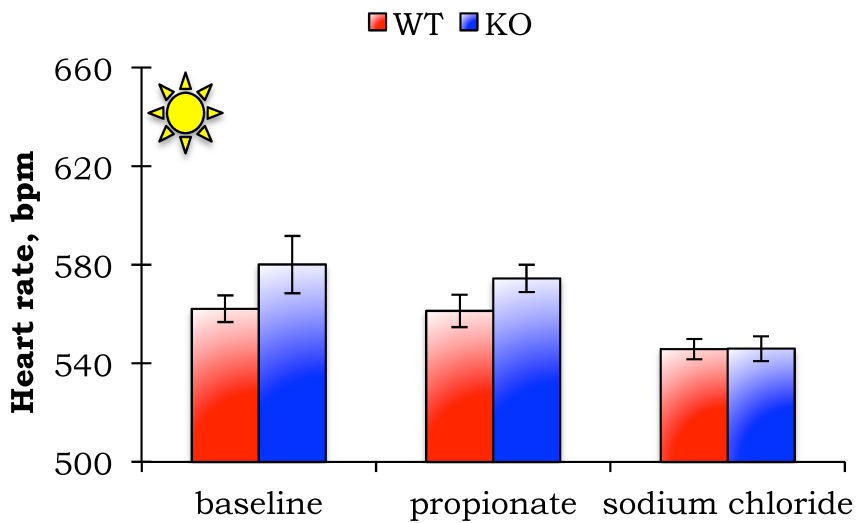


Figure 4.14: Mean arterial pressure and diastolic pressure in Gpr41 KO and WT mice during the treatment periods, both light cycle and dark cycle values are shown.





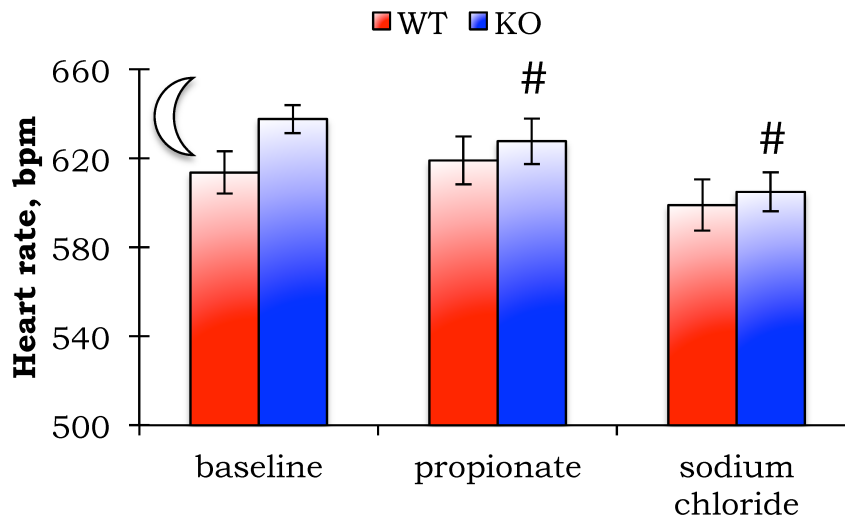


Figure 4.15: Heart rate is not significantly different between Gpr41 KO and Gpr41 WT mice during sodium propionate and sodium chloride treatment. Heart rate decreases in Gpr41 KO mice during propionate and sodium chloride treatment compared to baseline. #  $p < 0.05$  compared to Gpr41 KO baseline heart rate.

Body weights and plasma electrolytes were monitored in similar age-matched cohort of mice. Interestingly, body weights of Gpr41 KO mice on sodium propionate increased, whereas that of Gpr41 WT mice were relatively stable in an age matched cohort (Figure 4.16).

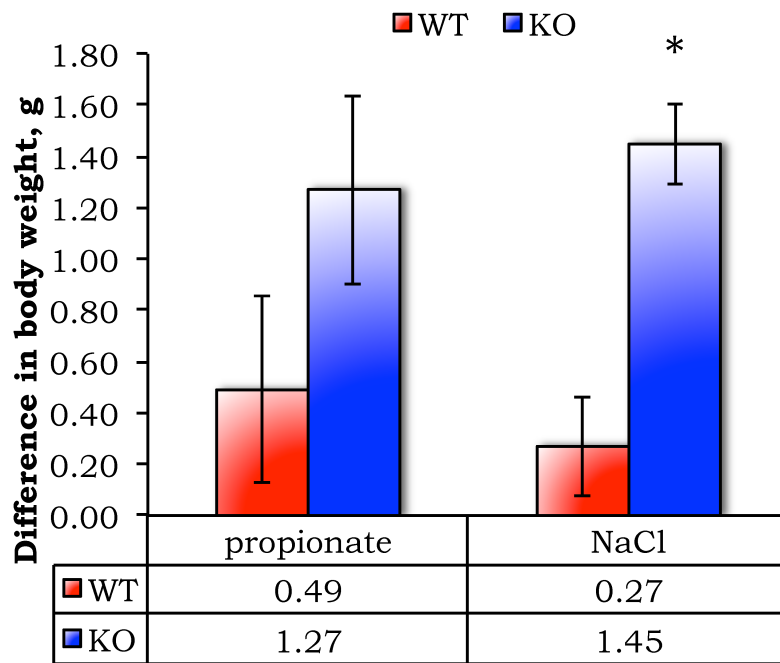


Figure 4.16: Body weight of Gpr41 KO mice increases on propionate and sodium chloride treatment. \*  $p < 0.05$ , comparison between genotypes.

Analysis of blood electrolytes during propionate and sodium chloride treatment showed an increase in plasma sodium in both genotypes during the sodium propionate treatment, but not during sodium chloride administration (Figure 4.17).

### Plasma sodium during treatments

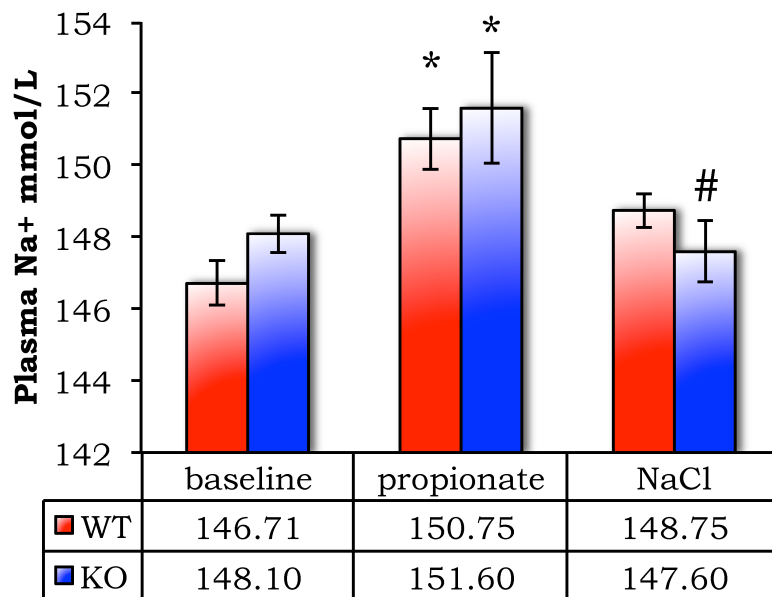


Figure 4.17: Plasma sodium increases during chronic sodium propionate treatment in both Gpr41 WT and Gpr41 KO mice

Table 4.2 Plasma electrolytes during baseline, sodium propionate and sodium chloride treatments							
		Baseline		Propionate		NaCl	
		WT	KO	WT	KO	WT	KO
mmol / L	Na	146.71	148.10	150.75	151.60	148.75	147.60
	K	6.01	6.22	6.00	6.06	6.10	5.96
	Cl	116.86	118.60	114.50	112.80	112.00	113.60
	iCa	1.14	1.17	1.22	1.28	1.25	1.27
	TCO2	15.29	15.00	20.75	18.40	24.25	21.00
mg/dL	Glucose	205.43	184.70	187.00	199.60	206.50	245.40
	BUN	18.57	20.00	20.25	21.00	16.75	19.60
	creatinine	<0.2	<0.2	<0.2	<0.2	0.20	0.20
% PCV	hematocrit	46.00	41.35	48.00	48.00	46.75	45.40
g/dL	hemoglobin	15.63	15.60	16.33	16.32	15.88	15.44
mmol/L	AnGap	21.43	21.70	22.50	27.20	19.25	19.80

Plasma samples collected for analysis of electrolytes during chronic sodium propionate treatment exhibited mild hemolysis, hence elevated potassium values

Table 4.2 Plasma electrolytes during baseline, sodium propionate and sodium chloride treatments							
		Baseline		Propionate		NaCl	
		WT	KO	WT	KO	WT	KO
mmol / L	Na	146.71	148.10	150.75	151.60	148.75	147.60
	K	6.01	6.22	6.00	6.06	6.10	5.96
	Cl	116.86	118.60	114.50	112.80	112.00	113.60
	iCa	1.14	1.17	1.22	1.28	1.25	1.27
	TCO2	15.29	15.00	20.75	18.40	24.25	21.00
mg/dL	Glucose	205.43	184.70	187.00	199.60	206.50	245.40
	BUN	18.57	20.00	20.25	21.00	16.75	19.60
	creatinine	<0.2	<0.2	<0.2	<0.2	0.20	0.20
% PCV	hematocrit	46.00	41.35	48.00	48.00	46.75	45.40
g/dL	hemoglobin	15.63	15.60	16.33	16.32	15.88	15.44
mmol/L	AnGap	21.43	21.70	22.50	27.20	19.25	19.80

Plasma samples collected for analysis of electrolytes during chronic sodium propionate treatment exhibited mild hemolysis, hence elevated potassium values

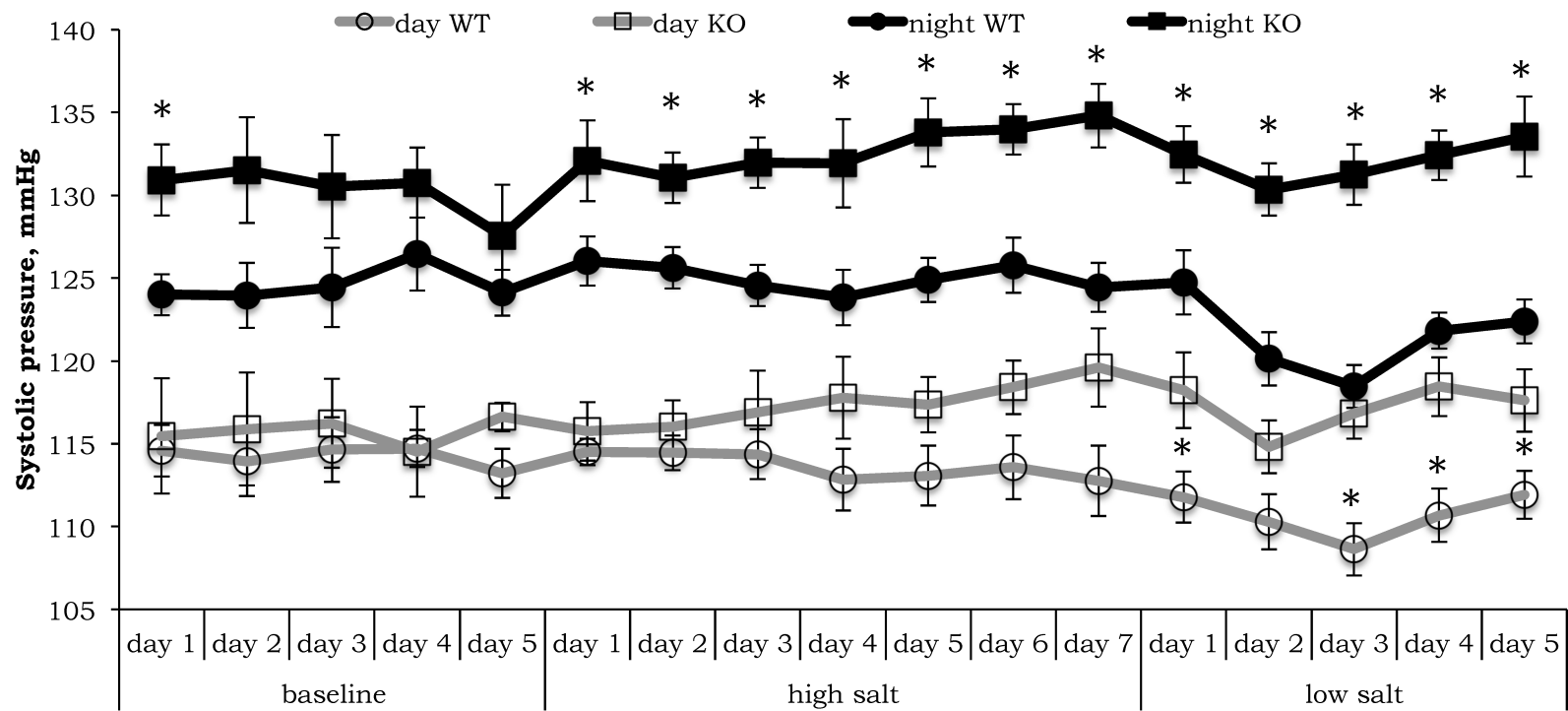


Figure 4.18: Gpr41 KO mice do not exhibit salt – sensitive hypertension. Squares represent values from KO mice and circles represent values from WT mice, filled squares and circles show dark cycle (night) values and open symbols represent light cycle (day) values. \*  $p < 0.05$ , comparison between genotypes.  $n=5$  (KO),  $6$  (WT).

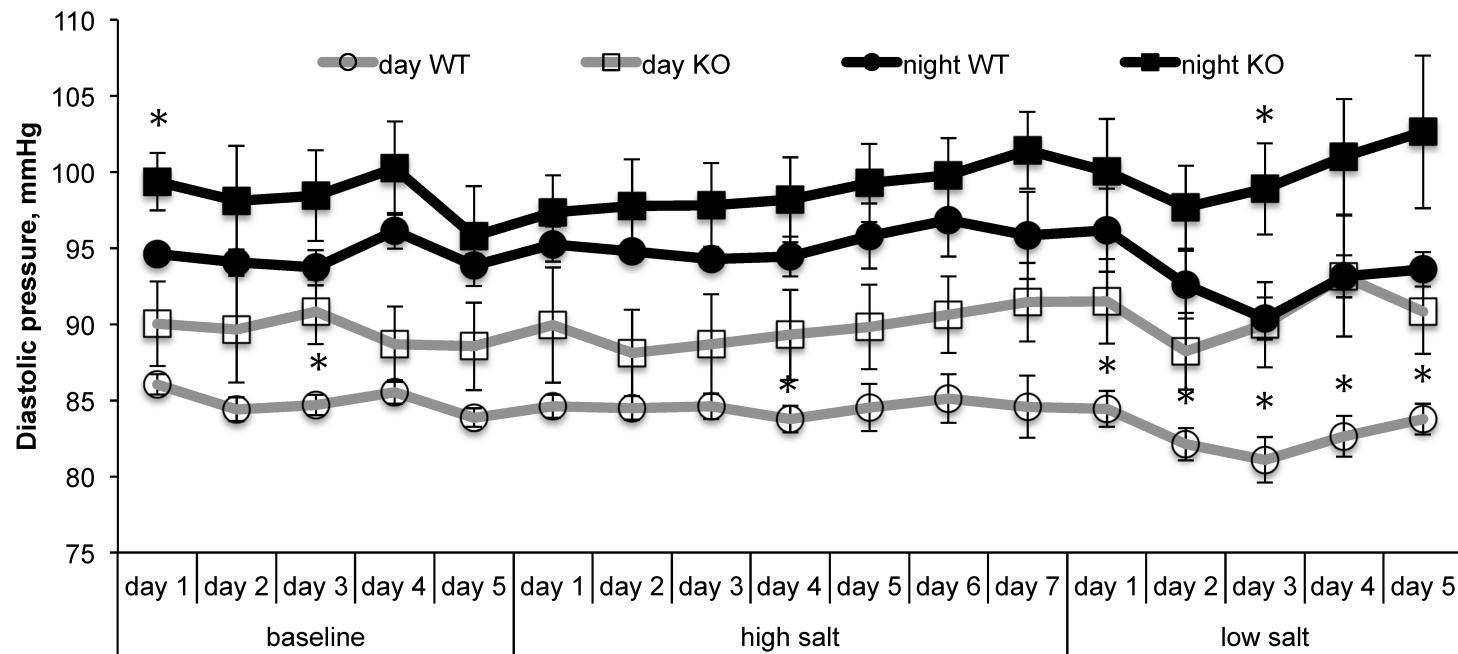


Figure 4.19: Diastolic pressures are mostly not different between genotypes during salt loading, a decrease in WT diastolic pressure is observed during the low salt treatment period. Squares represent values from KO mice and circles represent values from WT mice, filled squares and circles show dark cycle (night) values and open symbols represent light cycle (day) values. \*  $p < 0.05$ , comparison between genotypes.  $n = 5$  (KO),  $6$  (WT).

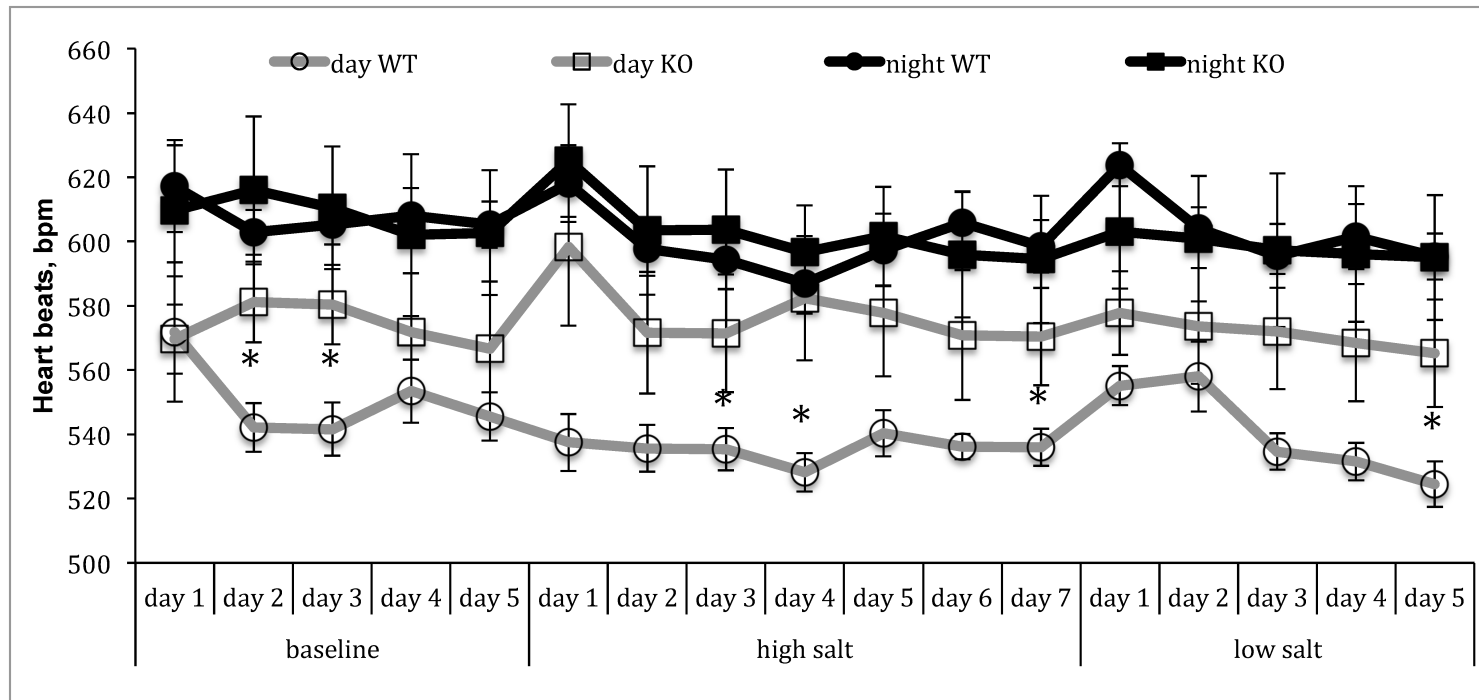


Figure 4.20: Heart rate is not different between the genotypes on diets with different salt contents. WT mice have lower heart rate during the light cycle on several days, but no significant differences are observed during the dark cycle. Squares represent values from KO mice and circles represent values from WT mice, filled squares and circles show dark cycle (night) values and open symbols represent light cycle (day) values. \*  $p < 0.05$ , comparison between genotypes.  $n = 5$  (KO),  $6$  (WT).



Heart rate doesn't differ significantly between Gpr41 KO and Gpr41 WT mice at baseline or during the high salt or low salt diets. There is a minor increase in heart rate observed in both genotypes immediately after switching to a new diet (Figure 4.19).

#### **4.5 Discussion**

Characterization of various physiological parameters in Gpr41 KO and WT mice revealed that

- (i) Plasma renin concentration was not different between Gpr41 KO and Gpr41 WT animals (both male and female). Olfr78 is expressed in renal afferent arteries and stimulates renin secretion.
- (ii) Plasma electrolytes are similar in 3-month-old Gpr41 KO and WT males and females. This indicates that on a large-scale level, ion balance in plasma is not perturbed in Gpr41 KO mice.
- (iii) Histological analysis of Gpr41 KO kidneys shows an apparent trend in decrease of glomerular size.
- (iv) Gpr41 KO mice are hypertensive at 3 months of age; they exhibit isolated systolic hypertension, elevated pulse pressure with no significant difference in diastolic pressure and heart rate compared to Gpr41 WT mice.
- (v) Analysis of vascular properties of Gpr41 KO and WT mice revealed that 6 – month – old Gpr41 KO mice exhibit increased pulse wave

velocity. On the other hand, isolated aortas do not exhibit any changes in their tensile properties.

### **Isolated systolic hypertension in Gpr41 KO mice**

Usually hypertension is characterized by an increase in both systolic pressure and diastolic pressure. Increased systolic pressure alone in Gpr41 KO mice indicates that they have isolated systolic hypertension, which could be a result of stiff, less compliant blood vessels, resulting in an increase of afterload. This coupled with an increase in  $dP/dt$  indicates that there is impaired relaxation of blood vessels in Gpr41 KO requiring a greater systolic pressure to pump blood into the aorta. Since Gpr41 is expressed in the endothelium, which modulates smooth muscle stiffness by secreting various factors, it is possible that Gpr41 acts on a key pathway in the endothelium to mediate vasodilation.

### **Hypertension in Gpr41 KO mice is vascular in nature**

Multiple lines of evidence indicate that the hypertension observed in Gpr41 KO is vascular in nature. First, similar plasma renin is similar in Gpr41 KO and WT mice. Similar plasma renin concentration in Gpr41 KO and WT mice indicates that the cause of hypertension is possibly vascular. A second line of evidence that the hypertension is likely vascular is the fact that the Gpr41 KO mice exhibit an isolated systolic

form of hypertension. A third line of evidence that the hypertension is vascular is the fact that it is not salt-sensitive in Gpr41 KO mice.

It is very intriguing that 3-month-old Gpr41 KO mice, which exhibit isolated systolic hypertension, do not have increased pulse wave velocity (PWV). 6-month-old Gpr41 KO mice have higher PWV, indicating that the compliance of Gpr41 KO blood vessels decreases faster with aging. This could indicate that increased systolic pressures exacerbate the age – associated decrease in blood vessel compliance, causing a decrease of the compliance of blood vessels in Gpr41 KO mice. If absence of Gpr41 in blood vessels increases age associated decrease in blood vessel compliance, Gpr41 could be an ideal target for treating resistant hypertension with hardening of the arteries that greatly decrease compliance.

Tensile testing of blood vessels to correlate the increased pulse wave velocity to possibly stiffer aortas showed no differences in tensile properties in intact vessels and increased compliance in decellularized aortas. Based on this evidence, it is possible that increased vascular tone or impaired signaling in the endothelium of Gpr41 KO mice could contribute to the development of isolated systolic hypertension. This line of evidence also rules out the possibility of increased collagen deposition and damaged elastin bands in Gpr41 KO blood vessels.

It was observed that Gpr41 KO mice do not exhibit salt sensitive hypertension. All the evidence accumulated till this point indicates that hypertension in Gpr41 KO mice is vascular in nature with minimal hormonal and renal components. Absence of a BP response to a high salt diet confirms the fact that Gpr41 KO mice have vascular dysfunction, leading to hypertension. Renal salt handling appears to be normal and able to compensate for a higher salt load in Gpr41 KO and WT mice.

Olfr78 mediates hypertension via an increase in plasma renin concentration, since SCFAs stimulate renin secretion from the juxtaglomerular apparatus in an Olfr78-dependent manner. Olfr78-induced hypertension is primarily hormonal (renin), whereas Gpr41-mediated hypertension seems to be primarily vascular in nature. This shows that even though Gpr41 and Olfr78 are activated by the same ligands and alter cellular cAMP in opposing directions upon activation; signal via strikingly different and unique mechanisms. This gives two novel BP regulation pathways that can be targeted by small molecule drugs or by dietary alterations to modulate BP in hypertension.

### **Vascular effects of SCFA – transient in nature?**

Previously, Gpr41 KO and WT mice showed different responses to acute SCFA doses, while wild-type (WT, C57BL/6) mice exhibited a hypotensive BP response to an acute SCFA bolus. It was expected that chronic SCFA

would increase BP in Gpr41 KO mice because Olfr78, which opposes the effect of Gpr41 acts unopposed in the KO mice, which lack Gpr41. An increase, if observed would have shed light on the mechanism of BP regulation involving Gpr41, under chronic exposure to SCFAs.

200mM sodium propionate delivered chronically to Gpr41 KO and WT mice in the drinking water did not have a lasting effect on blood pressure in Gpr41 KO and Gpr41 WT mice. This highlights the transient nature of BP response to SCFAs. Even in the acute dose response experiments, BP exhibited a step decrease and recovered in a period of 10 minutes. Since during analysis, we take into account the average systolic and diastolic BP values during the entire treatment period, we may not be observing transient changes in BP due to SCFA consumption. Furthermore, since 200mM propionate is delivered via drinking water *ad libitum*, there is no steady dosing of propionate and it is hard to assign minor variations in BP to propionate consumption. In fact, we observe a minor non-significant increase in systolic BP in both genotypes during sodium propionate and sodium chloride administration. Since Gpr41-mediated changes in BP are mainly vascular, it is a possibility that they are also transient and short-lived. On the other hand Olfr78 mediates an increase in plasma renin concentration, which would result in a sustained increase in BP over a longer period. This increase in plasma renin could result in the minor BP increases observed on sodium propionate.

Another plausible reason for the absence of a BP response to chronic SCFA treatment could be the inability of oral SCFA delivery to significantly increase plasma SCFA levels due to rapid uptake by tissues and small volume ingested. If this were the case, sustained delivery needs to be used as an alternative to oral delivery to study the BP effects of chronic SCFA delivery.

### **Renal histology and morphology**

Although a majority of this study was concerned with the role of Gpr41 in blood vessels and its downstream signaling in the endothelium, localization of Gpr41 in the renal glomerulus is equally important and crucial for blood pressure regulation. The trend of Gpr41 KO glomeruli to be smaller is consistent with the localization of Gpr41 in glomeruli and indicates that Gpr41 could possibly play a role development of proper structure and size of the glomerulus. This phenotype requires further investigation of renal parameters and glomerular filtration rate to understand the physiological role of Gpr41 in the kidney and glomeruli.

## **5 Signaling mechanisms of SCFAs in blood vessels**

### **5.1 Abstract**

Previous studies have found that SCFAs dilate blood vessels *ex vivo*. Using microvascular chambers to test vascular responses of tail arteries, we confirmed that both acetate and propionate dilate resistance vessels in a dose-dependent manner. This confirms previous reports that SCFAs dilate blood vessels and that Gpr41 could play a role in regulating vascular tone upon activation. We also found that SCFA-mediated vasodilation is dependent on the endothelium - consistent with a role for endothelial Gpr41 in mediating this response. In our attempts to narrow down the pathway of SCFA – mediated vasodilation, we blocked eNOS with L-NAME and saw that inhibition of eNOS doesn't inhibit SCFA-mediated vasodilation. SCFA-mediated vasodilation of tail arteries is mediated predominantly by an eNOS-independent mechanism.

## 5.2 Introduction

We have previously showed that SCFAs decrease BP via Gpr41. Other groups have showed that SCFAs dilate blood vessels *ex vivo*. SCFAs decrease BP by mediating vasodilation. Given that there are two SCFA receptors, Gpr41 in the endothelium and Olfr78 in vascular smooth muscle cells, it is important to decipher which component of blood vessels mediates the hypotensive response in order to further understand underlying signaling pathways and to use key players in the pathway as potential pharmacological targets to treat hypertension.

In this section, we analyzed vascular responses of tail arteries to SCFAs and isolated the component of blood vessels that mediates this response by comparing vascular responses of intact blood vessels and denuded vessels lacking functional endothelial cells. Since Gpr41 mediates a hypotensive response, we hypothesize that the endothelial layer would mediate SCFA-dependent vasodilation. We also attempted to identify the molecular mechanisms by which SCFAs signal beginning with eNOS, since it is an important pathway by which vasodilation is mediated and fits with the timeline of the response seen.



### **5.3 Materials and methods**

#### **Ex-vivo vascular relaxation experiments**

3-month-old male mice (Gpr41 WT and KO) were euthanized by CO<sub>2</sub> asphyxiation. Proximal segments of the tail artery were dissected rapidly and placed in cold Krebs-Ringer bicarbonate solution containing 118.3mM NaCl, 4.7mM KCl, 1.2mM MgSO<sub>4</sub>, 1.2mM KH<sub>2</sub>PO<sub>4</sub>, 2.5mM CaCl<sub>2</sub>, 25.0mM NaHCO<sub>3</sub>, and 11.1mM glucose (control solution). The tail arteries (either intact or with endothelium denuded) were cannulated at both ends with glass micropipettes, secured using 12-0 nylon monofilament suture, and placed in a microvascular chamber (Living Systems, Burlington, VT)[122, 123]. The arteries were maintained at a constant transmural pressure ( $P_{TM}$ ) of 60 mmHg in the absence of flow. The chamber was superfused with control solution, maintained at 37°C, pH 7.4, and gassed with 16% O<sub>2</sub>-5% CO<sub>2</sub>-balance N<sub>2</sub>. The chamber was placed on the stage of an inverted microscope (20X; Nikon TMS-F) connected to a video camera (CCTV camera; Panasonic). The vessel image was projected on a video monitor, and the internal diameter was continuously determined by a video dimension analyzer (Living Systems Instrumentation) and was monitored using a BIOPAC (Santa Barbara, CA) data acquisition system[122, 123]. The tail vessels were allowed to equilibrate at  $P_{TM}$  of 60mmHg for 30 minutes. After equilibration, the vessels were treated with increasing doses of sodium propionate and

sodium acetate in the superfusate and the internal diameter of the vessels were recorded over time. After propionate treatment, the reactivity of the vessels (and presence/absence of endothelium) was confirmed by acetylcholine.

## **5.4 Results**

Acute SCFAs mediate a hypotensive response via vasodilation. Human colonic arteries have been reported to exhibit vasodilation upon exposure to SCFAs[104]. The hypotensive response to SCFAs is primarily mediated by Gpr41, but is opposed by Olfr78[26]. In order to investigate the molecular mechanism and signaling events driven by SCFAs to mediate vasodilation, vascular responses of resistance arteries were examined upon addition of SCFAs in a vascular chamber (Figure 5.1, A)[123, 126-128]. Isolated resistance vessel from the tail exhibited vasodilation upon addition of increasing amounts of sodium propionate (Figure 5.1, B), indicating that this setup could be used to study downstream signaling events involved in this pathway.

Gpr41 is localized in the vascular endothelium and it has been established that Gpr41 acts to decrease blood pressure, based on acute dose responses[5, 26] and systolic hypertension observed in Gpr41 KO mice. Hence, it is possible that SCFA – mediated vasodilation observed is endothelium – dependent, consistent with a role for Gpr41.

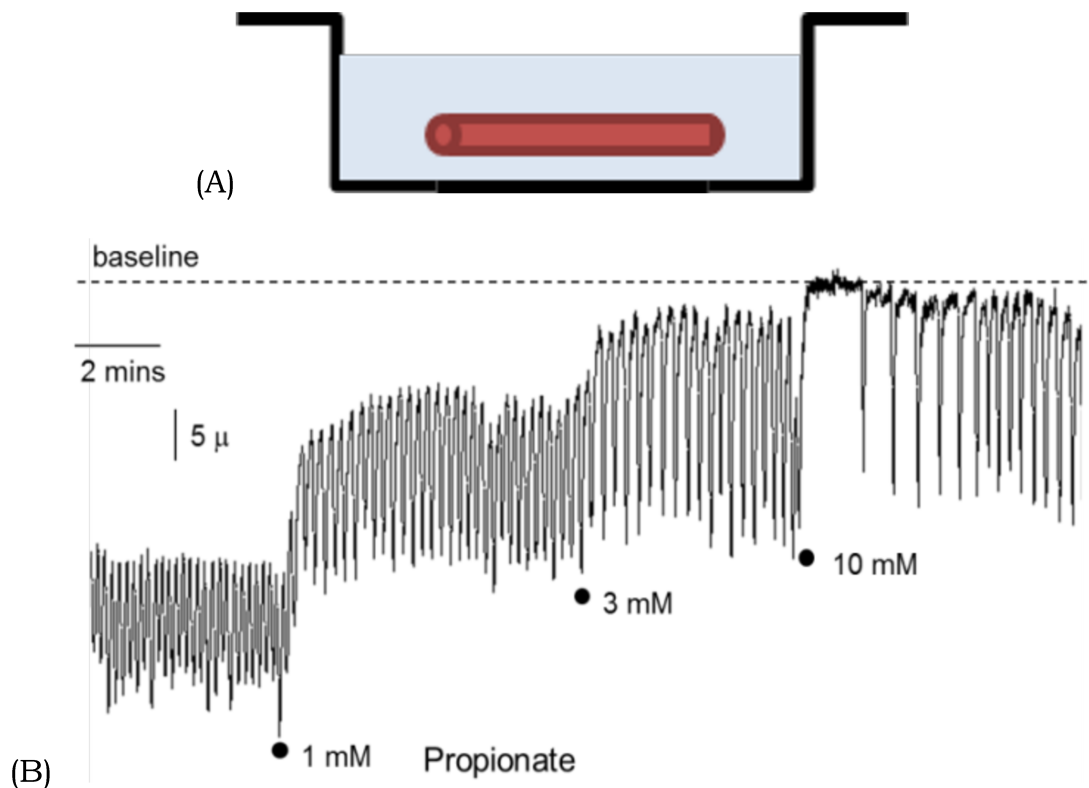


Figure 5.1: SCFAs induce vasodilation in murine tail resistance arteries (A) microvascular chamber setup, tail arteries are cannulated on each side by pipettes and maintained in a Krebs Ringers bath at 37C and 60mmHg transmural pressure. (B) A representative trace from vascular chamber experiment showing dilation of mouse-tail artery upon propionate treatment.

### **SCFA-mediated vasodilation is endothelium-dependent**

SCFAs propionate and acetate induced dose-dependent vasodilation of resistance arteries from the tail (representative traces shown in Figure 5.2, summarized data in Figure 5.3), with a dose-dependence that is

similar to the hypotensive response in vivo[26]. This SCFA – mediated vasodilation, was endothelium – dependent (Figure 5.2, 5.3), consistent with the localization of Gpr41. Intact arteries exhibit vasodilation in a dose – dependent manner upon SCFA treatment, the vasodilation was severely attenuated in the denuded arteries lacking functional endothelium.

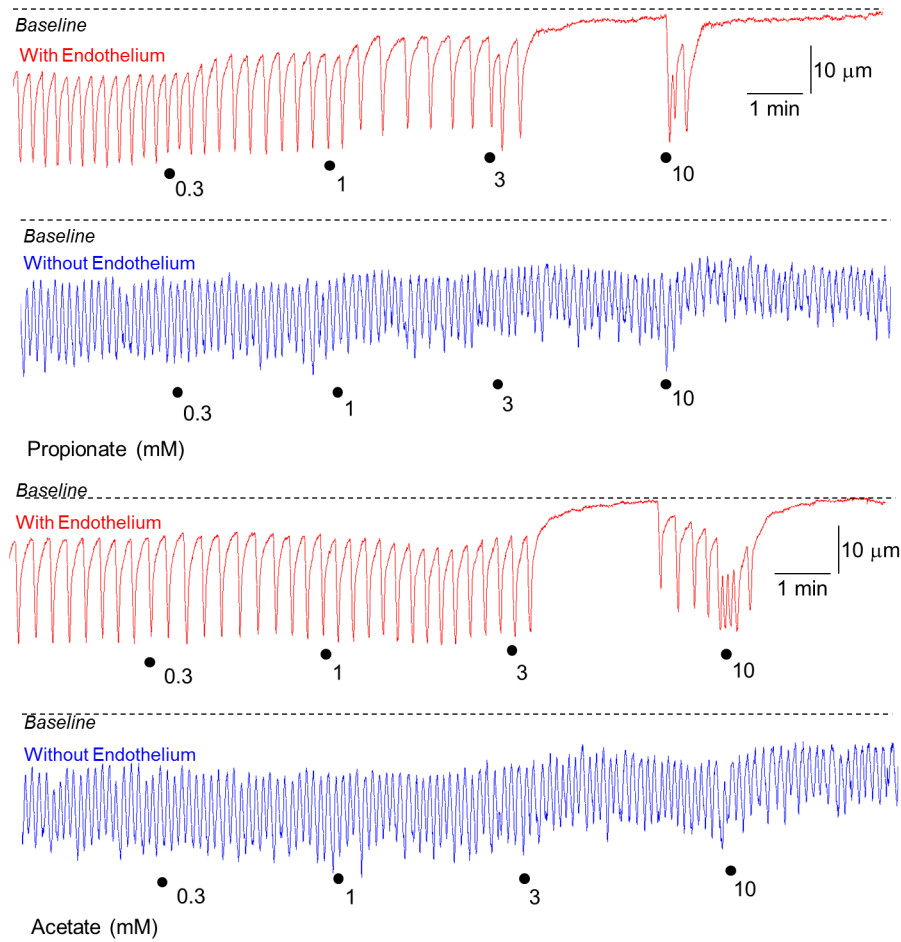


Figure 5.2: Endothelium mediates SCFA – mediated vasodilation – representative traces

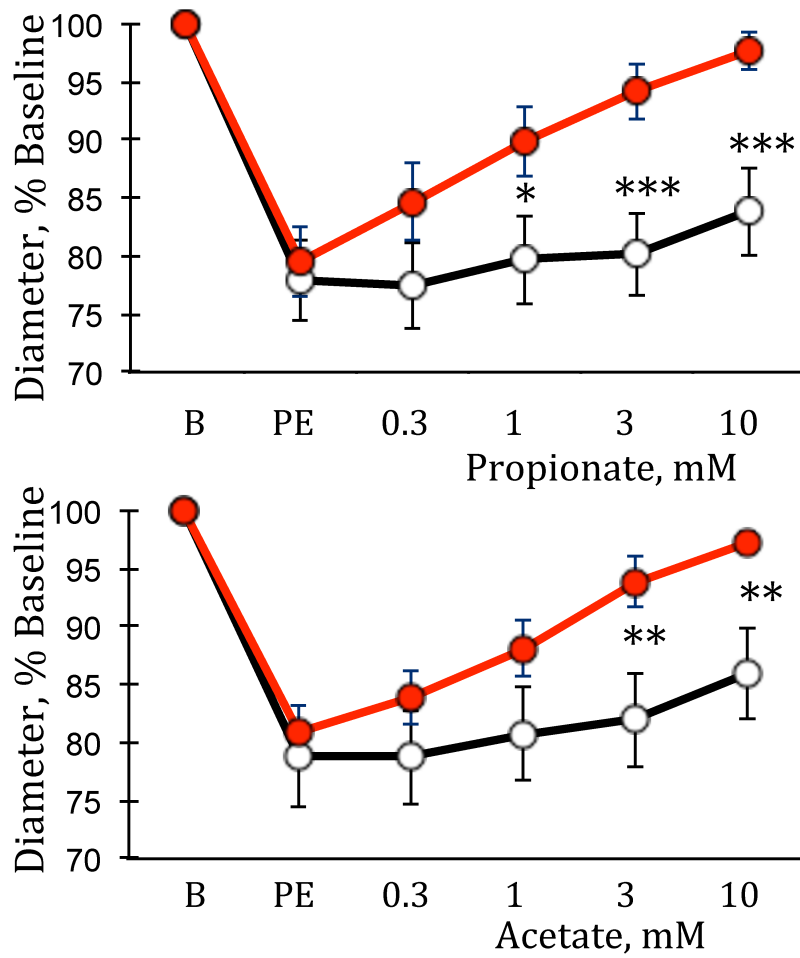


Figure 5.3: Endothelium mediates SCFA – mediated vasodilation (summarized data), \*  $p < 0.05$ , \*\*  $p < 0.01$ , \*\*\*  $p < 0.001$ , comparison between intact and denuded blood vessels.

The three major mechanisms by which endothelial cells facilitate vasodilation are

- (i) nitric oxide based, mediated via endothelial nitric oxide synthase (eNOS)
- (ii) prostacyclins and prostaglandins

(iii) endothelial – derived hyperpolarizing factor (EDHF)

Since the nature of hypotensive response to acute SCFA treatment in vivo is rapid and endothelium – dependent, it is possible that Gpr41 may induce vasodilation via eNOS; since nitric oxide mediated vasodilation is would match the timescale of responses observed.

### **SCFAs mediate vasodilation in an eNOS independent manner**

The next set of vascular chamber experiments were performed with SCFA (to mediate vasodilation) and L-NAME, a pharmacological inhibitor of eNOS to determine if the response was eNOS dependent. However, SCFA mediated vasodilation was not inhibited in the presence of L-NAME, indicating that SCFA-mediated vasodilation is mediated predominantly by an eNOS-independent mechanism (Figure 5.4, 5.5).

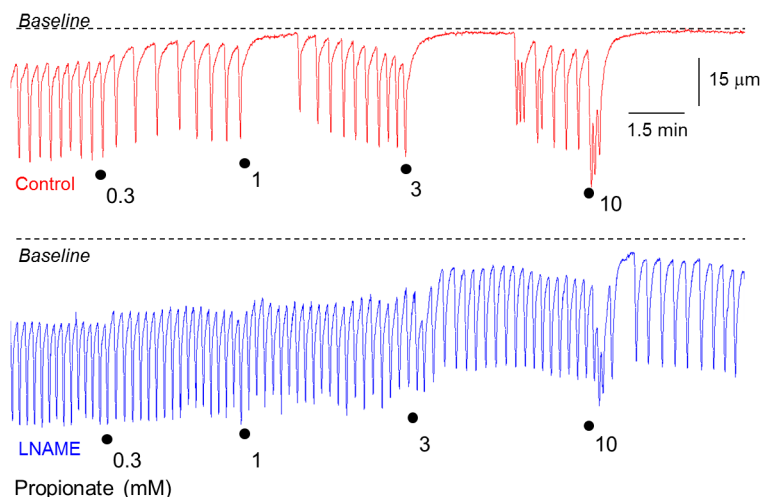


Figure 5.4: L-NAME doesn't significantly inhibit SCFA – induced vasodilation – representative trace

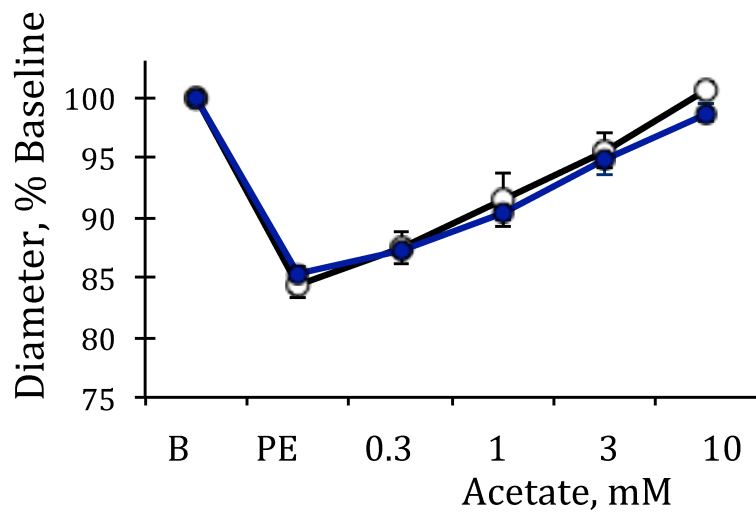
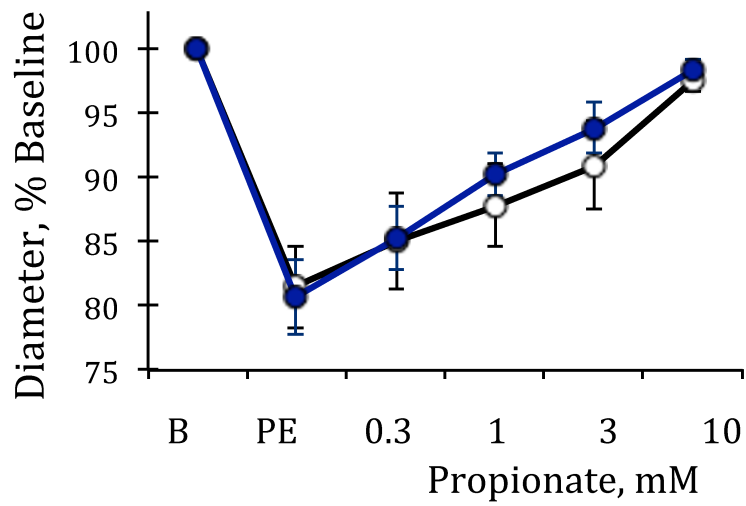


Figure 5.5: SCFA induce vasodilation in resistance vessels in an endothelium – independent manner – summarized data

Vasodilation observed upon eNOS inhibition is possibly mediated via prostacyclins or EDHF. Further experiments are required to determine the pathway of SCFA – mediated vasodilation.

## 5.5 Discussion

The mechanism of SCFA-mediated vasodilation was investigated and it was observed that

- (i) A functional endothelium is crucial for SCFA – mediated vasodilation in tail arteries. Denuded vessels lacking a functional endothelium do not vasodilate upon treatment with acetate and propionate.
- (ii) Inhibition of eNOS with L-NAME does not inhibit vasodilation of tail arteries upon SCFA treatment. The time scale of vasodilation seen with SCFAs and rapid recovery seen *in vivo* seemed to fit with role for eNOS in the response. Surprisingly, since L-NAME did not inhibit the vasodilation seen in tail arteries, it could be mediated by prostacyclins or EDHF. Further experiments are required to decipher the exact pathway.

### **Endothelium-dependent SCFA mediated vasodilation: A role for Gpr41?**

It has been shown previously that SCFAs mediate vasodilation. Our results confirm the observation and prove that the decrease in BP observed upon acute SCFA delivery is possibly via vasodilation. This is interesting because Gpr41 and Olfr78, the two major players in SCFA-mediated BP regulation are expressed in blood vessels, but Olfr78 is expressed in vascular smooth muscle cells and Gpr41 is expressed in the endothelium. The mechanisms by which these receptors mediate their



effects on BP are very different, even though they are localized to neighboring cell types in a blood vessel. Our observation that a functional endothelium is absolutely essential to mediate SCFA-dependent vasodilation is novel and consistent with our earlier finding of Gpr41 in the endothelium. This supports the hypothesis that Gpr41 mediates a hypotensive response, since Gpr41 is localized to the vascular endothelium. Gpr41 signals via the inhibitory G protein, Gi, which plays a major role in vasodilation events mediated by the endothelium. Further experiments with Gpr41 antagonists and vessels from Gpr41 KO mice are required to validate the role of Gpr41 in this pathway.

#### **SCFA and vasodilation: role for eNOS?**

Initially, it was assumed that eNOS might mediate SCFA-dependent vasodilation, since the time frame of both the *in vivo* BP response and *ex vivo* vasodilation are very rapid and *in vivo* BP recovers quickly too. Our attempts to monitor vasodilation in the presence of L-NAME, an eNOS inhibitor showed that SCFA-mediated vasodilation could occur even when eNOS was inhibited. This shows that SCFAs signal possibly via other endothelial dependent mechanisms to decrease BP.

## References

1. Marinissen, M.J. and J.S. Gutkind, *G-protein-coupled receptors and signaling networks: emerging paradigms*. Trends in pharmacological sciences, 2001. **22**(7): p. 368-376.
2. Böhme, I. and A.G. Beck-Sickinger, *Illuminating the life of GPCRs*. Cell Communication and Signaling, 2009. **7**(1): p. 16.
3. Heng, B.C., D. Aubel, and M. Fussenegger, *An overview of the diverse roles of G-protein coupled receptors (GPCRs) in the pathophysiology of various human diseases*. Biotechnology advances, 2013. **31**(8): p. 1676-1694.
4. Deshpande, D.A., et al., *Bitter taste receptors on airway smooth muscle bronchodilate by localized calcium signaling and reverse obstruction*. Nature medicine, 2010. **16**(11): p. 1299-1304.
5. Pluznick, J.L., *Renal and cardiovascular sensory receptors and blood pressure regulation*. American journal of physiology. Renal physiology, 2013. **305**(4): p. 44.
6. Douglas, J.E., et al., *A role for airway taste receptor modulation in the treatment of upper respiratory infections*. Expert review of respiratory medicine, 2016: p. 1-14.
7. Kang, N. and J. Koo, *Olfactory receptors in non-chemosensory tissues*. BMB reports, 2012. **45**(11): p. 612-622.

8. Amisten, S., et al., *An atlas of G-protein coupled receptor expression and function in human subcutaneous adipose tissue*. Pharmacology & therapeutics, 2014.
9. Foster, S.R., et al., *Bitter taste receptor agonists elicit G-protein-dependent negative inotropy in the murine heart*. FASEB journal : official publication of the Federation of American Societies for Experimental Biology, 2014.
10. Samuel, B.S., et al., *Effects of the gut microbiota on host adiposity are modulated by the short-chain fatty-acid binding G protein-coupled receptor, Gpr41*. Proceedings of the National Academy of Sciences of the United States of America, 2008. **105**(43): p. 16767-16772.
11. Tremaroli, V. and F. Bäckhed, *Functional interactions between the gut microbiota and host metabolism*. Nature, 2012. **489**(7415): p. 242-249.
12. Smith, P.M., et al., *The microbial metabolites, short-chain fatty acids, regulate colonic Treg cell homeostasis*. Science (New York, N.Y.), 2013. **341**(6145): p. 569-573.
13. Natarajan, N. and J.L. Pluznick, *From microbe to man: the role of microbial short chain fatty acid metabolites in host cell biology*. American journal of physiology. Cell physiology, 2014. **307**(11): p. 85.

14. Koh, A., et al., *From Dietary Fiber to Host Physiology: Short-Chain Fatty Acids as Key Bacterial Metabolites*. Cell, 2016. **165**(6): p. 1332-1345.
15. Zhu, W., et al., *Gut Microbial Metabolite TMAO Enhances Platelet Hyperreactivity and Thrombosis Risk*. Cell, 2016. **165**(1): p. 111-124.
16. Sekirov, I., et al., *Gut microbiota in health and disease*. Physiological reviews, 2010. **90**(3): p. 859-904.
17. Kau, A.L., et al., *Human nutrition, the gut microbiome and the immune system*. Nature, 2011. **474**(7351): p. 327-336.
18. Cox, L.M., et al., *Altering the Intestinal Microbiota during a Critical Developmental Window Has Lasting Metabolic Consequences*. Cell, 2014. **158**(4): p. 705-721.
19. Barros, A.F., et al., *Is there interaction between gut microbial profile and cardiovascular risk in chronic kidney disease patients? Future microbiology*, 2015. **10**: p. 517-526.
20. Mell, B., et al., *Evidence for a link between gut microbiota and hypertension in the Dahl rat*. Physiological genomics, 2015. **47**(6): p. 187-197.
21. Brestoff, J.R. and D. Artis, *Commensal bacteria at the interface of host metabolism and the immune system*. Nat Immunol, 2013. **14**(7): p. 676-84.

22. Henningsson, Å., I. Björck, and M. Nyman, *Short-chain fatty acid formation at fermentation of indigestible carbohydrates*. Food & Nutrition Research, 2001. **45**: p. 165-168.
23. Perry, R.J., et al., *Acetate mediates a microbiome-brain- $\beta$ -cell axis to promote metabolic syndrome*. Nature, 2016. **534**(7606): p. 213-217.
24. Priyadarshini, M., et al., *SCFA Receptors in Pancreatic  $\beta$  Cells: Novel Diabetes Targets?* Trends in Endocrinology & Metabolism, 2016.
25. Ulven, T., *Short-chain free fatty acid receptors FFA2/GPR43 and FFA3/GPR41 as new potential therapeutic targets*. Frontiers in endocrinology, 2012. **3**: p. 111.
26. Pluznick, J.L., et al., *Olfactory receptor responding to gut microbiota-derived signals plays a role in renin secretion and blood pressure regulation*. Proceedings of the National Academy of Sciences of the United States of America, 2013. **110**(11): p. 4410-4415.
27. Marette, A. and C. Jobin, *SCFAs Take a Toll En Route to Metabolic Syndrome*. Cell metabolism, 2015. **22**(6): p. 954-956.
28. Kelly, C.J., et al., *Crosstalk between Microbiota-Derived Short-Chain Fatty Acids and Intestinal Epithelial HIF Augments Tissue Barrier Function*. Cell host & microbe, 2015. **17**(5): p. 662-671.
29. Yu, X., et al., *Short-Chain Fatty Acids from Periodontal Pathogens Suppress Histone Deacetylases, EZH2, and SUV39H1 To Promote*

- Kaposi's Sarcoma-Associated Herpesvirus Replication*. Journal of virology, 2014. **88**(8): p. 4466-4479.
30. Venkatakrisnan, A.J., et al., *Molecular signatures of G-protein-coupled receptors*. Nature, 2013. **494**(7436): p. 185-194.
  31. Kroeze, W.K., D.J. Sheffler, and B.L. Roth, *G-protein-coupled receptors at a glance*. Journal of cell science, 2003. **116**(Pt 24): p. 4867-4869.
  32. Hill, S.J., *G-protein-coupled receptors: past, present and future*. Br J Pharmacol, 2006. **147 Suppl 1**: p. S27-37.
  33. Wettschureck, N. and S. Offermanns, *Mammalian G proteins and their cell type specific functions*. Physiol Rev, 2005. **85**(4): p. 1159-204.
  34. Thoen, W., J. Frazer, and D. Unett, *Functional assays for screening GPCR targets*. Current Opinion in Biotechnology, 2005.
  35. Tuteja, N., *Signaling through G protein coupled receptors*. Plant Signal Behav, 2009. **4**(10): p. 942-7.
  36. Rosenbaum, D.M., S.G. Rasmussen, and B.K. Kobilka, *The structure and function of G-protein-coupled receptors*. Nature, 2009. **459**(7245): p. 356-63.
  37. Le Poul, E., et al., *Functional characterization of human receptors for short chain fatty acids and their role in polymorphonuclear cell activation*. The Journal of biological chemistry, 2003. **278**(28): p. 25481-25489.

38. Brown, A.J., et al., *The Orphan G protein-coupled receptors GPR41 and GPR43 are activated by propionate and other short chain carboxylic acids*. The Journal of biological chemistry, 2003. **278**(13): p. 11312-11319.
39. Shaito, A., *Short Chain Fatty Acids Signaling through the G Protein-Coupled Receptor GPR41 in the Intestine*. Short Chain Fatty Acids Signaling through the G Protein-Coupled Receptor GPR41 in the Intestine., 2009.
40. Puhl, H.L., et al., *Human GPR42 is a transcribed multisite variant that exhibits copy number polymorphism and is functional when heterologously expressed*. Scientific reports, 2015. **5**: p. 12880.
41. Inoue, D., et al., *Short-chain fatty acid receptor GPR41-mediated activation of sympathetic neurons involves synapsin 2b phosphorylation*. FEBS letters, 2012. **586**(10): p. 1547-1554.
42. Bahar Halpern, K., et al., *GPR41 gene expression is mediated by internal ribosome entry site (IRES)-dependent translation of bicistronic mRNA encoding GPR40 and GPR41 proteins*. The Journal of biological chemistry, 2012. **287**(24): p. 20154-20163.
43. Kimura, I., et al., *Short-chain fatty acids and ketones directly regulate sympathetic nervous system via G protein-coupled receptor 41 (GPR41)*. Proceedings of the National Academy of Sciences of the United States of America, 2011. **108**(19): p. 8030-8035.

44. Tazoe, H., et al., *Expression of short-chain fatty acid receptor GPR41 in the human colon*. Biomedical research (Tokyo, Japan), 2009. **30**(3): p. 149-156.
45. Tazoe, H., et al., *Roles of short-chain fatty acids receptors, GPR41 and GPR43 on colonic functions*. Journal of physiology and pharmacology : an official journal of the Polish Physiological Society, 2008. **59 Suppl 2**: p. 251-262.
46. Yonezawa, T., Y. Kobayashi, and Y. Obara, *Short-chain fatty acids induce acute phosphorylation of the p38 mitogen-activated protein kinase/heat shock protein 27 pathway via GPR43 in the MCF-7 human breast cancer cell line*. Cellular signalling, 2007. **19**(1): p. 185-193.
47. Maslowski, K.M., et al., *Regulation of inflammatory responses by gut microbiota and chemoattractant receptor GPR43*. Nature, 2009. **461**(7268): p. 1282-1286.
48. Trompette, A., et al., *Gut microbiota metabolism of dietary fiber influences allergic airway disease and hematopoiesis*. Nature medicine, 2014. **20**(2): p. 159-166.
49. Cornall, L.M., et al., *The therapeutic potential of GPR43: a novel role in modulating metabolic health*. Cellular and molecular life sciences : CMLS, 2013.



50. Tunaru, S., et al., *Characterization of determinants of ligand binding to the nicotinic acid receptor GPR109A (HM74A/PUMA-G)*. Mol Pharmacol, 2005. **68**(5): p. 1271-80.
51. Tan, J., et al., *The role of short-chain fatty acids in health and disease*. Advances in immunology, 2014. **121**: p. 91-119.
52. Benyo, Z., et al., *GPR109A (PUMA-G/HM74A) mediates nicotinic acid-induced flushing*. J Clin Invest, 2005. **115**(12): p. 3634-40.
53. Writing Group, M., et al., *Heart Disease and Stroke Statistics-2016 Update: A Report From the American Heart Association*. Circulation, 2016. **133**(4): p. e38-60.
54. Mozaffarian, D., et al., *Heart disease and stroke statistics--2015 update: a report from the American Heart Association*. Circulation, 2015. **131**(4): p. e29-322.
55. Chobanian, A.V., et al., *Seventh report of the Joint National Committee on Prevention, Detection, Evaluation, and Treatment of High Blood Pressure*. Hypertension, 2003. **42**(6): p. 1206-52.
56. Carretero, O.A. and S. Oparil, *Essential hypertension. Part I: definition and etiology*. Circulation, 2000. **101**(3): p. 329-35.
57. Poulter, N.R., D. Prabhakaran, and M. Caulfield, *Hypertension*. Lancet, 2015. **386**(9995): p. 801-12.
58. Lifton, R.P., A.G. Gharavi, and D.S. Geller, *Molecular mechanisms of human hypertension*. Cell, 2001. **104**(4): p. 545-56.

59. Hollenberg, N.K., *Human hypertension caused by mutations in WNK kinases*. Curr Hypertens Rep, 2002. **4**(4): p. 267.
60. International Consortium for Blood Pressure Genome-Wide Association, S., et al., *Genetic variants in novel pathways influence blood pressure and cardiovascular disease risk*. Nature, 2011. **478**(7367): p. 103-9.
61. Mansia, G., et al., *2007 ESH-ESC Guidelines for the management of arterial hypertension: the task force for the management of arterial hypertension of the European Society of Hypertension (ESH) and of the European Society of Cardiology (ESC)*. Blood Press, 2007. **16**(3): p. 135-232.
62. Klarenbach, S.W., et al., *Identification of factors driving differences in cost effectiveness of first-line pharmacological therapy for uncomplicated hypertension*. Can J Cardiol, 2010. **26**(5): p. e158-63.
63. Victor, R.G. and M.M. Shafiq, *Sympathetic neural mechanisms in human hypertension*. Curr Hypertens Rep, 2008. **10**(3): p. 241-7.
64. Oparil, S., M.A. Zaman, and D.A. Calhoun, *Pathogenesis of hypertension*. Ann Intern Med, 2003. **139**(9): p. 761-76.
65. Beevers, G., G.Y. Lip, and E. O'Brien, *ABC of hypertension: The pathophysiology of hypertension*. BMJ, 2001. **322**(7291): p. 912-6.
66. Trott, D.W. and D.G. Harrison, *The immune system in hypertension*. Adv Physiol Educ, 2014. **38**(1): p. 20-4.

67. Harrison, D.G., *The immune system in hypertension*. Trans Am Clin Climatol Assoc, 2014. **125**: p. 130-38; discussion 138-40.
68. Harrison, D.G., et al., *Role of the adaptive immune system in hypertension*. Curr Opin Pharmacol, 2010. **10**(2): p. 203-7.
69. Mancia, G., et al., *2013 ESH/ESC Guidelines for the management of arterial hypertension: the Task Force for the management of arterial hypertension of the European Society of Hypertension (ESH) and of the European Society of Cardiology (ESC)*. J Hypertens, 2013. **31**(7): p. 1281-357.
70. Marinissen, M.J. and J.S. Gutkind, *G-protein-coupled receptors and signaling networks: emerging paradigms*. Trends Pharmacol Sci, 2001. **22**(7): p. 368-76.
71. He, W., et al., *Citric acid cycle intermediates as ligands for orphan G-protein-coupled receptors*. Nature, 2004. **429**(6988): p. 188-93.
72. Hwang, J.S., C.R. Im, and S.H. Im, *Immune disorders and its correlation with gut microbiome*. Immune Netw, 2012. **12**(4): p. 129-38.
73. Wang, Z., et al., *Gut flora metabolism of phosphatidylcholine promotes cardiovascular disease*. Nature, 2011. **472**(7341): p. 57-63.
74. Dahlqvist, G. and H. Piessevaux, *Irritable bowel syndrome: the role of the intestinal microbiota, pathogenesis and therapeutic targets*. Acta Gastroenterol Belg, 2011. **74**(3): p. 375-80.

75. DuPont, A.W. and H.L. DuPont, *The intestinal microbiota and chronic disorders of the gut*. Nat Rev Gastroenterol Hepatol, 2011. **8**(9): p. 523-31.
76. Vaziri, N.D., *CKD impairs barrier function and alters microbial flora of the intestine: a major link to inflammation and uremic toxicity*. Curr Opin Nephrol Hypertens, 2012. **21**(6): p. 587-92.
77. Vaziri, N.D., J. Yuan, and K. Norris, *Role of urea in intestinal barrier dysfunction and disruption of epithelial tight junction in chronic kidney disease*. Am J Nephrol, 2013. **37**(1): p. 1-6.
78. Natarajan, N. and J.L. Pluznick, *Olfaction in the kidney: 'smelling' gut microbial metabolites*. Experimental physiology, 2015.
79. Kim, S., et al., *6B.07: HYPERTENSIVE PATIENTS EXHIBIT GUT MICROBIAL DYSBIOSIS AND AN INCREASE IN TH17 CELLS*. Journal of hypertension, 2015. **33 Suppl 1**: p. 8.
80. Jose, P.A. and D. Raj, *Gut microbiota in hypertension*. Current opinion in nephrology and hypertension, 2015. **24**(5): p. 403-409.
81. Arumugam, M., et al., *Enterotypes of the human gut microbiome*. Nature, 2011. **473**(7346): p. 174-180.
82. Ussar, S., et al., *Interactions between Gut Microbiota, Host Genetics and Diet Modulate the Predisposition to Obesity and Metabolic Syndrome*. Cell metabolism, 2015.

83. Ridaura, V.K., et al., *Gut microbiota from twins discordant for obesity modulate metabolism in mice*. Science (New York, N.Y.), 2013. **341**(6150): p. 1241214.
84. Børnigen, D., et al., *Functional profiling of the gut microbiome in disease-associated inflammation*. Genome medicine, 2013. **5**(7): p. 65.
85. Mariat, D., et al., *The Firmicutes/Bacteroidetes ratio of the human microbiota changes with age*. BMC Microbiol, 2009. **9**: p. 123.
86. Sanz, Y. and A. Moya-Perez, *Microbiota, inflammation and obesity*. Adv Exp Med Biol, 2014. **817**: p. 291-317.
87. Yang, T., et al., *Gut dysbiosis is linked to hypertension*. Hypertension, 2015. **65**(6): p. 1331-40.
88. Yang, T., et al., *Gut dysbiosis is linked to hypertension*. Hypertension, 2015. **65**(6): p. 1331-1340.
89. Khalesi, S., et al., *Effect of probiotics on blood pressure: a systematic review and meta-analysis of randomized, controlled trials*. Hypertension, 2014. **64**(4): p. 897-903.
90. Burke, V., et al., *Dietary protein and soluble fiber reduce ambulatory blood pressure in treated hypertensives*. Hypertension, 2001. **38**(4): p. 821-6.
91. Kim, S., et al., *6b.07: Hypertensive Patients Exhibit Gut Microbial Dysbiosis and an Increase in Th17 Cells*. J Hypertens, 2015. **33 Suppl 1**: p. e77-8.

92. Van Orshoven, N.P., et al., *Postprandial hypotension in clinical geriatric patients and healthy elderly: prevalence related to patient selection and diagnostic criteria*. J Aging Res, 2010. **2010**: p. 243752.
93. Won, Y.-J.J., et al.,  *$\beta$ -Hydroxybutyrate modulates N-type calcium channels in rat sympathetic neurons by acting as an agonist for the G-protein-coupled receptor FFA3*. The Journal of neuroscience : the official journal of the Society for Neuroscience, 2013. **33**(49): p. 19314-19325.
94. Milligan, G., L.A. Stoddart, and A.J. Brown, *G protein-coupled receptors for free fatty acids*. Cellular signalling, 2006. **18**(9): p. 1360-1365.
95. Kim, M.H., et al., *Short-chain fatty acids activate GPR41 and GPR43 on intestinal epithelial cells to promote inflammatory responses in mice*. Gastroenterology, 2013. **145**(2): p. 396.
96. Becker, N., et al., *Human intestinal microbiota: characterization of a simplified and stable gnotobiotic rat model*. Gut microbes, 2011. **2**(1): p. 25-33.
97. Cani, P.D., A. Everard, and T. Duparc, *Gut microbiota, enteroendocrine functions and metabolism*. Current opinion in pharmacology, 2013. **13**(6): p. 935-940.

98. Remely, M., et al., *Effects of short chain fatty acid producing bacteria on epigenetic regulation of FFAR3 in type 2 diabetes and obesity*. Gene, 2014. **537**(1): p. 85-92.
99. Priyadarshini, M., et al., *Maternal short-chain fatty acids are associated with metabolic parameters in mothers and newborns*. Translational research : the journal of laboratory and clinical medicine, 2014. **164**(2): p. 153-157.
100. Kim, S., et al., *Perspectives on the therapeutic potential of short-chain fatty acid receptors*. BMB reports, 2014. **47**(3): p. 173-178.
101. Fung, K.Y., et al., *Butyrate-induced apoptosis in HCT116 colorectal cancer cells includes induction of a cell stress response*. Journal of proteome research, 2011. **10**(4): p. 1860-1869.
102. Hong, Y.-H.H., et al., *Acetate and propionate short chain fatty acids stimulate adipogenesis via GPCR43*. Endocrinology, 2005. **146**(12): p. 5092-5099.
103. Gamet, L., et al., *Effects of short chain fatty acids on growth and differentiation of the human colon cancer cell line HT29*. International journal of cancer, 1992. **52**(2): p. 286-289.
104. Mortensen, F.V., et al., *Short chain fatty acids dilate isolated human colonic resistance arteries*. Gut, 1990. **31**(12): p. 1391-4.
105. Milligan, G., L.A. Stoddart, and N.J. Smith, *Agonism and allosterism: the pharmacology of the free fatty acid receptors FFA2*

- and FFA3. British journal of pharmacology, 2009. **158**(1): p. 146-153.
106. Chang, A.J., et al., *Oxygen regulation of breathing through an olfactory receptor activated by lactate*. Nature, 2015. **527**(7577): p. 240-244.
  107. Katada, S., et al., *Odorant response assays for a heterologously expressed olfactory receptor*. Biochem Biophys Res Commun, 2003. **305**(4): p. 964-9.
  108. Eberle, J.A., P. Widmayer, and H. Breer, *Receptors for short-chain fatty acids in brush cells at the "gastric groove"*. Front Physiol, 2014. **5**: p. 152.
  109. Akiba, Y., et al., *Short-chain fatty acid sensing in rat duodenum*. J Physiol, 2015. **593**(3): p. 585-99.
  110. Kaji, I., et al., *Neural FFA3 activation inversely regulates anion secretion evoked by nicotinic ACh receptor activation in rat proximal colon*. The Journal of physiology, 2016.
  111. Offermanns, S., *Free Fatty Acid (FFA) and Hydroxy Carboxylic Acid (HCA) Receptors*. Annual review of pharmacology and toxicology, 2014. **54**: p. 407-434.
  112. Kumar, P. and N.R. Prabhakar, *Peripheral chemoreceptors: function and plasticity of the carotid body*. Compr Physiol, 2012. **2**(1): p. 141-219.



113. Høverstad, T. and T. Midtvedt, *Short-chain fatty acids in germfree mice and rats*. The Journal of nutrition, 1986. **116**(9): p. 1772-1776.
114. Peterson, K.S., et al., *Characterization of heterogeneity in the molecular pathogenesis of lupus nephritis from transcriptional profiles of laser-captured glomeruli*. J Clin Invest, 2004. **113**(12): p. 1722-33.
115. O'Rourke, M.F. and W.W. Nichols, *Aortic diameter, aortic stiffness, and wave reflection increase with age and isolated systolic hypertension*. Hypertension, 2005. **45**(4): p. 652-8.
116. Blacher, J., et al., *Aortic pulse wave velocity as a marker of cardiovascular risk in hypertensive patients*. Hypertension, 1999. **33**(5): p. 1111-7.
117. Ando, K. and T. Fujita, *Pathophysiology of salt sensitivity hypertension*. Ann Med, 2012. **44 Suppl 1**: p. S119-26.
118. Fujita, T., et al., *Factors influencing blood pressure in salt-sensitive patients with hypertension*. Am J Med, 1980. **69**(3): p. 334-44.
119. Weinberger, M.H., *Salt sensitivity of blood pressure in humans*. Hypertension, 1996. **27**(3 Pt 2): p. 481-90.
120. Chatterjee, S., et al., *Inhibition of glycosphingolipid synthesis ameliorates atherosclerosis and arterial stiffness in apolipoprotein E-/- mice and rabbits fed a high-fat and -cholesterol diet*. Circulation, 2014. **129**(23): p. 2403-2413.

121. Steppan, J., et al., *Exercise, vascular stiffness, and tissue transglutaminase*. Journal of the American Heart Association, 2014. **3**(2).
122. Nowicki, P.T., et al., *Redox signaling of the arteriolar myogenic response*. Circulation research, 2001. **89**(2): p. 114-116.
123. Chotani, M.A., S. Flavahan, and S. Mitra, *Silent  $\alpha$ 2C-adrenergic receptors enable cold-induced vasoconstriction in cutaneous arteries*. Silent  $\alpha$  2C-adrenergic receptors enable cold-induced vasoconstriction in cutaneous arteries, 2000.
124. Domanski, M.J., et al., *Isolated systolic hypertension : prognostic information provided by pulse pressure*. Hypertension, 1999. **34**(3): p. 375-80.
125. Safar, H., et al., *Aortic pulse wave velocity, an independent marker of cardiovascular risk*. Arch Mal Coeur Vaiss, 2002. **95**(12): p. 1215-8.
126. Jandu, S.K., et al., *Nitric oxide regulates tissue transglutaminase localization and function in the vasculature*. Amino acids, 2013. **44**(1): p. 261-269.
127. Zhou, Y., et al., *Acetylcholine causes endothelium-dependent contraction of mouse arteries*. American journal of physiology. Heart and circulatory physiology, 2005. **289**(3): p. 32.

128. Flavahan, S., et al., *Pressure-induced maturation of endothelial cells on newborn mouse carotid arteries*. American journal of physiology. Heart and circulatory physiology, 2013. **305**(3): p. 9.

## **7. Curriculum vitae**

**Niranjana Natarajan, M.Tech**

Graduate student

### **UNIVERSITY ADDRESS:**

Department of Physiology, JHUSOM

725 N. Wolfe Street, WBSB205

Baltimore, MD 21205

Phone: (410) 614-3082

Email: [nnataral@jhmi.edu](mailto:nnataral@jhmi.edu)

### **HOME ADDRESS:**

3120 Saint Paul Street, #B104

Baltimore, MD 21218

Phone: (607) 216-5259

### **PERSONAL:**

Date of Birth: 16 September, 1989

Place of Birth: Chennai, India

Citizenship: India

### **EDUCATION AND TRAINING:**

2011

B. Tech / M. Tech (dual degree,  
equivalent of BS / MS), Biotechnology,  
SASTRA University, Thanjavur, India

2011 – present                      Ph.D., Johns Hopkins University, SOM,  
 Baltimore, MD, U.S.A  
 Advisor: Dr. Jennifer Pluznick  
 Dissertation title: **“The interplay of gut  
 microbial metabolites and Gpr41 in  
 host blood pressure regulation”**

**PROFESSIONAL EXPERIENCE:**

May – July 2008	Summer Research Fellow, Indian Academy of Sciences,  Advisor: Dr. Siva Umapathy
June – Aug 2009	Summer Intern, University of Wisconsin, Madison, Khorana Fellowship (India – U.S.A. exchange program)  Advisor: Dr. Katrina Forest
June – Aug 2010	Summer Intern, Dartmouth College  Advisor: Dr. Albert Erives
Dec 2010 – April 2011	Research Assistant, Dartmouth College  Advisor: Dr. Albert Erives
Aug 2011 – present	Graduate Student, JHUSOM, Department of Physiology  Advisor: Dr. Jennifer Pluznick

### **AWARDS AND HONORS:**

2008	Indian Academy of Sciences, Summer research fellowship (SRF)
2009	Indian Academy of Sciences, Summer research fellowship (declined)
2009	Khorana Scholarship (Awarded jointly by Department of Biotechnology (DBT), India, Indo-US Science and Technology Forum (IUSSTF) and University of Wisconsin Madison (UWM) to 13 people out of a pool of over 500 students to pursue summer research at a lab in UWM)
2010	Regulatory Genomics Summer Internship at Dartmouth College
2013 - 2015	Selected for AAAS/Science Program for Excellence in Science
2014 – 2016	AHA pre-doctoral fellowship – Maggie Wimsatt Memorial Award
2014	Poster award – “Host – Microbiome interactions”, NIH NIDDK, September 9 – 10, 2014, Bethesda, MD
2016	Caroline tum Suden professional opportunity award, Experimental biology April 2 – 6, 2016

### **GRANT SUPPORT:**

AHA Pre-Doctoral Fellowship (2014-2016) – Maggie Wimsatt Memorial Award, (Direct costs – \$52,000)

### **SOCIETY MEMBERSHIPS:**

2012 - Present	American Physiological Society
2012 – Present	American Association for the Advancement of Science
2013 – Present	American Heart Association

### **PUBLICATIONS:**

1. Wei, Z., Seldin, MM., **Natarajan, N.**, Djemal, DC., Peterson, JM. and Wong, GW. C1q/tumor necrosis factor-related protein 11 (CTRP11), a novel adipose stroma-derived regulator of adipogenesis. J. Biol. Chem. 288, 10214–29 (2013). PMID: 23449976, PMCID: PMC3624406
2. Shepard, B.D., **Natarajan, N.**, Protzko, R. J., Acres, O. W. and Pluznick, J. L. A cleavable N-terminal signal peptide promotes widespread olfactory receptor surface expression in HEK293T cells. PLoS ONE 8, e68758 (2013). PMID: 23840901, PMCID: PMC3698168

3. Natarajan, N. and Pluznick, J. L. From microbe to man: the role of microbial short chain fatty acid metabolites in host cell biology. Am. J. Physiol., Cell Physiol. 307, C979–85 (2014). PMID: 25273884
4. Natarajan, N. and Pluznick, J. L. Olfaction in the Kidney: ‘Smelling’ gut microbial metabolites. Exp. Physiol. (2015). doi:10.1113/EP085285. PMID: 26238273

#### **MANUSCRIPTS IN PREPARATION:**

1. **Natarajan, N.**, Hori, D., Stepan, J., Flavahan, S., Flavahan, N.A., Berkowitz, D.E. and Pluznick, J.L. The role of Gpr41 in regulating blood pressure via microbial short chain fatty acid metabolites.
2. Aisenberg, W.H., Huang, J., Zhu, W., Rajkumar. P., Cruz, R., Santhanam, L., **Natarajan, N.**, Yong, H.M., Panettieri, R.R., Homann, O., Sullivan, J.K., Liggett, S.B., Pluznick, J.L. and An, S.A. Defining the primitive olfactory function in airway smooth muscle

#### **PUBLISHED ABSTRACTS:**

1. **Natarajan, N.** and Pluznick, J.L. BUMPT cells as a model system for studying olfactory receptor signaling in renal epithelial cells. The FASEB Journal 27, 1b865 (2013).
2. Shepard, B.D., **Natarajan, N.**, Protzko, R.J., Acres, A. and Pluznick, J.L. An N-terminal signal peptide increases total expression and



- enhances surface trafficking of olfactory receptors (ORs). The FASEB Journal 27, 731.732 (2013).
3. Yoon, A., **Natarajan, N.**, Aisenberg, W., De Santiago, B., Panettieri, R.A., Liggett, S.B., An, S.S. and Pluznick, J.L. Functional expression of the olfactory signaling system in human airway smooth muscle. Am J Respir Crit Care Med 189, A6662 (2014).
  4. Pluznick, J., Shepard, B.D., **Natarajan, N.**, Protzko, R.J. and Acres, A. A cleavable N-terminal signal peptide promotes widespread olfactory receptor surface expression in HEK293T cells. Chemical Senses, Vol. 39 80-80 (Oxford Univ Press, 2014).
  5. Aisenberg, W., Cruz, R., **Natarajan, N.**, Oh, J., Yong, H, Panettieri, R.A., Liggett, S.B., Pluznick, J.L., An, S.S. and Huang, J. Functional expression of the olfactory signaling system in human airway smooth muscle. Am J Respir Crit Care Med 191, A5594 (2015).
  6. **Natarajan, N.** and Pluznick, J.L. Short chain fatty acid metabolites lower blood pressure via endothelial Gpr41. The FASEB Journal 29, 811.815 (2015). (Selected for oral presentation)
  7. **Natarajan, N.**, Hori, D., Berkowitz, D.E. and Pluznick, J.L. Microbial short chain fatty acid (SCFA) metabolites lower blood pressure (BP) via endothelial G-protein coupled receptor (Gpr41). Hypertension 2015, (selected for oral presentation)
  8. Natarajan, N., Hori, D., Steppan, J., Flavahan, S., Flavahan, N.A., Berkowitz, D.E. and Pluznick, J.L. Microbial short chain fatty acid

(SCFA) metabolites lower blood pressure (BP) via endothelial G-protein coupled receptor (Gpr41). Submitted to Experimental Biology 2016, San Diego, CA

### **POSTERS PRESENTED:**

1. **Natarajan, N.**, Aly, K.A. and Forest, K.T. “*Xanthomonas campestris* CAP-like protein: Purification, characterization and structural analysis” at the 33rd Steenbock Symposium, University of Wisconsin, Madison, July 31, 2009
2. Dahlstorm, K.M., **Natarajan, N.** and Erives, A.J. Dissecting the functionality of an enhancer family. Presented at the 52nd Annual Drosophila Research Conference, San Diego, CA March 30-April 3, 2011

### **ORAL PRESENTATIONS:**

1. **Natarajan, N.**, & Pluznick, J. Interplay of microbiota and host GPCRs in regulating blood pressure. (Invited talk, Experimental Biology 2016, San Diego, CA)
2. **Natarajan, N.**, & Pluznick, J. Short chain fatty acid metabolites lower blood pressure via endothelial Gpr41. Presented at Experimental Biology, March 31, 2015. Boston, MA
3. **Natarajan, N.**, Hori, D., Berkowitz, D., Pluznick, J., Microbial short chain fatty acid (SCFA) metabolites lower blood pressure (BP) via

endothelial G-protein coupled receptor (Gpr41). Presented at  
Hypertension 2015, September 17, 2015, Washington D.C.

**PATENT:**

J Pluznick, **N Natarajan**, B Shepard

US Patent 20,150,087,053

Compositions and methods for increasing the expression and signaling of  
proteins on cell surfaces